Diffusion Models in Strongly Chaotic Hamiltonian Systems

A.N.Yannacopoulos

Department of Physics
University of Warwick

This thesis is submitted to the University of Warwick
in partial fulfillment of the requirements for admission
to the degree of Doctor of Philosophy

September 21, 1993

Abstract

The main subject of this thesis is the long time behaviour of strongly chaotic Hamiltonian systems and whether their behaviour can be modelled with diffusion processes. The problem of diffusion caused by chaos in a particular area preserving map on the torus, the web map is studied. The formalism is then generalised for the study of diffusion in higher dimensional symplectic maps on the cylinder and general results are obtained. A numerical method for the calculation of diffusion coefficients for chaotic maps is described. Finally, the problem of diffusion in phase space in the case where chaos coexists with structures such as stable islands is studied .

Being undecided:

Chapter 1 is for Nicos

Chapter 2 is for Jenny

Chapter 3 is for Helen

Chapter 4 is for Helen (2)

Chapter 5 is for Electra

and

Chapter 6 is for ME!

Ἁρμονίη ἀφανὴς φανερῆς κρείττων
(Ηράκλειτος, απόσπ. 54)

Contents

FIGURE CAPTIONS.

Acknowledgments

First of all I would like to thank Prof. G.Rowlands for his excellent supervision and guidance. His help has been invaluable both in physics and in real life. I would also like to thank Dr. R.S.Mackay and Dr. G.King for helpful discussions and suggestions.

Thanks are due to Prof. C.Polymilis of the University of Athens for introducing me to the world of nonlinear physics, and for helpful discussions and support throughout the accomplishment of this work, Prof. K.Hidjanidis, Prof. G.P.Triberis, Dr. D.Frantzeskakis and Prof. G.Kontopoulos also for helpful discussions, seminars and a great deal of encouragement.

A great deal of thanks go to some special friends and colleagues whose presence made life better and easier in Warwick (and not only!). I want to thank Electra, for sharing everything with me, and for being there whenever I needed her. Thanks (the order is inessential) also go to Thanasis Kontos, Jim Charalambakis, Xanthi Zianni, Iakovos Danielidis, George Leftheriotis, Vasilis Karavolas, Dej Jaracensutasinee and Mike Allen.

Of course, I am indebted to my parents Jenny and Nicos for all their moral and financial support, and their interest throughout this period. Without them this thesis would not have been here.

Finally, for financial support I would like to thank the Hellenic State Scholarship Foundation (SSF) for a three year studentship. I would also like to thank Prof. Rowlands, the Physics Department of the University of Warwick and Dr. G.King and Dr. A.Provenzale for arranging financial support for attending some conferences and workshops.

Declaration

Except where otherwise indicated, this thesis contains an account of my own independent research undertaken in the Department of Physics, University of Warwick between October 1989 and May 1993, under the supervision of Prof. G.Rowlands. Some of this work has appeared in the scientific literature in the following joint publications:

Publications

1)A.N.Yannacopoulos and G.Rowlands:'Diffusion Coefficients for the Web Map' Physics Letters A. Volume 155 (1991) 133-136

2)A.N.Yannacopoulos and G.Rowlands:'Diffusion Coefficients for Higher Dimensional Symplectic Maps of the Cylinder' Physica D 57 (1992) 355-374

3)A.N.Yannacopoulos and G.Rowlands:'Calculation of Diffusion Coefficients for Chaotic Maps' Physica D 65 (1993) 71-85

4)A.N.Yannacopoulos and G.Rowlands:'A Model for the Coexistence of Diffusion and Accelerator Modes in Area Preserving Maps' To appear in J.Phys.A

Presentations at Conferences.

1)A.N.Yannacopoulos and G.Rowlands:'Diffusion Coefficients for the Web Map'. Poster presented in the Eight General Conference of the European Society in Collaboration with the Netherlands Physical Society. Amsterdam, the Netherlands September 4-8 1990.(A full version of this work appeared later in Phys.Lett A)

2)A.N.Yannacopoulos and G.Rowlands:'Calculation of Diffusion Coefficients for Chaotic Maps'. Poster presented in Chaotic Dynamics. Theory and Practice NATO ASI. July 11-20, 1991, Patras Greece.

3)A.N.Yannacopoulos and G.Rowlands:'Modelling Chaos With Diffusion Processes.' Short talk presented in Chaotic Advection, Tracer Dynamics and Turbulent Dispersion NATO ARW, May 24-28, 1993, Italy.

Chapter 1

Statistical Description Of Dynamical Systems.

1.1 Introduction

The main subject of this thesis is the long time behaviour of Hamiltonian dynamical systems, whether under certain conditions this behaviour can be approximated by a diffusion process and if so what is the appropriate value of the transport coefficients (diffusion coefficient). In this section a few important ideas about Hamiltonian systems, symplectic maps and chaotic behaviour are given.

A Hamiltonian dynamical system can be defined as a set of $2D$ differential equations

$$\frac{d\mathbf{x}}{dt} = \mathbf{J}\frac{\partial \mathbf{H}}{\partial \mathbf{x}} \tag{1.1}$$

where $\mathbf{J}$ is the $2D \times 2D$ dimensional matrix defined by

$$\mathbf{J} = \begin{pmatrix} \mathbf{0} & \mathbf{1} \\ -\mathbf{1} & \mathbf{0} \end{pmatrix} \tag{1.2}$$

where $\mathbf{0}$ is the $D \times D$ matrix of zero elements and $\mathbf{1}$ is the $D \times D$ unit matrix, $\mathbf{x}$ is the 2D-dimensional vector $\mathbf{x} = (\mathbf{q}_1, \ldots, \mathbf{q}_D, \mathbf{p}_1, \ldots, \mathbf{p}_D)$, where the p's are generalised momentum coordinates and the q's are generalised position coordinates and $H(\mathbf{p}, \mathbf{q})$ is a real valued function. A Hamiltonian system has the

property that it preserves the Lebesgue measure in the $(\mathbf{p}, \mathbf{q})$ space, called the phase space. The evolution of the vector of positions and momenta $\mathbf{x}$ in time can be thought of as a flow in the phase space.

The continuous time Hamiltonian dynamical system of equation (1.1) is often replaced by a discrete time dynamical system which is called the Poincaré map. The Poincaré map can generally be obtained by the following procedure. We cut the 2D-dimensional phase space by a (2D-1) dimensional manifold Σ chosen in such a way that the flow defined by the Hamiltonian dynamical system is everywhere transverse to it [6,H83]. We then take the orbit of each point in Σ and follow it until its first return to Σ with the same orientation with which it started off. The initial point is then mapped to the point of the first return and so on. This procedure then defines a map $\mathbf{P} : \Sigma \rightarrow \Sigma$. This is a discrete time dynamical system which is called the Poincaré map. The process of passing from the continuous time Hamiltonian system to the discrete time Poincaré map is shown in fig.1.1. Another situation where a Poincare map is derivable is the case where we have a Hamiltonian system with a periodic dependence on time with a period say T. Then a Poincare map is defined by stroboscopically observing the flow at times which are multiples of the period. It is the map that takes $\mathbf{x}(0)$ to $\mathbf{x}(T)$ and then to $\mathbf{x}(2T)$ and so on.

The fact that the reduced discrete time dynamical system originally comes from a Hamiltonian system is reflected in the fact that the Poincare map retains the symplectic property. That is, assuming that we have the Poincaré map $\mathbf{P}$ from some manifold Σ to itself, then the Jacobian matrix $\mathbf{P}$ of this map satisfies the condition

$$\mathbf{P}\mathbf{J}\mathbf{P}^T = \mathbf{J} \tag{1.3}$$

where $\mathbf{P}^T$ denotes the transposed Jacobian matrix of the Poincaré map and $\mathbf{J}$ is the matrix defined in equation (1.2).

Of special importance to the study of Hamiltonian dynamical systems are the periodic orbits. Periodic orbits are orbits that close on themselves after some time which is called the period of the periodic orbit. The periodic orbits of the continuous Hamiltonian systems correspond to fixed points of some pe-

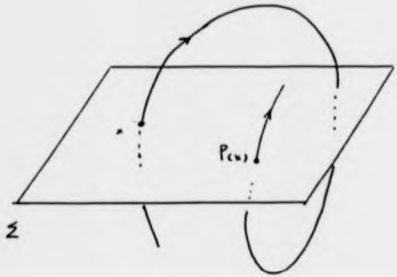

Figure 1.1. Construction of a Poincaré surface of section.

riod (not necessarily the period of the continuous orbit) for the Poincare map of the system. The periodic orbits can either be stable (elliptic) or unstable (hyperbolic). The elliptic orbits act as centers in phase space around which the motion is ordered (quasiperiodic), whereas the hyperbolic orbits act as scatterers in phase space, and nearby orbits will diverge from them at an exponential rate in certain directions. For hyperbolic orbits we can define the notion of stable and unstable manifolds. These are composed of all the points in phase space which for infinite time approach or diverge from the hyperbolic orbit respectively. As we will see in the next paragraph the hyperbolic orbits and their stable and unstable manifolds are responsible for the emergence of very complicated, quasi-random, behaviour in Hamiltonian systems which is called chaotic behaviour.

A basic concept useful in the study of motion in Hamiltonian systems is that of a separatrix. One could generally say that a separatrix is a special orbit(s) of the system which connects the hyperbolic periodic orbits. In order to be able to give a more detailed idea of what a separatrix is we should introduce the model of the simple pendulum. This consists of a rigid and massless bar with a weight attached to the end. The upper part of the bar is fixed at some point and the system is allowed to move under the influence of the gravitational force. The Hamiltonian of the system is given by

$$H = \frac{1}{2}p^2 - A\cos\theta \tag{1.4}$$

where p is the momentum of the weight and θ is the angle of deviation from the vertical position and A is a constant depending on the mass of the weight and the gravitational acceleration. It is easy to see that the pendulum has three fixed points (equilibrium states). One is at p=0 and $\theta = 0$ which corresponds to the pendulum hanging down with no initial velocity. This is a stable fixed point since any small perturbation of the pendulum from that state would be counterbalanced by the effect of the gravitational force and would bring the pendulum back to the stable equilibrium state. The other two fixed points are at p=0 and $\theta = \pm\pi$ corresponding to the upright position of the pendulum. These two are unstable equilibrium points since a small perturbation would

drive this system away from this initial state and the system would not be able to get back there. We can imagine two orbits connecting these two unstable (hyperbolic) fixed points. One is the orbit starting from the upright equilibrium (or better, arbitrarily close to it) at $\theta = -\pi$ and then falling down, passing from the $\theta = 0$ point but with a large velocity, and continuing to go upwards (because of having enough energy) to approach the point $\theta = \pi$. Of course since it started with a momentum equal to zero as it approaches the point $\theta = \pi$ it is going to deccelerate gradually and in consequence it is going to approach this point at $t \to \infty$. By the same reasoning it takes infinite time for the orbit to leave the point $\theta = -\pi$. So this special orbit approaches one hyperbolic fixed point at $t \to -\infty$ and the other at $t \to \infty$. The other orbit of the same kind is one with the same behaviour, only that it goes from left to right rather than from right to left. These two orbits are called the separatrix orbits. In figure.1.2 they are shown in a phase plane diagram. As is understandable, orbits having less energy than the separatrix orbit are going to correspond to oscillations of different amplitudes and orbits with greater energy than the separatrix orbits correspond to rotations of the pendulum. Therefore the separatrix orbits separate qualitatively different motions.

In the case of the pendulum, the separatrix is formed by the smooth joining up of the stable and unstable manifolds of the hyperbolic fixed points and is sometimes called homoclinic or heteroclinic orbit. This is generally the case in integrable systems, that is Hamiltonian systems where the number of integrals of motion (constants of motion) is equal to the dimension of the momentum vector.

When a small, time dependent periodic perturbation is added to the pendulum, destroying integrals of motion and making the system nonintegrable, the smooth separatrix orbit is disrupted (because of the transverse intersection of the stable and unstable manifolds that form it) and a chaotic layer is created around the old separatrix solution (figure 1.2). Inside the chaotic layer the systems dynamics are very complicated and look as if they are generated by a random process. The reason why such behaviour occurs near the separa-

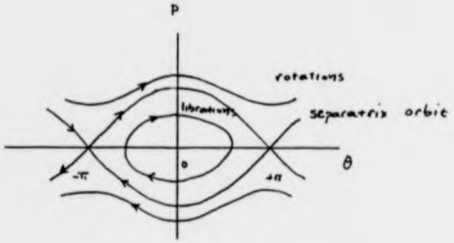

Figure 1.2. Phase plane of the pendulum.

trix is that near the separatrix and especially near the hyperbolic fixed point, the force experienced by a particle from the unperturbed system is very small and so the time dependent perturbation becomes dominant. So the orbit can switch from librations to rotations under the influence of the perturbing force and back again. Since the periods of the motions near the separatrix are becoming infinite (this can be obtained simply by studying more carefully the example of the pendulum) the switches from one type of motion to another will be uncorrelated and so it will be very irregular [A88].

This kind of behaviour, described for the simple pendulum, can arise locally in every nonlinear Hamiltonian system. This can be sketched in a hand waving way by the following reasoning. The example of the pendulum is the prototype for any nonlinear resonance and it is seen that separatrices occur often in dynamical systems. Suppose that we have a nonlinear system which is integrable and is perturbed by some arbitrary perturbation which conserves the Hamiltonian property of the system. It can be proved that a new set of coordinates $(\mathbf{I}, \phi)$ for the system exists in which the Hamiltonian of the perturbed system can be written in the form (see for example [Ar89])

$$H(\mathbf{I}, \phi) = H_0(\mathbf{I}) + \epsilon \sum_{\mathbf{n}} A_{\mathbf{n}} \cos(\mathbf{n}.\phi) \tag{1.5}$$

where ϵ is a small perturbation parameter and the perturbation is expanded in a Fourier series. This new set of coordinates is such that in the unperturbed case the $\mathbf{I}$'s are constants of the motion and $\phi = \omega t + \mathbf{c}$ where $\omega = \frac{\partial H_0}{\partial \mathbf{I}}$ and $\mathbf{c}$ is a constant vector. This new set of coordinates is called action-angle variables [Ar89], [Gi80]. It is not hard to see and prove that if the perturbation is small enough then the most important term in the perturbation is the most slowly varying one [Ar89]. This term is the one satisfying the condition $\omega.\mathbf{n} = \mathbf{0}$. We then say that this is a resonant term and the truncated Hamiltonian (retaining in the perturbation series only the slowly varying term) is said to describe a nonlinear resonance. It is not difficult to show (see for example [LL83]), that with the appropriate canonical transformation [1] the Hamiltonian for the non-

[1] A transformation is called canonical if the equations of motion in the new coordinate system are still in Hamiltonian form, eq.(1.2) [Gi80]

linear resonance can be brought in the form of the Hamiltonian describing the pendulum. In the case of a nonlinear resonance a separatrix is the curve separating islands (which correspond to trapped orbits in the resonance) from the rest of phase space (which corresponds to untrapped orbits). So in analogy with the case of the pendulum (now the role of the time dependent perturbation is played by the neglected quickly varying terms in the perturbation series), a chaotic layer where very complicated and quasi-random behaviour occurs, is created around the separatrix of any nonlinear resonance. Since in a nonlinear system a large number of resonances can occur, the interaction of those (resonance overlap, see for example [C'79]) can lead to widespread chaotic behaviour of the system.

A huge amount of analytical and theoretical work has been done on the issues of stability and how and when this is lost we are led to chaotic behaviour. Nowdays we have explicit results on when the constants of motion (or local constants of motion) are destroyed and why (for example the several versions of the KAM theory to be mentioned in Chapter 2 or the renormalisation approach to the breakdown of tori in phase space bearing regular orbits, corresponding to the survival of certain local integrals of motion under the perturbation [M85]).

1.2 Statistical description of dynamical systems using the Fokker-Planck equation

It is well known that very simple low-dimensional dynamical models may show very complicated dynamics and this has been called chaotic dynamics. Even though the underlying dynamical system is deterministic, the chaotic dynamics, due to its complexity and to properties like the exponential instability of neighboring orbits, can be modeled by statistical methods and in particular by kinetic equations. The idea is to a get a simpler description of the chaotic motion by looking at the evolution of a distribution of orbits in phase space rather than the evolution of single orbits. Going to such a description means that some information about the system is inevitably lost, at the gain of getting

a simpler coarse-grained description of the chaotic system which can then give us information about measurable quantities of the system.

The kinetic equations used are usually of the Fokker-Planck type. The Fokker-Planck equation is the simplest type of kinetic equation and corresponds to the coarse-grained description of a stochastic system with the minimum amount of memory, that is, it is equivalent to a Markovian process. Of course it is readily understood that such a description is not exact but in many cases it is a very good approximation.

Methods similar in nature to the ones used by Prigogine and the Brussels group [P62],[L88] for the derivation of kinetic equations from the Hamiltonian dynamics of infinite systems have been devised to show rigorously that under some conditions (strong enough stochasticity is the main one) the dynamics of a chaotic Hamiltonian system with as little as two degrees of freedom can be modeled in the first approximation by a kinetic equation of the Fokker-Planck type for the evolution of a distribution function in momentum space [P85]. Such rigorous methods complement the 'heuristic' derivation of the Fokker-Planck approximation to the dynamics in momentum space for Hamiltonian systems [LL83]. It should be mentioned here that for Hamiltonian systems it is possible to have an even simpler kinetic description. As it has been shown by Landau, for a Hamiltonian system, the Fokker-Planck equation can be reduced to a diffusion equation (see for example [LL83]).

Once we accept the idea of approximating the chaotic dynamics with a kinetic equation of the Fokker-Planck type the next obvious problem is the calculation of the transport coefficients that enter the kinetic equation. Various analytical methods have been devised for the calculation. An attempt is made here to present briefly the most important of these, namely the correlation function method, characteristic function method the path integral method, and the Fourier path method.

The Fokker-Planck equation in momentum space is of the form

$$\frac{\partial P(\mathbf{p},t)}{\partial t} = -\frac{\partial (BP)}{\partial p} + \frac{1}{2}\frac{\partial^2 (DP)}{\partial p^2} \tag{1.6}$$

where P is a distribution function in momentum space, p is a vector of momenta,

D is the diffusion tensor and B the friction tensor.

For a Hamiltonian system, the Fokker-Planck equation can be reduced to the diffusion equation

$$\frac{\partial P(\mathbf{p},t)}{\partial t} = \frac{1}{2}\frac{\partial}{\partial \mathbf{p}} D(\mathbf{p}) \frac{\partial P(\mathbf{p},t)}{\partial \mathbf{p}} \tag{1.7}$$

In the case where the momentum or action space is one dimensional, the diffusion coefficient is defined by

$$D = lim_{t\to\infty} \frac{< (p_t - p_0)^2 >}{2t} \tag{1.8}$$

where p_t is the momentum at time t and the angle bracket denotes an ensemble average over a number of orbits in a part of phase space of physical interest. It is also a good approximation for Hamiltonian systems with two degrees of freedom or equivalently for area preserving maps where now p is the action variable.

In the case of higher dimensional systems, a diffusion tensor should be introduced instead of the diffusion coefficient. The diffusion tensor would be of the form

$$D = lim_{t\to\infty} \frac{< (\mathbf{p}_t - \mathbf{p}_0)(\mathbf{p}_t - \mathbf{p}_0) >}{2t} \tag{1.9}$$

and it gives the correlation between the different degrees of freedom. However we are going to look at the case of two-dimensional systems only for the time being. The case of higher dimensional systems will be considered later.

In the next two sections we present the derivation of the Fokker Planck equation as a means of describing the evolution of a chaotic dynamical system.

1.3 Derivation of the Fokker-Planck equation for dynamical systems

In this section we sketch two different derivations of the Fokker Planck description of deterministic systems. The first is a derivation of the Fokker Planck description for chaotic Hamiltonian maps [CR81] and the second is a generalisation of the Liouville operator method used by Prigogine and others (see eg

[P62]) in irreversible statistical mechanics. The second method is formulated for continuous time systems but the results can be easily generalised to mappings.

We will first present the approach of Cohen and Rowlands for the derivation of the Fokker-Planck equation.

Assume a mapping of the form

$$p_{n+1} = p_n + F(\theta_n, p_n) \tag{1.10}$$

$$\theta_{n+1} = \theta_n + G(\theta_n, p_n) \tag{1.11}$$

where p and θ are action angle variables (see for example [G80]). We wish to obtain a kinetic equation description for the evolution of the action variable p. Following Cohen and Rowlands [CR81] we define a distribution function $P(p, \theta, t)$ such that $P(p, \theta, t)dpd\theta$ is the number of particles in the volume element $dpd\theta$ of the phase plane. In the original derivation a noise term was added to the map to help randomisation of motion but here we omit it and assume that randomisation of the motion and decay of correlations is due only to chaos. We are going to look at the evolution of

$$N(p, t) = \int d\theta P(p, \theta, t) \tag{1.12}$$

which is the number of particles per unit of p.

In a time Δt corresponding to n iterations of the map, the particles which originally were in position (p,θ) move to position (p', θ') which is fully determined by the map. Then

$$P(p', \theta', t + \Delta t) = P(p' - \Delta p, \theta' - \Delta\theta, t)det(\frac{(p, \theta)}{(p', \theta')}) \tag{1.13}$$

The second factor of the right hand side of the above equation is the Jacobian of the map which gives the contraction of the initial volume of phase space due to the dynamics of the map. However, since we are dealing here with symplectic maps (area preserving) this Jacobian is always equal to 1. This equation can be written, using the map, in the form

$$P(p', \theta', t + \Delta t) = \int dudv P(p' - u, \theta' - v, t)\delta(p' - p - u)\delta(\theta' - \theta - v) \tag{1.14}$$

where the initial values p,θ are regarded as functions of the final values p', θ' In the above relation $p' = p + u$ and $\theta' = \theta + v$ after n iterations of the map. Assuming that the changes in the action coordinate p are small we may Taylor expand the integrand of the previous equation in p and obtain

$$P(p', \theta', t + \Delta t) = \sum_{k=0}^{\infty} \frac{(-1)^k}{k!} \frac{\partial^k}{\partial p^k} \int du dv u^k P(p', \theta' - v, t) \delta(p' - p) \delta(\theta' - v - \theta) \tag{1.15}$$

Performing integration over v and θ' we obtain

$$N(p', t+\Delta t) = \int P(p', \theta', t+\Delta t) d\theta' = \sum_{k=0}^{\infty} \frac{(-1)^k}{k!} \frac{\partial^k}{\partial p^k} \int du d\theta' u^k P(p', \theta', t) \delta(p' - p) \tag{1.16}$$

Since the Jacobian for the transformation defined by the map is one, we can change variables from u,θ' to p,θ without changing the form of the integral. Finally we integrate over p to obtain

$$N(p, t + \Delta t) = \sum_{k=0}^{\infty} \frac{(-1)^k}{k!} \frac{\partial^k}{\partial p^k} \int d\theta P(p, \theta, t) (\Delta p(p, \theta))^k \tag{1.17}$$

where $\Delta p = p' - p$ is defined as a function of the initial p and θ.

Taking Δt small enough so that the change in the action during this interval is small but also large enough such that $n \gg 1$, we can truncate the series defined in the above equation to second order in Δp and replace $N(p, t + \Delta t)$ with $N(p, t) + \Delta t \frac{\partial N}{\partial t}$ to obtain

$$\frac{\partial N}{\partial t} = \int d\theta \frac{\partial}{\partial p} (\eta P + k \frac{\partial P}{\partial p}) \tag{1.18}$$

where

$$\eta = \frac{1}{n\tau_c} (-\Delta p + \frac{1}{2} \frac{\partial}{\partial p} (\Delta p)^2) \tag{1.19}$$

and

$$k = \frac{(\Delta p)^2}{2n\tau_c} \tag{1.20}$$

and τ_c is such that $\Delta t = n\tau_c$. It is easy to see that by assuming that the chaotic process results in a randomisation of the values of θ as a function of time, the distribution functions in phase space will not depend on the angle variables and so the above equation reduces to the Fokker-Planck equation with well defined transport coefficients.

A similar approach has been adopted by Lieberman and Lichtenberg [LL83] in their derivation of the Fokker-Planck equation for chaotic maps.

This approach depends heavily on the convergence of the Taylor series in equation (1.17) and the randomisation of the angle coordinate. These conditions are expected to be true for a fully chaotic region.

1.4 Alternative derivation of the Fokker-Planck equation

An alternative derivation of the Fokker-Planck equation for nonlinear chaotic systems was obtained by Petrovsky [P84],[P85]. This derivation, gives more explicit results for the region of validity of the Fokker-Planck equation and its connection with chaos. In his two papers he used a formal perturbation theory of the Liouville equation to study the asymptotic evolution of a distribution function near a perturbed separatrix in phase space. He proved that the asymptotic evolution of such a distribution function is given by a kinetic equation of the Fokker-Planck type. His method of deriving the Fokker-Planck equation is analogous to that used by Prigogine and coworkers (see for example [P62] or [L89]) for the derivation of kinetic equations for the case of non equilibrium statistical mechanics in an infinite system.

Here we sketch briefly the method and the results of Petrosky [P84],[P85]. Assume a nonlinear Hamiltonian system written in action-angle variables $p_1, p_2, \theta_1, \theta_2$ in such a way that the periods of oscillations in θ_1, θ_2 are $\frac{\partial I}{\partial p_1}$ and $\frac{\partial I}{\partial p_2}$ respectively. The system is nonlinear, so these periods depend on the actions.

Let us now introduce a distribution function $P(p, \theta, t)$ of orbits in the stochastic region. The evolution of this distribution function under the dynamics is given by Liouville's equation (see for example [P62]) which is of the form

$$\frac{\partial P(\mathbf{p}, \theta, t)}{\partial t} = \hat{L} P(\mathbf{p}, \theta, t) \tag{1.21}$$

where $\hat{L} = i[H, \,]$ is the Liouville operator. The square brackets denote the Poisson bracket and the distribution function is normalised in the stochastic

region of phase space.

If the Hamiltonian is written in the form $H = H_0 + K\hat{V}$ where K is a small perturbation parameter then the Liouville operator can be written in the form $L = \hat{L}_0 + K\delta\hat{L}$ where

$$\hat{L}_0 = -i\omega.\frac{\partial}{\partial\theta} \tag{1.22}$$

and

$$\delta\hat{L} = i\frac{\partial V}{\partial\theta}.\frac{\partial}{\partial\mathbf{p}} - i\frac{\partial V}{\partial\mathbf{p}}.\frac{\partial}{\partial\theta} \tag{1.23}$$

where $\omega = \frac{\partial H_0}{\partial \mathbf{p}}$ are the unperturbed frequencies of the system. The normalised eigenfunctions of the unperturbed Liouville operator are given by

$$\Phi_{k_1,k_2}(\theta) = \frac{(\Delta k_1 \Delta k_2)^{\frac{1}{2}}}{2\pi}\exp(i(k_1\theta_1 + k_2\theta_2)) \tag{1.24}$$

and form a complete orthonormal set in which we can analyse the initial distribution function $P(\mathbf{p}, \theta, 0)$. Petrosky [P84],[P85] in analogy with the original work of Prigogine [P62], assumes a distribution function of the particular form

$$P(\mathbf{p}, \theta, 0) = \frac{\Delta k_1 \Delta k_2}{(2\pi)^2}\sum_{k_2}(P_{0k_2}(\mathbf{p}) + \Delta k_1 \sum_{k_1}^{\infty} P_{k_1 k_2}(\mathbf{p})\exp(ik_1\theta_1))\exp(ik_2\theta_2) \tag{1.25}$$

It is seen that this distribution function has a δ-singularity in k_1 in the Fourier representation. The existence of this singularity is essential for the derivation of the kinetic equation [P85]. Not all possible distribution functions have this property. For example a distribution function corresponding to a single trajectory will not have the δ-singularity. The existence of this singularity is related to the existence of homoclinic points in the ensemble chosen. In [P85] it was conjectured and checked with specific examples that a probability distribution containing homoclinic points possesses this δ-function singularity in the Fourier representation. Of course, as is well known, homoclinic points are the skeleton of chaos, so the assumption of Petrosky [P85] is understandable since it just states that a kinetic equation can be obtained only in the region of phase space where homoclinic points exist, that is where chaotic behaviour occurs. Furthermore, he was able to show that the condition for the existence of nonzero kinetic operators (the operators that define the kinetic equation) is equivalent

to the condition that the stable and unstable manifolds of the hyperbolic point intersect transversely, that is, the Melnikov function (which defines the distance between the stable and the unstable manifolds of a hyperbolic fixed point) has a number of non degenerate zeros.

We are interested in the evolution of the momentum (action) components of the distribution function because usually diffusion in chaotic systems occurs in the actions. For this reason we define the projection operator

$$\hat{P} = \int\int d\theta_1 d\theta_2 \tag{1.26}$$

which performs an averaging over the angle variables. We now find the equations giving the asymptotic behaviour of $\hat{P}P$.

The formal solution of the Liouville's equation is given by the resolvent operator of the Liouvillian, $(z - \hat{L})^{-1}$ in a Laplace transform representation, and can be written as

$$P(\mathbf{p},\theta,t) = \exp(-i\hat{L}t)P(\mathbf{p},\theta,0) = \frac{1}{2\pi i}\int_\Gamma dz \exp(-izt)\frac{1}{z-\hat{L}}P(\mathbf{p},\theta,0) \tag{1.27}$$

where the contour Γ lies above the real axis of z and goes from $-\infty$ to ∞ for $t > 0$. After some algebraic manipulations we can obtain a perturbation series for the evolution of $\hat{P}P$.

$$\hat{P}P(\mathbf{p},\theta,t) = \frac{1}{2\pi i}\sum_{n=0}^{\infty}\int_\Gamma dz \exp(-izt)\frac{1}{z^{n+1}}(\psi(z))^n(P + \hat{D}(z))P(\mathbf{p},\theta,0) \tag{1.28}$$

where we define the operators

$$Q = 1 - \hat{P} \tag{1.29}$$

$$\psi(z) = \hat{P}\hat{L}Q\frac{1}{z - Q\hat{L}Q}Q\hat{L}\hat{P} \tag{1.30}$$

and

$$\hat{D}(z) = \hat{P}\hat{L}Q\frac{1}{z - Q\hat{L}Q}. \tag{1.31}$$

In analogy with the theory of Prigogine et al [P62] for infinite systems Petrosky [P84],[P85] called ψ the collision operator and $\hat{D}$ the destruction operator.

The asymptotic contribution in equation (1.28) for $t \to \infty$ is obtained by evaluating the singularities of the integrand at z=0. Assuming that the singularities of $\frac{1}{z^{n+1}}$ are isolated from the singularities of the analytically continued

operators $\psi(z)$, $\hat{D}(z)$, an assumption which is shown by Petrovsky to be satisfied, the asymptotic solution for $t \to \infty$ can be obtained by finding the residue of the integrand in equation (1.28). The asymptotic solution then takes the form

$$P^{\prime}P(\mathbf{p},\theta,t) = \sum_{n=0}^{\infty} \frac{i}{n!} \frac{\partial^n}{\partial z^n} \exp[-izt](\hat{\psi}(z))^n (\hat{P} + \hat{D}(z))\mathbf{P}(\mathbf{p},\theta,0))_{z=+i0} \quad (1.32)$$

where $z=+i0$ means that the residue is taken for analytically continued kinetic operators from the upper half plane of z. This equation is equivalent to

$$\frac{\partial}{\partial t} P(\mathbf{p},\theta,t) = \int_0^t dt' \psi(t') \mathbf{P}\mathbf{P}(\mathbf{p},\theta,t-t') \quad (1.33)$$

where $\psi(t)$ is the Laplace transform of the collision operator $\hat{\psi}(z)$ defined by the relation

$$\hat{\psi}(z) = i \int_0^{\infty} dt \exp(izt)\psi(t). \quad (1.34)$$

The integral in the right hand side of equation (1.33) can be expanded in a perturbation series in K, the lowest order of which gives the result

$$\frac{\partial}{\partial t} P(\mathbf{p},\theta,t) = \pi K^2 \sum_{\mathbf{k}}^{'} \frac{\partial}{\partial \mathbf{p}} .\mathbf{k}\Delta\mathbf{k}_1 \mid V_{\mathbf{k}} \mid^2 \delta(\mathbf{k}.\omega)\mathbf{k}.\frac{\partial}{\partial \mathbf{p}} \Delta\mathbf{k}_1 P(\mathbf{p},\theta,t) \quad (1.35)$$

where $V_{\mathbf{k}}$ are the Fourier components of the perturbation V in a Fourier series in the angles θ.

As the separatrix is approached, the period of oscillation in one of the angles, say θ_1 becomes infinite in which case $\Delta k_1 \to 0$ and the summation over k_1 may be replaced with an integral over k_1 that is $\Delta k_1 \sum_{k_1} \to \int dk_1$. Then, making the canonical coordinate transformation $(p_1, p_2) \to (p_1, H_0)$ the kinetic equation obtained can be transformed to the Fokker-Planck equation

$$\frac{\partial}{\partial t} P_1(p_1, H_0, t) + \frac{\partial}{\partial p_1}(-\frac{1}{2} D(p_1, H_0) \frac{\partial}{\partial p_1} \Delta k_1 P_1(p_1, H_0, t)) = 0 \quad (1.36)$$

where $P_1(p_1, H_0, t) = P(p_1, p_2, t)$ and $D(p_1, H_0) = 2\pi K^2 \Delta k_1 \sum_{\mathbf{k}}^{'} \mid k_1 V_{\mathbf{k}} \mid^2 \delta(\mathbf{k}.\omega)$ is the diffusion coefficient. The diffusion coefficient is well defined near the separatrix and can be calculated for particular models by changing the summation over $\mathbf{k}_1$ to an integration.

The derivation given in this section depends explicitly on the existence of a broken separatrix and homoclinic points, and one expects the Fokker-Planck

equation to be good in the neighbourhood of such points. It is a local derivation for the kinetic equation. The kinetic equation for a wider part of phase space can be obtained by a properly chosen averaging method over different patches of phase space for which the method described above can be properly used.

In the above it has been demonstrated that the Fokker-Planck equation can be used to describe systems where chaotic motion dominates. We now consider some methods that can be used to calculate the transport coefficients that enter the Fokker-Planck equation.

1.5 The correlation function method

We are interested in the calculation of the diffusion coefficient for chaotic area preserving maps of the form

$$p_{n+1} = p_n + f(\theta_n, p_n) \tag{1.37}$$

$$\theta_{n+1} = \theta_n + g(\theta_n, p_n) \tag{1.38}$$

where f,g are functions periodic in both the variables θ,p or linear in the variable p.

We first present a method given by Karney et al [KRW82],[CM81]. This method was originally proposed for doubly periodic area preserving maps with noise. The noise was introduced to ensure ergodicity. The case we are interested in are chaotic maps without noise terms, that is fully deterministic maps, so the method is presented in a form slightly different from its original version. The role of noise here is played by the extended stochasticity required for the method to work.

The diffusion coefficient given by equation (1.8) can be rearranged as follows Define

$$a_n = p_{n+1} - p_n \tag{1.39}$$

Then

$$p_n - p_0 = \sum_{j=0}^{n-1} a_j \tag{1.40}$$

and

$$(p_n - p_0)^2 = \sum_{j=0}^{n-1} a_j^2 + 2\sum_{l=0}^{n-2}\sum_{p=l+1}^{n-1} a_l a_p \qquad (1.41)$$

Taking the ensemble average we get

$$< (p_n - p_0)^2 > = \sum_{j=0}^{n-1} < a_j^2 > +2\sum_{l=0}^{n-2}\sum_{p=l+1}^{n-1} < a_l a_p > . \qquad (1.42)$$

Since the average is taken over an invariant part of phase space and the measures are conserved the average over initial conditions is time ranslation invariant and $< a_p a_l > = < a_{p-l} a_0 >$. We can rewrite the second term in the right hand side of the sum as follows

$$\sum_{l=0}^{n-2}\sum_{p=l+1}^{n-1} < a_l a_p > = \sum_{j=1}^{n-1}\sum_{p=0}^{n-1}(n-j) < a_j a_0 > \qquad (1.43)$$

where $j = p - l$. The diffusion coefficient is then given by

$$D = lim_{n\to\infty}(\frac{1}{2n}\sum_{j=0}^{n-1} < a_j^2 > + \sum_{j=1}^{n-1}\frac{(n-j)}{n} < a_j a_0 > \qquad (1.44)$$

In the limit $n \to \infty$ the first part of the sum can be taken in good approximation to be

$$\frac{1}{n}\sum_{j=1}^{n} < a_j^2 > = < a^2 > \qquad (1.45)$$

where a^2 is the time average of $a^2 = (\Delta p)^2 = f^2(\theta, p)$. The second part becomes

$$lim_{n\to\infty}\sum_{j=1}^{n}(1 - \frac{j}{n}) < a_j a_0 > \qquad (1.46)$$

and if $< a_j a_0 >$ decays fast enough in j

$$\sum_{j=0}^{\infty} < a_j a_0 > . \qquad (1.47)$$

The time averages through which the diffusion coefficient has been defined are difficult to handle analytically. In order to be able to use the expansion of the diffusion coefficient given above to get analytical expressions we make the assumption of ergodicity in which case time averages may be replaced by phase space averages. These are easier to handle analytically. In this case $lim_{n\to\infty}\frac{1}{n}\sum_{j=0}^{n} a_j^2$ can be approximated by $< a(p,\theta) >_N = < f(p,\theta) >_N$ where

the angle brackets now denote an average over the whole ergodic region of the phase space. Similarly $< a_{m+p} a_p >_R = < f(\theta_m, p_m) f(\theta_0, p_0) >_R$.

The maps we are interested in are periodic in both coordinates (doubly periodic maps) and so they can be thought of as maps of the torus. The ergodic region of phase space R over which the phase space averaging will be performed can be taken to be the unit torus, thus providing convergence of the phase space averages. According to the above assumptions the diffusion coefficient can be written in the form

$$D = \frac{1}{2} C_0 + \sum_{\tau=1}^{\infty} C_\tau \tag{1.48}$$

where

$$C_\tau = \frac{1}{(2\pi)^2} \int_0^{2\pi} \int_0^{2\pi} d\theta_0 dp_0 a_\tau a_0 \tag{1.49}$$

a_τ and a_0 are functions of θ_0, p_0. It is then seen that the diffusion coefficient for a chaotic map is just the infinite sum of all the momentum autocorrelation functions.

Some remarks are in order now. To obtain the above expression, which can be easily used for the analytical calculation of the diffusion coefficient of chaotic maps, the assumption that the dynamics in phase space is ergodic has been used. Such an assumption has not been proven except for a very limited number of specially chosen ideal systems. In most cases it is nothing else but an approximation. The above method proposed relies heavily on the fact that the ergodic approximation is good enough and this is best achieved if the dynamics are strongly chaotic. This is why, for maps which are perturbations of integrable maps, the method works only for large values of the perturbation parameter, unless a noise term is introduced to help ensure the ergodic properties.

A second drawback to the calculation of D is the actual convergence of the infinite series of correlation functions defining the diffusion coefficient. The convergence of this series requires fast enough (exponential) decay of the correlation functions C_τ with τ. This is equivalent to a fast enough memory loss for the system under consideration. In the original paper where this method was proposed [KRW82], the fast enough decay of the correlation functions was

ensured by the introduction of a noise term. However if a system is sufficiently chaotic , such a fast decay may be obtained from the local exponential instability without the need for the introduction of a noise term. This is not of course always the case and slow algebraic decay of the correlation functions, due for example to island structures in phase space, causes difficulties in the numerical and analytical calculation of the diffusion coefficient for chaotic systems [MO86]. Such difficulties are discussed in detail in Chapter 5 of this thesis.

Due to the drawbacks of this method, discussed above, the approximations of the diffusion coefficients obtained using correlation functions, must be checked by computations.

1.6 Characteristic function method

A method similar in nature to the one proposed by Karney et al [KRW82] is the one proposed by Cary and Meiss [CM81]. Cary and Meiss were interested in the calculation of the diffusion coefficient for area preserving maps of the form

$$p_{n+1} = p_n + K f(\theta_n) \tag{1.50}$$

$$\theta_{n+1} = \theta_n + p_{n+1} \tag{1.51}$$

where f is a periodic function. These maps are also doubly periodic maps and can be thought of as maps of the unit torus. The general class of characteristic functions were defined

$$\Lambda_k^N(m_0, m_1, ..., m_k) = < exp(i \sum_{j=0}^{k} m_j \theta_{n+j}(\theta_0, p_0)) >_R \tag{1.52}$$

where θ_{n+j} is a function of the initial conditions θ_0, p_0 through the iterations of the map. The angle brackets denote an average over the region R of phase space. R is supposed to be an invariant under the dynamics of the map chaotic region of phase space and because of the double periodicity of the class of maps under consideration the region R can be taken to be the whole unit torus.

These characteristic functions are the Fourier transforms of the joint probability distribution $P_k^N(p_0, p_1, ..., p_k)$, which gives the probability of finding a

particle at y_j at time j (j=0,1,....k) given that it was initially in the region R of phase space. It is then clear that the characteristic functions can give a complete statistical description of the dynamics of the map. Here however we are only interested in the diffusion coefficient. As was shown in the previous section the diffusion coefficient can be written as the infinite sum of correlation functions

$$D = \frac{1}{2}C_0 + \sum_{r=1}^{\infty} C_r \tag{1.53}$$

where $C_r = < f(\theta_0)f(\theta_r) >_R$ for the special class of maps considered by Cary and Meiss.

Taking the Fourier decomposition of $f(\theta)$ to be

$$f(\theta) = \sum_{l=-\infty}^{\infty} f_l exp(il\theta) \tag{1.54}$$

the correlation functions can be expressed in terms of the characteristic functions as follows

$$C_r = \sum_{m,n} f_m f_n \chi_r(m, 0, ..., 0, n) \tag{1.55}$$

where the characteristic functions can be calculated from the recursion relation

$$\chi_r^R(m_0, m_1, ..., m_k) = \sum_{l=-\infty}^{\infty} g_l(m_k K)\chi_{k-1}^R(m_0, m_1, ..., m_{k-2}, m_{k-2} - m_k, m_{k-1} + 2m_k + l) \tag{1.56}$$

and where

$$g_l(K) = \frac{1}{2\pi}\int_0^{2\pi} exp(il\theta - iKf(\theta))d\theta \tag{1.57}$$

Using this recurrence relation Meiss et al [MCG83] managed to get the principal terms in the diffusion coefficient, that is resum all the terms in (1.53) to a certain order in the perturbation parameter K.

We will review this method briefly since it can only be used for maps which are of a rather simple form such as the standard map.

The diffusion coefficient is written as a sum of all the correlation functions (see for example the previous section) and as was shown before, the correlation functions can be expressed only in terms of one particular class of the characteristic functions $\chi_r(m, 0, ..., 0, n)$. Iterating this recursion relation for

the characteristic functions for this particular class of characteristic functions Meiss et al [MCG83] found the following relation

$$\chi_k^{l_0}(l_k, 0, ..., 0, l_0) = \sum_{l_1, l_2, ..., l_{k-1}=-\infty}^{\infty} \prod_{j=0}^{k-1} g_{\nu_j}(lK) \chi_1^{l_0}(l_k - l_{k-2}, l_{k-1}) \qquad (1.58)$$

where $l_{-1} = 0$ and $\nu_j = l_{j-1} - 2l_j + l_{j+1}$.

The maps under consideration are supposed to be of such form that for $K \gg 1, g_\nu(lK) \ll 1$ when $(\nu, l) \neq (0, 0)$ in order to ensure the convergence of the series defining the characteristic functions. For the standard map for example the g's are just Bessel functions of the first order and this condition is satisfied.

An approximate expression for the characteristic functions has been obtained (for the particular case of the standard map) by performing a summation of the principal terms [MCG83]. The principal terms are those with the maximum number of factors $g_\nu(lK)$ equal to unity. For the case of the standard map where these factors are Bessel functions this requires $l_j = \nu_j = 0$ for each such factor. Since l_0 is fixed we set $l_1 = \nu_1 = 0$ and obtain (l_2, ν_2) by the recursion relation for the l's and the ν's. Then we set all the remaining odd l's and ν's equal to 0 and calculate the even ones according to the recursion relation. All the even l's and ν's are given in terms of the fixed value of l_0. This trajectory in (j,l) space, which should not be confused with the Fourier space trajectories used by Rechester et al [RRW81], terminates at j=k-2 with $l_{k-2} = l_k$. A nontrivial result can be obtained if $l_k \neq 0$ and this condition gives us that k must be even and $l_k = (-1)^{\frac{(k-2)}{4}} l_0$. This principal term contributes to the characteristic function in question the term

$$\chi_k^{l_0}(l_k, 0, ..., l_0) = (g_{-2l_0}(l_0 K))^{\frac{k}{2}} g_{2(-1)^{(k-2)/4} l_k} \qquad (1.59)$$

where the superscript l^0 refers to the principal part. The principal contribution in the case where k is odd can be obtained similarly. However for the case of the standard map it turns out that in the case of k odd, not all odd order l and ν 's must be zero. If we assume that this is l_{j0} for j_0 odd, then it is easy to calculate l_{j_0-1} and l_{j_0} in terms of l_0 and l_k. The contribution from such principal paths can then be written down [MCG83].

Having obtained the principal term contributions to the characteristic functions χ_k, we can calculate the principal contribution to the force correlation functions C_k through which the diffusion coefficient can be defined. It is found that

$$C_k = < f(\theta_k) f(\theta_0) >_R = \frac{1}{2}(\chi_k(1,0,...,0,-1) - \chi_k(1,0,...,0,1)) \qquad (1.60)$$

for the special case of the standard map and then the principal term contribution to these are

$$C_k^P = \frac{1}{2}(-J_2(K))^{k/2} \quad k \quad even \qquad (1.61)$$

and

$$-\frac{k-1}{k+1}\frac{1}{K}\frac{d}{dK}(-J_2(K))^{(k+1)/2} \quad k \quad odd \qquad (1.62)$$

The diffusion coefficient can then be found by summing up the C_k's for k=0 to ∞. This is obtained as a geometric series and gives the final result

$$D^P = \frac{K^2}{4}[\frac{1 - J_1^2(K) - J_2^2(K) + 2J_2^3(K)}{(1 + J_2(K))^2}]. \qquad (1.63)$$

This result is more accurate than other results for the standard map (for example [RRW81],[CR81]) since it has been obtained by taking into account an infinite number of terms that add up to give a contribution of the order of $O(\frac{1}{K^2})$, which were not taken into account using the previous methods. As is rightly remarked by Rowlands and Bland [BR86] the expression given for D^P can be thought of as a Padé approximation to the diffusion coefficient using the expansion given by Retchester et al [RRW81].

The method of Meiss et al [MCG83] though efficient in calculating and resumming an infinite number of correlations whose total effect is of a given order, can not be used in maps which are not doubly periodic (i.e maps of the torus), at least in its original form, and becomes algebraically complicated if the map is not of a simple form such as the standard map. However, it has recently been used in higher dimensional symplectic maps of the torus [KM90] with some success.

1.7 The path integral method for the estimation of the diffusion coefficient

Another interesting method for the calculation of the diffusion coefficient for chaotic dynamical systems expressed as area preserving maps is the path integral method or Fourier space path method formulated by Rechester, Rosenbluth and White [RW80],[RRW81], Cohen and Rowlands [CR81] and others. The method was formulated initially for the standard map with a noise component. Later a method similar in spirit to the Fourier space path method has been formulated for more general area preserving maps such as the radial twist maps by Hatori et al [HKI85]. In the latter approach a noise component was not introduced into the map. Here we briefly sketch these two approaches without introducing the noise term. The noise term was used to ensure the ergodic properties of the map so that a kinetic description would be appropriate. However here we assume that the role of the noise is played by the intrinsic stochasticity of the system caused by the strong chaotic properties of the deterministic dynamical system in question.

We will start by introducing the approach of Hatori et al [HKI85]. A similar approach was also followed by Rowlands and Hland [RR86] for the specific case of the standard map.

Let us assume an area preserving map of the form

$$p_{n+1} = p_n + k f(\theta_n) \tag{1.64}$$

$$\theta_{n+1} = \theta_n + a(p_{n+1}) \tag{1.65}$$

where $f(\theta)$ is a periodic function of period 2π and $a(p)$ is any function. The above area preserving map is called the radial twist map (RTM). For general choices of the function $a(p)$ the map in question is a map of the cylinder, that is, a map with periodicity only in the angle variable θ. However for special choices of the function $a(p)$, for example if a is a linear function of p, or a periodic function of p, the map can be thought of as a map of the torus, that is a map with periodicity in both the action and the angle variables. The well known standard map is an example of the latter case with $f(\theta)=\sin(\theta)$ and $a(p)=p$.

Following Hatori et al [HKI85] we define the diffusion coefficient for the map as

$$D = lim_{N\to\infty} \frac{<(p_N - p_0)^2>}{2N} \tag{1.66}$$

where the brackets denote an average over the initial angle θ_0. Iterating the map N times we get that

$$I_N = <(p_N - p_0)^2> = \int_0^{2\pi} \dots \int_0^{2\pi} d\theta_0 I_N^2 \Pi_{j=1}^{N-1} \delta(\theta_j - \theta_{j-1} - a(I_j^*)) d\theta_j \tag{1.67}$$

where $I_j = K\Sigma_{l=0}^{j-1} f(\theta_l)$ and p_0=0 is assumed. Taking the Fourier decompositions of the δ functions the above equation can be written in the form

$$I_N = \sum_{m_1=-\infty}^{\infty} \dots \sum_{m_{N-1}=-\infty}^{\infty} \int_0^{2\pi} \dots \int_0^{2\pi} d\theta_0 \dots d\theta_{N-1} I_N^2 exp(\sum_{j=1}^{N-1} i2\pi m_j(\theta_j - \theta_{j-1} - a(I_j^*))) \tag{1.68}$$

where the m_j's take integer values.

We can now evaluate perturbatively the integral I_N. Since the exponential term in the integral can be written as a product of N-1 exponentials, which are always less or equal to one and contain one n, the main contribution to I_N comes from the part obtained by putting all the m_j's equal to zero. This choice for the m_j's then gives

$$I_N = \int_0^{2\pi} \dots \int_0^{2\pi} d\theta_0 \dots d\theta_{N-1} I_N^2 \tag{1.69}$$

or equivalently

$$I_N = \int_0^{2\pi} \dots \int_0^{2\pi} d\theta_0 \dots d\theta_{N-1} K^2 (\sum_{l=0}^{N-1} f(\theta_l))^2 \tag{1.70}$$

This term gives the so called random phase approximation, in which the $\theta^l s$ are supposed to be statistically independent, that is $<\theta_n \theta_m> = <\theta_n^2> \delta_{nm}$. This is easily seen since taking all the $m_j^l s$ to be zero is equivalent to replacing all the delta functions in the integral expression for I_N, equation (1.67) by unity. This means we assume that the values of the angle θ, as a function of the time, are not related to each other by the mapping equations, that is, the system loses its memory in one iteration. For the simple case where $f(\theta) = sin\theta$ we readily obtain that $I_N^{(0)} = \frac{K^2}{4} 2N$ and this part of I_N gives a finite contribution

to the diffusion coefficient $D_{QL} = \frac{K^2}{2}$. Here the index QL means the quasilinear approximation discussed above.

The higher approximations may be obtained by first taking $m_k = 0$ for $k \neq j$ and $m_j \neq 0$ for j=1,...,N-1 then $m_j \neq 0, m_{j+1} \neq 0$ and $m_k = 0$ for $i \neq j, j+1$ and j=1,....N-2 and so on. This essentially means that we treat the $\theta's$ as independent after one iteration of the map, two iterations of the map and so on. In order to calculate the contributions from these higher approximations the following Fourier decompositions will have to be used

$$exp(iqa(p)) = \int_{-\infty}^{\infty} dk \sigma(k,q) exp(ikp) \tag{1.71}$$

and

$$exp(iqf(\theta)) = \sum_{m=-\infty}^{\infty} F_m(q) exp(im\theta) \tag{1.72}$$

The derivation of the contributions of the higher approximations is cumbersome and depends heavily on the particular properties of the functions $\sigma(k,q)$ and $F_m(q)$. For example, for the standard map where a(p)=p and $f(\theta) = sin\theta$ and consequently $\sigma(k,q) = \delta(k-q)$ and $F_m(q) = J_m(q)$ (where J_m is the Hessel function of order m) the first three corrections have been calculated explicitly and were shown to give the following result for the diffusion coefficient [C'R81], [HK85], [HR86]

$$D = \frac{K^2}{2}(\frac{1}{2} - J_0(K) + J_1^2(K)) \tag{1.73}$$

For more general maps Hatori et al [HK85] proved that the corrections to the quasilinear result to I_N go off as $N^{\frac{1}{2}}$ for $N \to \infty$ thus giving no finite corrections to the quasilinear result for the diffusion coefficient. The condition for this to happen is that $\sigma(k,q)$ has no singular behaviour as a function of k.

In the approach of Rechester, Rosenbluth and White [RRW81], Cohen and Rowlands [C'R81] (see also [MLL85]) equation (1.67) was written for the evolution of a probability distribution $P(p,\theta,t)$ of orbits in the phase space of the map, under the iterations of the map. This equation was obtained starting from the conservation of the number of particles under the iteration of the map. This property can be expressed as

$$\frac{dP}{dt} = 0 \tag{1.74}$$

or equivalently

$$\frac{\partial P}{\partial t} + \frac{\partial \theta}{\partial t}\frac{\partial P}{\partial \theta} + \frac{\partial p}{\partial t}\frac{\partial P}{\partial p} = 0 \tag{1.75}$$

where in the integer time n in the map has been substituted by a continuous time t and the variables p and θ can be found as functions of the time t by the iteration of the radial twist map.

The appropriate initial condition for the probability distribution is

$$P(p,\theta,0) = \frac{1}{2\pi}\delta(p - p_0) \tag{1.76}$$

The solution to equation (1.76) is given by

$$P(p,\theta,t) = \int_0^{2\pi} G(\theta - \theta')P(\theta', p - K\sin\theta', t-1)d\theta' \tag{1.77}$$

where $G(\theta - \theta', p)$ is the Greens function given in the form

$$G(\theta - \theta', p) = \frac{1}{2\pi}\sum_{m=-\infty}^{\infty} exp(im(\theta - \theta' - a(p)) = \delta(\theta - \theta' - a(p)) \tag{1.78}$$

Substitution of this equation gives the following result for the probability distribution

$$P(\theta,p,t) = \int_0^{2\pi} d\theta'\delta(\theta - \theta' - a(p))P(\theta', p - K\sin\theta', t-1) \tag{1.79}$$

The above equation just states that the particle being in position p,θ of phase space at time t is just the particle that was in position p', θ' ,such that $p = p' + K\sin\theta'$, $\theta = \theta' + a(p)$, at time t-1.

Let us introduce the Fourier transform of the probability function

$$P(p,\theta,t) = \frac{1}{(2\pi)^2}\sum_{m=-\infty}^{\infty}\int_{-\infty}^{\infty} dk a_m^t(k) exp(i(m\theta + kp) \tag{1.80}$$

Using this Fourier decomposition, equation (1.77) gives

$$a_m^t(k) = \int_0^{2\pi} d\theta' exp(-im\theta')\int_{-\infty}^{\infty} dp exp(-i(kp + ma(p))P(\theta', p + K\sin\theta', t-1) \tag{1.81}$$

If a(p)=p, then we have the case of the standard map and the analysis is tractable. In the more general case the analysis is difficult because of the complicated form of the integral over p. However for intermediate times such

that the action p has not changed much we may linearise a(p) around the initial value of the momentum p_0 and write

$$a(p) = a(p_0) + (p - p_0)\frac{da}{dp}|_{p=p_0} \tag{1.82}$$

Therefore, from now on, for simplicity, we will assume that a(p)=p. Then using the identity

$$exp(\pm i\beta sin\theta) = \sum_{m=-\infty}^{\infty} J_m(\beta)exp(\pm im\theta), \beta > 0 \tag{1.83}$$

we can obtain from equation (1.79) the recursion formula for the Fourier amplitudes $a^t_m(k)$

$$a^t_m(k) = \sum_{k'=-\infty}^{\infty} J_{(k'K)}a^{t-1}_{m'}(k') \tag{1.84}$$

where the following relations have to be fulfilled

$$k' = k + m \quad and \quad m' = m - lagnk' \tag{1.85}$$

With the help of this recursion formula one can in principle calculate the long time behaviour of the distribution function P(p,θ,t). The diffusion coefficient we are interested in can be calculated directly from the quantities a^t_m in the following way. The diffusion coefficient is defined by

$$D = lim_{N\to\infty}\frac{< (p_N - p_0)^2 >}{2N} \tag{1.86}$$

The νth moment of the probability distribution P(p,θ,t) can be given by

$$< p^\nu > = \int P(p,\theta,t)p^\nu dpd\theta = lim_{k\to 0}(i\frac{\partial}{\partial k})^\nu a^N_0(k) \tag{1.87}$$

so that

$$D = lim_{k\to 0} -\frac{1}{N}\frac{\partial^2}{\partial k^2}a^N_0(k) \tag{1.88}$$

[CR81].

Thus we see that in order to calculate the diffusion coefficient we must calculate a^N_0 in the limit $N \to \infty$. This can be done in a perturbative way.

Let us iterate that the recursion relation (1.84) N times, starting with the initial condition

$$a^0_m(k) = \delta_{m0}exp(-ikp_0) \tag{1.89}$$

corresponding to the probability distribution

$$P(p,\theta,0) = \frac{1}{2\pi}\delta(p-p_0) \tag{1.90}$$

Every iteration can be thought of as a path in the (m,k) space. The iterations will be performed backwards in time and since we are interested in the limit $k \to 0^+$ and m=0, all the paths we are interested in should end at the point (m,k)=(0,0). There is a large number of such paths, each one of those giving a contribution to $a_0^N(0^+)$. The simplest path is the one that never leaves the origin, that is all the k's and m's are equal to zero. This path contributes the term

$$a_0^N(k) = (J_0(kK))^N a_0^0(0) \tag{1.91}$$

and this gives the contribution to the diffusion coefficient

$$D = \frac{K^2}{4} \tag{1.92}$$

which is nothing but the quasilinear approximation.

The corrections to this main contribution are obtained using paths in the Fourier space that leave the origin. From the recursion relation (1.84) we see that leaving or returning to the origin once gives factors of $J_l(kK)$ and since we are interested in the limit $k \to 0^+$ we only have a contribution to the diffusion coefficient from such parts of a path if and only if $l = \pm 1$. This is because the second derivatives with respect to k of $J_l(kK)$ with $l \geq 2$ go to zero as $k \to 0^+$. For large K, because of the Bessel function contribution at each step, we can construct a series in ascending powers of Bessel functions by considering paths with an increasing number of steps spent away from the origin. This is in complete analogy with the approach used by Hland and Rowlands [HR86] and Hatori et al [HK185] where the approximation was based on the number of iterations of the map before randomisation of the angle variables. The number of iterations allowed before randomisation of the angles is equal to the number of steps spent away from the origin. However in the way presented by Hland and Rowlands [HR86] or Hatori et al [HK185], the physical justification for the approximation used is more apparent.

The construction and the enumeration of the appropriate graphs remains to be done. We will not need to go through this in detail since the construction of graphs depends on the particular map considered. We just give the simplest corrections. The path with the fewer number of steps spent outside the origin is the path

$$(0,0) \to (0,1) \to (1,-1) \to (0,0). \tag{1.93}$$

This can be traversed in N steps in N-2 different ways, that is remaining at the origin before moving S=0,1,...N-3 iterations. The contribution of these N-2 paths to $a_0^N(k)$ is

$$a_0^N(k) = (N-2)(J_0(kK'))^{N-3}J_{-1}(kK')J_{-1}(kK')J_2((1+k)K') \tag{1.94}$$

and this contributes to the diffusion coefficient a correction term of $-\frac{N-2}{4}J_2(K')$. Note that this result is the same as that of Hatori et al [HKI85].

1.8 Markov models for transport in phase space

All the models for transport in phase space considered up to now were more or less in the same spirit and were based on the calculation of the various transport properties, such as the diffusion coefficient, in terms of correlation functions which are obtained by averaging over parts of phase space. It is evident that such models can not give a very detailed description of the transport processes throughout phase space.

A different class of models which is based mainly on the geometrical characteristics of the dynamical system in question are the Markov models for transport in phase space. These can give more localised information on transport through phase space, at the expense of having to obtain detailed information on the characteristics of the particular dynamical system in question, such as position of hyperbolic unstable orbits, stable and unstable manifolds etc. Models of this sort have been proposed by Mackay et al [MMP84], Benslimon and Kadanof [BK84], Dana et al [DMP89] and Wiggins and coworkers (see for example the monograph [W92]).

The strategy of such models can be summarised as following. Suppose that the transport between two disjoint parts of phase space R_1 and R_2 is to be studied. Two disjoint regions can only communicate if a partial barrier exists between them. A partial barrier permits some flux of phase space through it and can be either a cantorus (a cantorus is just an invariant curve of the map that has an infinite number of holes in it and has the structure of a Cantor set) or a set of stable and unstable manifolds of a hyperbolic periodic orbit that intersect permitting a part of phase space to be transported by the action of the map.

Before introducing models of this form we must give the basic mechanism of transport. Assume that a hyperbolic fixed point for a map M exists in phase space and let us call it S. Then for this point there exists a stable and an unstable manifold which are the set of points which if mapped to $t \to \infty$ approach S and if mapped by the inverse mapping to $t \to -\infty$ approach S respectively. These two manifolds, which we shall call $W^s(S)$ and $W^u(S)$ (the superscript s denotes the stable one and the superscript u denotes the unstable one), must intersect at an infinity of points (each one of which is the image of the other under M) which are called homoclinic points. The intersection of these manifolds is equivalent to the nonintegrability of the system because it has been proved that in the case of an integrable system the stable and the unstable manifolds of the hyperbolic fixed point of the map will have to be smoothly connected. Suppose for simplicity that $W^s(S)$ and $W^u(S)$ intersect in such a way that there is only one homoclinic point q with the property that the segment of $W^s(S)$ from S to q and the segment of $W^u(S)$ from S to q intersect only at q (a point with such properties is called a primary intersection point by Easton [E86]). It is easy to prove that if M is a diffeomorphism then the images and preimages of primary intersection points (pips) are again pips (see eg [W92]). We can see that between the pip q and $M^{-1}(q)$ we have an s-shaped region of finite area (which is defined by the stable and unstable manifolds of S) that was called a turnstile by Mackay et al [MMP84]. If we call L_{12} the part of the turnstile between $M^{-1}(q)$ and t (see figure 1.3) and L_{21} the part of the turnstile

between t and q (where t is a homoclinic point but not a pip) then we see that under the action of the map the area in L_{12} is mapped to an intersection of the manifolds lying 'outside' the area enclosed by $[Sq]^u$ and $[qS]^s$ which we will call for simplicity R_1 ($[Sq]^u$ denotes the segment of the unstable manifold between S and q). The same thing applies for the area in L_{21} which starts 'outside' the area R_1 (that is in R_4) and under the action of the map M is mapped inside it (see figure 1.3). So we see that through the turnstiles, that are formed by the broken separatrix, we can have communication between two distinct areas of phase space. This is the basic mechanism of transport between two regions of phase space which are distinct but are connected by partial barriers. It is easily seen that the afore mentioned mechanism is present in the case of hyperbolic orbits of period greater than one. We can then define the flux of phase space out of region R_1 and into region R_4 which is nothing else but the area of L_{12}. This area can be obtained for area preserving maps using the action formalism [MMP84] or using the Melnikov function [W92].

We are now able to formulate the transport problem. In order to study the transport through the phase space of an area preserving map we have to break the phase space into disjoint areas that cover the whole of phase space, that is we have to generate a Markov partition for the map. These disjoint regions can communicate through partial barriers like turnstiles or overlap of turnstiles formed by stable and unstable manifolds of different hyperbolic periodic orbits. Suppose that each of the disjoint areas forming the Markov partition has area A_i which can be calculated. If the flux between two such regions is ΔW_{ij}, which is given by the common area of the appropriate turnstiles, then a Markov model can be obtained for the transport process through phase space with transition probabilities $p_{ij} = \frac{\Delta W_{ij}}{A_i}$ from region i of the partition to region j. This Markov model can then be solved giving information about how different parts of phase space can communicate. Of course the problem of choosing the right partition remains. Mackay et al got round this problem by choosing a partition of phase space in terms of resonances. A resonance is a region of phase space bounded by pieces of stable and unstable manifolds of a hyperbolic ordered periodic

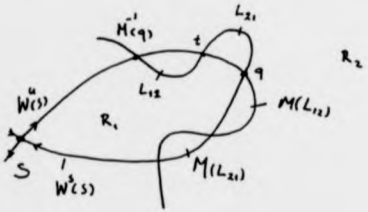

Figure 1.3. Transport through a broken separatrix.

orbit [MMP87]. Then the turnstiles of the resonance is the total area (flux) exchanged by this resonance and the rest of phase space. It can be proved that with the right choice of boundaries for each resonance, two resonances will not overlap while for a given region bounded by two KAM curves the total area of the resonances is equal to the area. That means that the resonances form a complete partition of phase space and all chaotic orbits except a set of measure 0 must lie in this partition. Two resonances can only communicate through overlaps of their turnstiles. In choosing such a partition the areas of the different regions can be obtained quite easily (though with considerable numerical effort) through the action formalism of area preserving maps and same goes for the turnstiles area.

Markov models are very interesting and can give detailed results for transport in parts of phase space where the formalism presented in the previous sections is not appropriate. They can be used in cases when we have weak chaos, such as when we are close to the critical value of the perturbation parameters for the onset of transport, that is when a KAM curve is just beginning to break up. On the other hand the methods described up to now need the existence of strong chaos and are valid for large values of the perturbation parameters.

Markov models have been used successfully by several authors for simple maps such as the standard map and the sawtooth map and for the latter exact results have been obtained (see for example [DMP89], [D90] , [MMP84], [W92]). The above presentation of such models is certainly incomplete but a more complete presentation is beyond the scope of this thesis since our work is based on the class of models based on correlation function methods. We think that such models should be used to get an overall idea of the transport through phase space and then the Markov models which require a great deal of numerical work should be used for the parts of phase space or regions in parameter space that the correlation function models are seen to be inadequate. Furthermore since the Markov models are not yet sufficiently well formulated for systems of dimension greater than 2 (except perhaps for some partial results by Wiggins [W92]) we have to use the techniques of the previous sections which

have already been shown to work successfully.

In the present thesis, as mentioned above, we focus on the investigation of correlation function models for the study of diffusion in strongly chaotic maps. In such cases correlation function methods are appropriate since for strongly chaotic motions the effect of ordered structures such as islands is small and more detailed or refined descriptions are not urgently necessary at least in the stage of getting some basic information on the system. As a final remark here we can see that combinations of the two models can be made. For example Markov models that are appropriate in certain parts of phase space can be used to obtain the proper boundary conditions to be used in the description of the system in question by a diffusion equation.

1.9 Motivation for this Work.

As mentioned earlier, the main subject of this thesis is the long time behaviour of chaotic Hamiltonian dynamical systems. In this section I want to present the main motivations for undertaking such a study, by mentioning some of the applications of such a problem.

By now it is well understood that a great number of the dynamical systems that appear in nature can become chaotic, so being able to quantify observables for a chaotic system is of great importance for applications.

One of the most important problems of this sort is that of charged particle confinement. If we consider charged particles in an axisymmetric magnetic mirror, or for example the earth's magnetic field, then these are dynamical systems of two degrees of freedom, and the details of the particle trajectories give information about the confinement of particles by the fields. Depending on the geometry and strength of the applied fields, there can be a transition from regular motion to global stochasticity. The presence of stochastic motion leads to an enhancement of particle losses either out of the mirror machine or to the poles in the case of the earth's magnetic field. The long time behaviour of this dynamical system will give us information on the leakage rate of particles from the field, information of paramount importance for the design of magnetic

mirrors and the entry of charged particles into the earth's ionosphere.

Another important class of problems where this study is of relevance, is the problem of charged particle heating. The motion of charged particles in specially selected electromagnetic field configurations can become chaotic. This chaotic motion, which comes from the modification or destruction of invariants of motion due to the interaction of resonances may lead to a more effective transfer of energy from the electromagnetic field to the particles, that is more effective heating of the charged particles. One of the most common schemes is the use of the resonance between the gyrofrequency and the electromagnetic wave. An example of such a heating scheme is the web map, proposed by Zaslavskii et al [ZZS86] where electrons rotating in a magnetic field interact with an electrostatic wave packet propagating perpendicularly to the magnetic field. The long time evolution of a probability distribution in the momenta (or actions) gives important information on the evolution of the kinetic energy of an initial ensemble of particles and the effectiveness of this scheme as a heating mechanism. Thus the construction of kinetic equations for the evolution of such probability distributions in the case where motion becomes chaotic will be of great practical importance.

Last, but not least, in this small indicative list of problems related to the study of the long time properties of chaotic Hamiltonian systems, is the problem of chaotic advection. It was found recently, that the motion of tracer particles, even in a two dimensional, incompressible laminar flow, can become chaotic if the laminar flow is time dependent [O89]. The equations of motion for the tracer particles can be written in Hamiltonian form. The long time behaviour for such a system will give information on the dispersion of passive tracers in the flow and on how effective mixing due to chaos is. There is a wide range of problems related to that, such as the dispersion of contaminants in the atmosphere or the oceans, or effective mixing of reacting substances in the chemical industry.

The contents of this thesis, are not going to deal with any specific applications, except for Chapter 2 where the study of transport in a particular system, associated with charge particle heating, the web map, is presented. The rest

of it is devoted to the study of some general problems that appear when the problem of transport caused by chaos in Hamiltonian dynamical systems is considered.

Chapter 2

Diffusion in the Web Map.

2.1 Introduction

We have seen in Chapter 1 that a deterministic dynamical system can give rise to complicated, irregular motion which looks very similar to noise. This kind of motion is called chaotic motion. Importantly, unlike noise chaotic motion is perfectly deterministic. This irregular motion is extremely sensitive to initial conditions as applied to the deterministic system. In a more formal language, this corresponds to an exponential divergence of nearby orbits, a property which is quantified by the introduction of the Lyapunov numbers [LL83]. Chaotic solutions of a dynamical system have (maximal) Lyapunov exponents which are positive, while regular or periodic solutions have negative maximal Lyapunov exponents. Another point which should be made, is that usually the correlation functions for chaotic motion are more structured than those for noise, particularly white noise.

The chaotic behaviour first arises near the separatrix solution. As mentioned already in section 1.1 a separatrix is a special orbit(s) of the system which passes from the hyperbolic periodic orbits. In the integrable case (where no chaos is possible) like for example the pendulum, the separatrix is formed by the smooth joining up of the stable and unstable manifolds of the hyperbolic fixed points and is sometimes called homoclinic or heteroclinic orbit. The separatrix separate qualitatively different orbits. For example in the case of the

unperturbed pendulum whose phase portrait is shown in figure 1.2 the separatrix solution is the solution separating oscillatory from rotating orbits that joins up the hyperbolic fixed points corresponding to the unstable equilibrium points of the pendulum. The example of the pendulum is the prototype for any nonlinear resonance and it is seen that separatrices occur often in dynamical systems. In the case of a nonlinear resonance a separatrix is the curve separating islands (which correspond to trapped orbits in the resonance) from the rest of phase space (which corresponds to untrapped orbits).

When a small, time dependent periodic perturbation is added to the pendulum, the smooth separatrix orbit is disrupted (because of the transverse intersection of the stable and unstable manifolds that form it) and a chaotic layer is created around the old separatrix solution (figure 2.1) . Inside the chaotic layer the systems dynamics are very complicated and look as if they are generated by a random process. The reason why such behaviour occurs near the separatrix is that near the separatrix and especially near the hyperbolic fixed point, the force experienced by a particle from the unperturbed system is very small and so the time dependent perturbation becomes dominant. So the orbit can switch from librations to rotations and back again under the influence of the perturbing force. Since the periods of the motion near the separatrix approach infinity (this can be obtained simply by studying more carefully the example of the pendulum) the switches from one type of motion to another will be uncorrelated and so it will be very irregular [A88].

A stochastic web appears when many stochastic layers intersect in phase space. The existence of stochastic webs in Hamiltonian systems of more than two degrees of freedom has been known since 1960 (a phenomenon called Arnold diffusion, see for example [LL83]) However it is only recently that such stochastic webs have been reported for lower dimensional Hamiltonian systems namely systems of $1\frac{1}{2}$ degrees of freedom (that is one degree of freedom plus a time periodic perturbation) in the physical context of charged particles rotating in a steady and homogeneous magnetic field interacting with electrostatic waves [ZSU88].

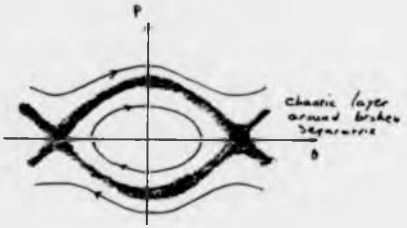

Figure 2.1. Chaotic region around the separatrix area.

2.2 Spider webs.

The standard system for such webs is that of a linear oscillator perturbed by a time periodic perturbation as is discussed in detail in the next sections. The simplest model for a stochastic web is a linear oscillator with a sinusoidal wave. Such a system is said to produce a spider web and is described by the Hamiltonian [CSZ88]

$$H = \frac{p^2}{2} + \frac{\omega_0 x^2}{2} + K\cos(kx - \omega t) \tag{2.1}$$

A physical situation described by such a Hamiltonian is that of the motion of a charged particle in a homogeneous static magnetic field (this is equivalent to a harmonic oscillator of frequency ω_0, the Larmour frequency) perturbed by an electrostatic wave propagating perpendicularly to the magnetic field. We can easily go to action angle variables (J,θ) for the harmonic oscillator. Then the nonlinear perturbation when, expanded in a Fourier series, introduces into the motion a series of resonances between the unperturbed motion and the perturbation. The resonance condition is

$$m\omega_0 = n\omega \tag{2.2}$$

When we have a resonance a stochastic web appears in phase space that has a rotational symmetry (see figure 2.2) . It is clear from the figures that the phase space consists of 2m concentric rays along which the chaotic layers are aligned and in between the rays we have elliptic islands corresponding to stable motion. More details about how the structure of the spider web is obtained are given later.

The width of the chaotic layer of the web depends exponentially on the perturbation parameter [CNP87]

$$\Delta H = \frac{const}{K} exp(-\frac{const}{K}) \tag{2.3}$$

The constant is independent of K but depends on the part of phase plane we are in. The exact expression for ΔH shows that the width of the stochastic layer becomes smaller as we move out in the phase plane. Bearing in mind that diffusion of orbits through the channels of the stochastic web to remote regions

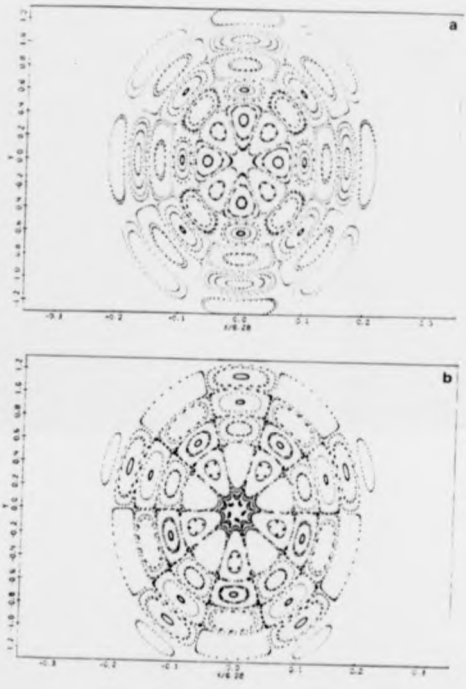

Figure 2.2. Phase plane for the spider web map for various symetries after [CNP87].

of phase space is possible, one readily sees that the reduction in the width of the stochastic layer as we move out in the phase plane corresponds to the fact that high energy paticles have less probability to diffuse to high kinetic energies than low energy particles. This is not true for all kinds of stochastic webs. It is possible to construct stochastic webs with chaotic layers having a uniform width all over the phase space (see section 2.3).

To study the structure of the spider web in more detail we first take an appropriate canonical transformation, namely

$$x = (\frac{2n_0 I}{\omega_0})^{\frac{1}{2}} cos(\frac{\phi}{n_0} - \omega t) \tag{2.4}$$

$$p = (2n_0 I\omega_0)^{\frac{1}{2}} sin(\frac{\phi}{n_0} - \omega t). \tag{2.5}$$

Then in the case of exact resonance $n_0\omega_0 = \omega$,the Hamiltonian of the system reduces to

$$H = H_0 + V \tag{2.6}$$

$$H_0 = \frac{K\omega^2}{k} J_{on}(k(\frac{2n_0 I}{\omega_0})^{\frac{1}{2}}) cos n\phi \tag{2.7}$$

$$V = \frac{K\omega^2}{k} \sum_{m=0,n=-\infty}^{+\infty} J_n(k(\frac{2n_0 I}{\omega_0}))^{\frac{1}{2}} cos(\frac{n\phi}{n_0} + (\frac{n}{n_0} - 1)\omega t) \tag{2.8}$$

where J_n is the Bessel function of order n.

With this canonical transformation we have changed to action-angle variables for the harmonic oscillator and changed to a moving coordinate frame rotating with the frequency of the oscillator. In this way we may separate slow and fast variables, and thus set a formal framework for the use of perturbation theory.

The part H_0 of the Hamiltonian is the integrable part (unperturbed hamiltonian). Under certain conditions, namely that the pertubation is on a much faster time scale than the unperturbed motion, the Hamiltonian H_0 provides a good approximation to the full motion. This part of H generates in the phase plane a separatrix network that is extended all over the phase plane. Information concerning the form of the separatrix network generated by H_0 can be gained from the hyperbolic singular points of H_0. According to Chernikov et

al [CSZ88] the separatrix network consists of concentric circles that are crossed by $2n_0$ rays.

The time-dependent part of the Hamiltonian , V, plays the role of the perturbation that disrupts the separatrix network created by H_0 and is responsible for the formation of stochastic layers (chaotic layers) about lines defined by the separatrices of the unperturbed system. This is the way a stochastic web is created and these features are illustrated in figure 2.2. The width of the stochastic web can be found by approximating the particle motion near a separatrix by a mapping (separatrix mapping) and taking the local phase instability condition for the occurence of stochasticity as proposed by Zaslavskii and Chirikov [ZC72] and is given by equation (2.3).

The existence of an infinite connected stochastic web at first sight looks incompatible with the KAM theorem (named after Kolmogorov Arnold and Moser who first proved versions of it). According to this theorem some of the invariant tori of the unperturbed system (those not carying resonant or equivalently periodic orbits) should survive under the perturbation for small enough values of the perturbation (see for example [LL83]) These tori should then be barriers for the communication of the chaotic layers along the resonances thus ruling out the posibility for the existence of an infinite connected stochastic web. An important condition for the KAM theorem to hold is that the unperturbed system is not degenerate, that is the determinant of the Hessian matrix of the unperturbed Hamiltonian (written in the action angle variables) should not be zero. This condition states that for the KAM theorem to hold, a resonance condition should be localised in phase space. According to Chernikov et al [CSZ88] one of the important reasons that the infinite stochastic web exists for the linear oscillator, when perturbed by the resonant perturbation, is that the unperturbed system is degenerate, thus making the KAM theorem inapplicable in some parts of phase space. The degeneracy arises from the fact that the unperturbed system is linear.

This degeneracy of the unperturbed system is immediately removed by considering a nonlinear oscillator (in which case the frequency of oscillations de-

pends on the energy or momentum of the oscillator) in the place of the harmonic one. Then, the KAM theorem is applicable and this makes the existence of a stochastic web infinitely extended in phase space impossible. The theorem implies that for some finite K there will be an invariant curve in the phase space that impedes stochastic diffusion across it. In this case stochastic layers are separated by KAM surfaces (due to the low dimensionality of the system) and consequently cannot intersect. It is however possible that certain finite segments of the stochastic web may remain in certain parts of phase space. This is more probable in the parts of phase space where oscillations are small and the nonlinear oscillator can well be approximated by a linear oscillator. This idea is supported by numerical calculations [CNP87].

2.3 The web map.

According to Chernikov et al [CSZ88] there is the possibility of the existence of an infinite stochastic web with a uniform width as distinct to the case of the spider web, where the width of the stochastic web decreases exponentially as we move away from the origin in the phase plane. An appropriate model of this kind is a linear oscillator perturbed by a force E which consists of an infinite number of sinusoidal forces with a harmonically related frequencies, namely

$$E(x,t) = A \sum_{n=-\infty}^{+\infty} sin(kx - n\omega t) \tag{2.9}$$

Importantly this can be re-expressed in the form

$$E(x,t) = Asin(kx) \sum_{n=-\infty}^{+\infty} \delta(t - nT) \tag{2.10}$$

where $T = \frac{2\pi}{\omega}$.

The corresponding Hamiltonian takes the form

$$H = \frac{p^2}{2} + \frac{\omega_0^2 x^2}{2} + Acos(kx) \sum_{n=-\infty}^{+\infty} \delta(t - nT) \tag{2.11}$$

This Hamiltonian describes the motion of a charged particle in a homogeneous and static magnetic field , perturbed by an electrostatic wave packet propagating perpendicularly to the magnetic field.

The equations of motion of the particle between two actions of the δ-functions at time $t = nT^-$ and $t = (n+1)T^-$ (where the minus sign denotes just before this time instant) are linear and hence admit a full analytic solution. The action of the perturbation is to impose an impulse at time t=nT that changes the momentum of the particle by a known factor that depends on the position of the particle at the time it experience the impulse. Hence, the motion of the particle described by this Hamiltonian can be described by a difference equation relating the momentum and the position of the particle before and after the nth kick by the delta function that is at time $t = nT^-$ and $t = (n+1)T^-$ respectively. The corresponding mapping is exact and is [ZZS86]

$$u_{n+1} = (u_n + K\sin v_n)\cos\alpha + v_n\sin\alpha \tag{2.12}$$

$$v_{n+1} = -(u_n + K\sin v_n)\sin\alpha + v_n\cos\alpha \tag{2.13}$$

where $\alpha = 2\pi/q$, $v_n = v(t = nT^-)$, $u_n = u(n = nT^-)$ and $K = \frac{AkT^2}{q}$. For brevity we are going to call this map, the web map M_{ws}.

In the case of exact resonance where q a integer, this map has some remarkable properties (the case of resonance means that during one period of the harmonic oscillator exactly q delta pulses act on it). It is the generator of a tiling of the whole phase plane with a stochastic web which has uniform thickness. It also has some interesting symmetry properties. For certain resonances the stochastic web exhibits a novel kind of symmetry, the so called quasicrystal symmetry. This is the symmetry observed recently in some materials like Mn-Al for example that are crystals with five-fold or seven-fold rotational and translational quasisymmetry [SHGC'84].

Along the stochastic layers of the web the particle motion resembles a random walk and at least according to Zaslavskii et al [ZZS86] particles can diffuse through this stochastic network to high kinetic energies, while the motion of the particles inside the tiles is regular. The properties of the web have been studied both numerically and analytically. Here its most important properties are reviewed briefly.

The Hamiltonian of the system consists of two parts. The first part is a linear oscillator. This part of the Hamiltonian has a degenerate rotational symmetry.

The second part of the Hamiltonian describes the interaction of particles with the wave packet. This part of the Hamiltonian has a translational symmetry (symmetry with respect to translation $x \to x + \frac{2\pi}{k}$). These two symmetries compete. Normally the interaction of the two symmetries should lead to a destruction of both. However when the linear oscillator is in resonance with the perturbation it is possible that the degenerate rotational symmetry breaks into a rotational symmetry with respect to angles of rotation $\alpha = \frac{2\pi}{q}$. The coexistence of rotational symmetry and translational symmetry is only possible if q=1,2,3,4,6. The cases where q=1,2 are trivial, q=1 corresponding to the so called cyclotron resonance and q=2 corresponding to the half-integer cyclotron resonance and lead to uniform acceleration without diffusion as readily seen from the map. The cases q=3,4,6 correspond to the formation of a stochastic web exhibiting the well known crystal symmetries. In the case of q=4 the stochastic web is a square mesh. In the case of q=3,6 the stochastic web has a kagome structure [ZSU89] and consists of hexagonal and triangular cells. In the case where q=5,7,8... the coexistence of rotational and translational symmetries is no longer possible. In this case exact symmetry gives place to quasisymmetry (at least for small values of K) and the stochastic web exhibits quasicrystal symmetry. For example the case q=5 corresponds to a five-fold quasisymmetry, q=7 corresponds to a seven fold quasisymmetry. In figure 2.3 some pictures of the stochastic web for various symmetries are shown.

Quasicrystal symmetries are much more complicated than ordinary symmetries. One way of studying their properties is by using the mapping M_q and is the one to be used in the following. Alternative ways have been used in the past such as Penrose partitions or the Landau theory [ZSU89].

In the following we sketch briefly how the above results concerning the structure of a stochastic web can be obtained quantitatively :

By writing the map in the form

$$M_\alpha = R_\alpha(1 + KS) \tag{2.14}$$

[ZZS86] where R_α is the rotation operator with respect to an angle α and $S\phi = (sinv, 0)^T$ where $\phi = (v, u)^T$, one can show that for the exact resonance

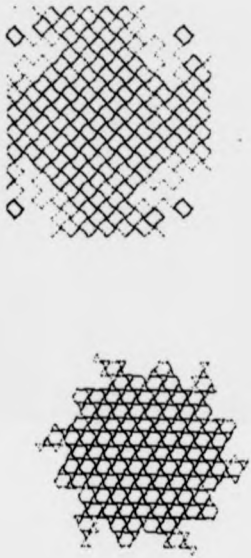

Figure 2.3. Phase plane of the web map for various symmetries after [ZSU89].

condition $\alpha = \frac{2\pi}{q}$, if the point ϕ in the phase space is a fixed point of M_α, then the points $R_{\alpha}\phi, R^2_{\alpha}\phi, \ldots, R^{q-1}_{\alpha}\phi$ are also fixed points of the mapping M_α. This result is true to an accuracy of $O(K^2)$. This is not the case when we do not have an exact resonance. Intuitively we can understand that the structure of the web may be approximated for small values of K by the separatrix network created in the unperturbed system. It is then easy to see that because the unstable fixed points of the mapping M_α have rotational symmetry, with angle of rotation $\alpha = \frac{2\pi}{q}$, the separatrix network created by the system, and in turn the stochastic web, must possess the same symmetry

By taking appropriate canonical transformations similar to those used in the case of the spider web ([CSZ88], [ZSU89]) we can write the Hamiltonian (2.11) in the form

$$H = H_q + V_q \tag{2.15}$$

where

$$H_q = -\frac{K}{q}\sum_{j=1}^{q} cos\xi_j \tag{2.16}$$

with

$$\xi_j = xcos(\frac{2\pi j}{q}) + ysin(\frac{2\pi j}{q}) \tag{2.17}$$

and

$$V_q = -\frac{2K}{q}\sum_{m=-\infty}^{\infty}\sum_{j=1}^{q} cos\xi_j cos(\frac{2\pi m(r-j)}{q}) \tag{2.18}$$

Geometrically $\xi_j = R\epsilon_j$ where R is a state vector in phase space and ϵ_j is a unit vector which defines a vertex of a regular polygon. H_q plays the role of the hamiltonian of the averaged motion of the particle over the Larmour period and is an integrable hamiltonian. It forms a separatrix net in the phase plane that gives the basic structure of the stochastic web. For example in the case q=4, H_4 gives a separatrix network that has square symmetry. In the case q=3,6, $H_3 = H_6$ gives a triangular and hexagonal separatrix network. The separatrix network for q=5,7,8... gives more complicated structures.

The role of the perturbation V_q is to disrupt the separatrix network and form narrow stochastic layers along the separatrices. The instability of motion near the separatrix network of the unperturbed system that is caused by

the perturbation leads to the occurence of the stochastic layer. This may be illustrated in the following way, for the particular case of four-fold symmetry The full equations of motion are linearised about the separatrix solution corresponding to the Hamiltonian H_4. As a result in the long time limit a Mathieu equation is obtained for the deviation from the unperturbed separatrix motion whose solution is found to be unstable for the parameter values appropriate to the problem (details are given in Appendix 2.1).

Zaslavskii et al [ZZS86] made an estimate of the width of the stochastic layer keeping only two terms in the perturbation. According to their estimate the width of the stochastic layer is proportional to $exp(-\frac{\text{constant}}{K})$ where the constant is independent of the position in phase plane. The stochastic web then has a uniform width over all the phase plane. The thickness of the web increases as K is increased and for $K > 1$ the width of the channels of the web becomes comparable to the size of the cells of the web.

An important set of properties of the hamiltonian H_q is related to the singular points of the hamiltonian. In the case where q=3,4,6 i.e when the web has a crystal symmetry, the hyperbolic singular points of the hamiltonian are located on surfaces of constant energy E. Thus if we plot the distribution p(E) of the hyperbolic singular points of H_q versus E (p(E) is the averaged number of hyperbolic singular points with energy E over a part of phase space) we can see that this distribution exhibits some delta function peaks for some values of E. This fact is responcible for the existence of a connected separatrix network for the unperturbed problem in the case of the full crystal symmetry. In the case of quasicrystal symmetry the set of hyperbolic points of the hamiltonian H_q is no longer located on a constant energy surface but they are distributed over a large energy range [CSU87]. As a consequence the hyperbolic singular points density as a function of the energy is blurred with certain maxima at certain energy values. This indicates an element of disorder associated with quasicrystal symmetry. Similar results hold for the elliptic singular points.

There are also some important properties of H_q associated with the Van Hove singularities in the density of states p(E). These are singularities associ-

ated with the singular points of H_q. In the case of crystal symmetries there exist sharp singularities in the density of states. These sharp singularities are associated with the delta functions in the distribution of the singular points. In the case of the quasicrystal symmetries such singularities are considerably smoothed. The position of these smoothed features corresponds exactly to the position of the maxima for the distribution of the singular points of H_q. The smoothing of the singularities in the case of quasicrystal symmetry is a distinctive property of this kind of symmetry and is an indication of a more disordered structure than a normal crystal symmetry [CSU87]. Results for the density of states for q=3,4,6 can be obtained analytically whereas for q=5,7,8,... the calculation is possible only numerically [ZSU89].

2.4 Study of Diffusion in the web map.

As was mentioned in the previous section for a large range of values of the perturbation parameter K a connected web of stochastic layers of a certain symmetry exists in phase space through which transport of orbits to remote parts of phase space is possible. For sufficiently large K the mapping becomes chaotic over most of the phase plane and motion on the phase plane is describable by a diffusion process. In this section the method of Karney,Rechester and White (KRW) [KRW82], already described in detail in the introduction of the thesis, is used to obtain the analytical form for this diffusion constant [YR91] as a function of K for q=3,4,6 where the crystal symmetry can be invoked,a necessary condition for the application of the KRW method. According to this method the diffusion constant D can be expressed in terms of the correlation functions such that:

$$D = lim_{n\to\infty} \frac{< n^2 >}{n} = C_0 + 2\sum_{m=1}^{\infty} C_m \tag{2.19}$$

where

$$C_m = \frac{1}{(2\pi)^2}\int_0^{2\pi}\int_0^{2\pi} a_m a_0 dv_0 du_0 \tag{2.20}$$

and

$$a_m = v_{m+1} - v_m \tag{2.21}$$

and the integration is over all initial values u_0 and v_0. The infinite series converges provided the correlation functions C_m decay rapidly enough (exponentially),an assumption which is valid for large enough values of the stochasticity parameter K.The quantities a_m are given as functions of u_0 and v_0 by successive iterations of the map.This method of calculation of the diffusion coefficient can be only used for maps which are doubly periodic,period 2π so that the averaging used,namely over u_0 and v_0, of the correlation functions is valid. Thus in order to use this approach for the present problem it is first necessary to eliminate the highly correlated rotation of the particles around the tiles that constitute the phase plane. This is done by removing the twist out of the map which is accomplished by iterating the map q times.This new map is then used for the calculation of the diffusion coefficient.

We present below the calculation of the diffusion coefficient for each of the cases of the hexagonal symmetry (q=3) and the square symmetry (q=4).

2.4.1 Hexagonal symmetry (q=3)

Iterating the map 3 times to remove the twist we obtain exactly

$$u_{n+3} = u_n + K sin v_n - \frac{K}{2}(sin A_n + sin B_n) \tag{2.22}$$

$$v_{n+3} = v_n + K sin v_n (sin A_n - sin B_n) \tag{2.23}$$

where:

$$A_n = -u_n sin\omega - K sin\omega sin v_n + v_n cos\omega \tag{2.24}$$

$$B_n = u_n sin\omega + v_n cos\omega + K sin\omega sin v_n - K sin\omega sin A_n \tag{2.25}$$

In terms of v and A this map reduces to

$$v_{n+1} = v_n + K sin A_n + K sin(v_n + A_n + K sin A_n) \tag{2.26}$$

$$A_{n+1} = A_n - K sin(v_n + A_n + K sin A_n) - K sin v_{n+1} \tag{2.27}$$

where $K'=K\sin\alpha$ and n+3 is replaced by n+1.This map is doubly periodic in $[0,2\pi]\times[0,2\pi]$

The method of KRW [KRW82] may now be applied directly to the above map and we find to first order

$$D = (C_0 + 2C_1)\frac{1}{3} \tag{2.28}$$

(The 1/3 factor is the appropriate scaling factor to allow for the fact that the web map is iterated three times for each iterate of (2.26) and (2.27)) where:

$$C_0 = K^4 \tag{2.29}$$

$$\begin{aligned} C_1 = \quad & \frac{K^4}{2} J_{-1}(K) + K^2 J_0^2(K) - K^4 J_2^2(K) + \\ & \frac{K^2}{2} \sum_n J_n(K) J_{1-n}((1+n)K) J_n(K) - \\ & \frac{K^2}{2} \sum_n J_n(K) J_{-1-n}((n+1)K) J_{2+n}(-K) \end{aligned} \tag{2.30}$$

Neglecting terms of $O(K^{-2})$ we finally obtain (Note $J_n(K) \sim K^{-\frac{1}{2}}$) :

$$D = \frac{K^2}{4} - \frac{K^4}{4} J_1(K) + \frac{K^2}{2} J_0^2(K) - \frac{K^4}{4} J_1^2(K) - \frac{K^2}{2} J_2^2(K) \tag{2.31}$$

The value of $\frac{D}{K^2}$ as a function of K is shown as a continuous line in Fig.2.4 . Also shown are numerical values obtained by iterating the mapping for 10^5 times and taking an ensemble average over 10^4 different initial conditions.We observe that the analytical calculations give an oscillatory form of $\frac{D(K)}{K^2}$.The numerical results verify this oscillatory behaviour and particularly good agreement is found for the values of K near where the diffusion coefficient is a minimum.

2.4.2 Existence of accelerator modes and their effect on diffusion.

The discrepancy between the numerical and the analytical results can be attributed to the presence of accelerator modes (see for example [LL83]). For this particular map these exist for $K=2l\pi$ (l integer) at the lattice points $(\frac{\pi}{3},\frac{\pi}{3}),(\frac{2\pi}{3},\frac{2\pi}{3})$,$(\frac{\pi}{2},\frac{3\pi}{2}),(\frac{3\pi}{2},\frac{\pi}{2})$ etc (n is any integer). Trajectories which pass

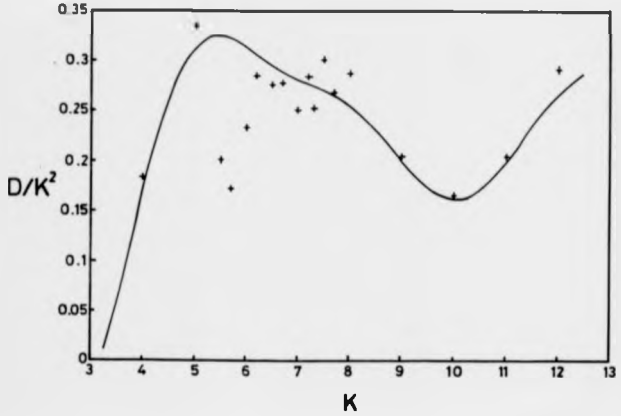

Figure 2.4. The diffusion coefficient divided by K^2 as a function of the parameter K for the case of hexagonal symmetry.

close to these points, experience an acceleration for a number of iterates.This gives rise to an enhancement in the effective diffusion hence the maxima as calculated analytically.Since the particle is undergoing an acceleration its motion is highly correlated.This gives rise to the discrepances between the analytic and numerical results as the present method for the calculation of the diffusion coefficient depends on the sufficiently rapid decay of the correlation functions. Furthermore as particles move in and out of the acceleration region in phase space they give rise to oscillations in the value of D as a function of time (or the number of iterates).This behaviour has been observed in the numerics.Importantly these oscillations in D are responsible for the scatter of the numerical results for D around the simple curve obtained from the analytical results ,apparent in figure 2.4 for K values about $2l\pi$.

When $K=(2l+1)\pi$, l=integer the accelerator modes that existed for $K=2l\pi$ are replaced by period-2 fixed points.Therefore we expect a decrease in the diffusion coefficient near this value of K and indeed this is what we observe. Furthermore the agreement between the numerical and the analytical results for these values of K is surprisingly good.This is expected since near these values of K ,most of the information on the dynamics is contained in two iterations of the map whereas the analytic value of D obtained here was found by taking into account exactly the first two correlation functions, that is essentially taking into account the randomisation of v only after two iterations.Thus the analytical method used in calculating the diffusion coefficient for these particular values of K is perfectly adequate to capture the dynamical behaviour of the system.

2.4.3 Square symmetry (q=4)

In the case of the four fold symmetry we proceed in an analogous way. We remove the twist from the map by iterating four times and change from n+4 to n+1 to obtain the doubly periodic map:

$$u_{n+1} = u_n + K sin v_n + K sin(v_n - K sin(u_n + K sin v_n)) \qquad (2.32)$$

$$v_{n+1} = v_n - K sin(u_n + K sin v_n) - K sin(u'_n \qquad (2.33)$$

where:

$$C'_n = u_n + K\sin v_n + K\sin(v_n - K\sin(u_n + K\sin v_n)) \qquad (2.34)$$

There is no need to perform a change of variables in this map as we did in the case q=3 since it is already doubly periodic in $[0,2\pi]\times[0,2\pi]$ in the original variables u and v.

The diffusion constant is still of the form of (2.28) (only that the scaling factor of 3 must now be replaced by a scaling factor of 4 allowing for the fact that four iterates of the original map correspond to one iterate of the map (2.32),(2.33)) with

$$C'_0 = K^2 + K^2 J_0(K) \qquad (2.35)$$

and

$$\begin{aligned} C'_1 = \; & \frac{K^4}{2} J_0(K) + K^2 \sum_n J_n(K) J_{-n}(K) J_0(nK) - K^2 \sum_n J_0^2(K) J_2(nK) + \\ & \frac{K^2}{2} \sum_n \sum_m \sum_l J_n(K) J_m(nK) J_l((1-m)K) J_{-m}((n+l)K) J_{n+l}(-K) - \\ & \frac{K^2}{2} \sum_n \sum_m \sum_l J_n(K) J_m(nK) J_l((1-m)K) \times \\ & J_{2-m}((n+l)K) J_{n+l}(K) \end{aligned} \qquad (2.36)$$

Neglecting terms of order $O(K^{-3})$ we finally obtain:

$$D = \frac{K^2}{4} + \frac{K^4}{2} J_0(K) + \frac{K^2}{2} J_0^2(K) \qquad (2.37)$$

This same analytical expression for D has been obtained using a different method by Afanasiev et al [ACSZ90].

The analytic and numerically obtained values of D as function of K are shown in Fig.2.5 . By analogy with the discussion of the q=3 case we associate the general behaviour of D with K as due to the presence of accelerator modes and periodic orbits.

Furthermore one can observe that the agreement between the numerical and analytical results in the case of the square symmetry is much better than in the case of the hexagonal symmetry. This may be due to the fact that in the case of hexagonal symmetry the fixed points and separatrix net have a much more complicated structure than for the square symmetry.

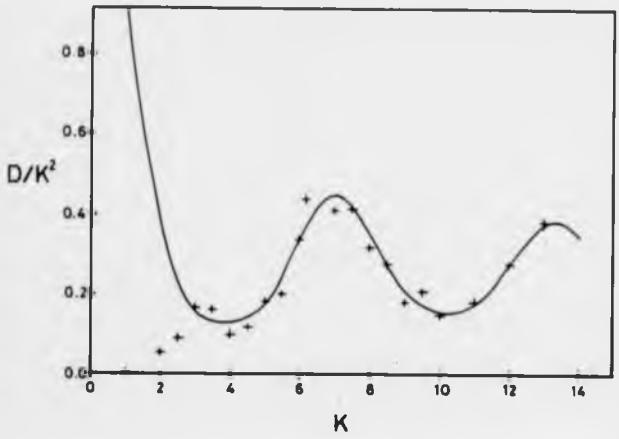

Figure 2.5. The diffusion coefficient divided by K^2 as a function of the parameter K for the case of the square symmetry.

2.4.4 Six-fold symmetry (q=6)

For this case the analytic form for the diffusion constant is :

$$D = \frac{K^4}{4} + \frac{K^4}{4} J_3(K) + \frac{K^4}{2} J_0^2(K) - \frac{K^4}{4} J_1^2(K) - \frac{K^4}{2} J_3^2(K) \qquad (2.38)$$

The variation of D/K^4 with K shows the characteristic oscillatory behaviour as found in the cases of q=3 or 4.

2.4.5 Two-fold symmetry (q=2)

In the case where q=2 the map is an accelerator mode (over the whole phase space) and a diffusion approximation to the motion is no longer applicable. The map in that case can be readily solved every two iterates to give $u_n = u_0 + nv_0$ and $v_n = v_0$ where n is an even integer. This is readily seen since the series defining D for the u variable diverges for all K.

2.4.6 Quasicrystal symmetries

The case of the quasicrystal symmetries of the web (q=5,7,8...) presents fundamental difficulties since it is not possible to manipulate the map into a doubly periodic form where KWH method is applicable. New numerical methods have to be developed since ensemble averaging over initial conditions must now include the whole of phase space and can no longer be reduced by invoking periodicity to averaging over the region $[0,2\pi]\times[0,2\pi]$.

Such problems, in a more general context, will be considered in Chapters 3 and 4.

2.5 Conclusions

In this chapter a short introduction to the properties of the web map has been given. The web map was chosen as a subject of study because it is a map which presents many interesting dynamical properties which are inherent in linear dynamical systems which are resonantly driven or dynamical systems which can be closely approximated by such a model. The diffusion coefficients for the

web map in the case of the crystal symmetries have been obtained analytically and shown to compare well with numerical results. The symmetry of the web is found to play a significant role in the value of the diffusion constant describing the motion of particles through phase space.

Chapter 3

Diffusion Coefficients For Higher Dimensional Symplectic Maps on the Cylinder.

3.1 Introduction.

One of the important methods for the calculation of the diffusion coefficient of area preserving maps is the correlation function method [KRW82]. The correlation function method has been used successfully for the calculation of the diffusion coefficient of chaotic maps which were doubly periodic i.e for maps of the torus. For such maps the correlation functions which are ensemble averages over the whole phase space can be written as an ensemble average over the unit torus thus ensuring the convergence of the integrals defining them. Maps of this form are the standard map or the web map for which the correlation function method has been used successfully for the calculation of the diffusion coefficient (see for example [KRW82], Chapter 2 and [YR91]).

The study of diffusion in higher dimensional symplectic maps is a relatively new subject. However the correlation function method has been used in higher

dimensional maps of the generalised torus $S^d \times S^d$ [KM90] such as the generalised Froeschle map [F72] to yield values for the diffusion tensor.

Symplectic maps on the unit torus, that is doubly periodic symplectic maps are just particular cases of symplectic maps which arise in physical problems. In general a symplectic map arising from a physical situation such as a wave particle interaction or a plasma confinement problem will not be periodic in the action variables. A doubly periodic map is usually the result of a local approximation to the full map which is a map of the generalised cylinder. For such maps the correlation function method as formulated by Karney et al [KRW82] can no longer be used. The double periodicity of the map is broken and the ensemble averages over the whole phase space which is supposedly chaotic can no longer be reduced to ensemble averages over the unit torus. The latter averages being convergent are relatively easy to calculate.

In this chapter the correlation function method is extended to the calculation of the diffusion tensor for symplectic maps on the generalised cylinder. In the next section the method as applied to symplectic maps of arbitrary dimension on the cylinder is introduced. In sections 3.3 and 3.4 this method is applied to symplectic maps of two (d=1) and higher dimensions respectively to obtain analytic forms for the approximate diffusion coefficients and in particular their variation with parameters that define the symplectic maps. These estimates are compared, in section 3.5, with values obtained numerically.

3.2 Extension of the Correlation Function Method to Maps on the Cylinder.

Assume a symplectic map of the form:

$$\mathbf{p}_{n+1} = \mathbf{F}(\mathbf{p}_n, \boldsymbol{\theta}_n, \mathbf{K}) \tag{3.1}$$

$$\boldsymbol{\theta}_{n+1} = \mathbf{G}(\mathbf{p}_n, \boldsymbol{\theta}_n, \mathbf{K}) \tag{3.2}$$

where $(\mathbf{p}_n, \boldsymbol{\theta}_n) \in R^d \times S^d$, which implies that the map is periodic in the angle variables $\boldsymbol{\theta}$, and $\mathbf{K}$ is a set of parameters. For a range of values of $\mathbf{K}$, it is

assumed that the map becomes chaotic. Furthermore the chaotic regions cover a substantial part of the phase space whilst KAM surfaces are well separated and islands of coherent motion are not large. The simple standard map with

$$F(p,\theta) = p + K\sin\theta \tag{3.3}$$

and

$$G(p,\theta) = \theta + F(p,\theta) \tag{3.4}$$

satisfies these conditions for $K > 6$.

For such cases a statistical description of the motion is more appropriate. The dynamics is often approximated by a diffusion process and described by a Fokker-Planck equation of the form (see Chapter 1)

$$\frac{\partial P(\mathbf{p},t)}{\partial t} = \frac{\partial}{\partial \mathbf{p}} D(\mathbf{K}) \frac{\partial P(\mathbf{p},t)}{\partial \mathbf{p}} \tag{3.5}$$

where P is a probability distribution in the momenta in phase space. Such a description is complete once the diffusion coefficient or the diffusion tensor $D(\mathbf{K})$ is known. The diffusion tensor is defined to be the asymptotic rate of spread of the second moment of the momentum distribution:

$$D = lim_{n\to\infty} \frac{< \mathbf{\Delta p_n} \mathbf{\Delta p_n} >_R}{2n} \tag{3.6}$$

where $\mathbf{\Delta p_n}$ is the momentum change after n iterations of the map. The possibility of the existence of a nonzero diffusion tensor for general maps is discussed in appendix 3.2. The averages are taken over a set of initial conditions set up on an area of phase space R which is invariant under the dynamics of the map. D is taken to be independent of this initial set. If R is taken to be a connected ergodic region of phase space, that is a region of phase space where time averages and space averages exist and are equal, the diffusion tensor can easily be rewritten in terms of the momentum autocorrelation functions following Karney et al [KRW82], Kook and Meiss [KM90]

$$D = \frac{C_0}{2} + \sum_{r=1}^{\infty} C_r \tag{3.7}$$

where

$$C_r = < (\mathbf{p_1} - \mathbf{p_0})(\mathbf{p_{r+1}} - \mathbf{p_r}) >_R \tag{3.8}$$

This method was used by Kook and Meiss [KM90] for maps of the higher dimensional torus $S^d \times S^d$, where the averages on R were reduced, due to periodicity in both the angle and the momentum variables to averages on the unit (2d dimensional) torus. Thus convergence of the integrals defining the ensemble averages is ensured.

The maps we are interested in can not be written as maps of the torus since they are not doubly periodic (that is periodic in both the momentum and the angle variables as for example the standard map in the case where d=1 or the Froeschlé map in the case where d=2). To study the behaviour of the diffusion tensor for such maps the correlation function method has to be extended to maps which are only singly periodic.

The invariant connected ergodic region R is taken to be the whole cylinder $R^d \times S^d$. This approximation is true for maps where the chaotic dynamics extend over the whole of phase space. Then to ensure convergence we define the averaging over phase space in the following manner:

$$< A(\mathbf{p}, \boldsymbol{\theta}) >_R = \lim_{r \to \infty} \frac{\int_0 \int_0^{2\pi} \mathbf{A}(\mathbf{p}, \boldsymbol{\theta}) \mathbf{dp} \mathbf{d}\boldsymbol{\theta}}{(2\pi r)^d} \tag{3.9}$$

If the map is periodic with period T in the Rth direction one can break the interval from 0 to ϵ into units of width T. Then because of the periodicity one can write

$$\frac{1}{\epsilon} \int_0^{\epsilon} A(p_R) dp = lim_{m \to \infty} \frac{1}{mT} (m \int_0^T A(p_R) dp_R) = \frac{1}{T} \int_0^T A(p_R) dp_R \tag{3.10}$$

(where the explicit dependence of the observable function on the other coordinates has been suppressed) , giving the usual definition of the phase space average used by Karney et al [KRW82].

To illustrate this generalisation we first consider the case of one dimensional cylinder maps.

3.3 One Dimensional Cylinder Maps.

Assume a symplectic map of the cylinder of the form:

$$p_{n+1} = p_n + f(p_n, \theta_n) \tag{3.11}$$

$$\theta_{n+1} = \theta_n + g(p_n, \theta_n) \tag{3.12}$$

(For this map to be symplectic one must have $f_p + g_\theta + f_p g_\theta - g_p f_\theta = 0$,where the subscript denotes partial derivative with respect to that variable.) The functions f and g are assumed to be periodic in the angle variable θ. We assume that the motion is chaotic over the whole phase space.

It is convenient to introduce the following Fourier decompositions:

$$f(p,\theta) = \sum_m \int_{-\infty}^{+\infty} a_m(k) exp(im\theta + ikp) dk \tag{3.13}$$

$$exp(\epsilon f(p,\theta)) = \sum_m \int_{-\infty}^{+\infty} a_m(k,\epsilon) \exp(im\theta + ikp) dk \tag{3.14}$$

$$exp(\epsilon g(p,\theta)) = \sum_m \int_{-\infty}^{+\infty} b_m(k,\epsilon) \exp(im\theta + ikp) dk \tag{3.15}$$

The quasilinear approximation to the diffusion coefficient of maps is given by C_0, and we may write

$$C_0 = < (p_1 - p_0)^2 >_H = < f^2(p_0, \theta_0) >_H \tag{3.16}$$

where R is the whole cylinder R×S. Introducing the Fourier decompositions we have

$$C_0 = < \sum_{m,n} \int_{-\infty}^{+\infty} a_m(k) a_n(k') exp(i(m+n)\theta) exp(i(k+k')p) dk dk' >_H \tag{3.17}$$

$$= lim_{\epsilon \to 0} \frac{1}{\epsilon} \int_0^\epsilon \sum_m \int_{-\infty}^{+\infty} a_m(k) a_{-m}(k') exp(i(k+k')p) dk dk' dp \tag{3.18}$$

For C_0 to be non-zero it is necessary that the integral

$$\sum_m \int_0^\epsilon \int_{-\infty}^{+\infty} a_m(k) a_{-m}(k') exp(i(k+k')p dk dk' dp = O(\epsilon) \tag{3.19}$$

which implies that

$$\sum_m \int_{-\infty}^{+\infty} a_m(k) a_{-m}(k') exp(i(k+k')p) dk dk' \tag{3.20}$$

is independent of p or equivalently that the Fourier amplitudes $a_m(k)$ are of singular nature such that

$$\sum_m a_m(k) a_{-m}(k') \propto \delta(k+k') \tag{3.21}$$

The solution to this functional equation is $a_m(k) = a_m \delta(k)$ in which case the quasilinear diffusion coefficient is

$$D_{ql} = \frac{1}{2} C_0 = \frac{1}{2} \sum_m a_m a_{-m} \tag{3.22}$$

A simple example of such a map is the well studied standard map.

To consider corrections to the quasilinear result it is nessecary to look at the higher correlation functions: The rth correlation function is defined by:

$$C_r = < f(p_r, \theta_r) f(p_0, \theta_0) >_H \tag{3.23}$$

Using the Fourier decompositions for f we have:

$$f(p_r, \theta_r) = \sum_{m_0} \int_{-\infty}^{+\infty} a_{m_0}(k_0) exp(i m_0 \theta_r + i k_0 p_r) dk_0 \tag{3.24}$$

and then using the map

$$\begin{aligned} f(p_r, \theta_r) = \textstyle\sum_{m_0} \int_{-\infty}^{+\infty} a_{m_0}(k_0) exp(i m_0 [\theta_{r-1} + g(p_{r-1}, \theta_{r-1})]) \\ exp(i k_0 [p_{r-1} + f(p_{r-1}, \theta_{r-1})]) dk_0 = \end{aligned} \tag{3.25}$$

$$\begin{aligned} \textstyle\sum_{m_0, n_1, n_1} \int_{-\infty}^{+\infty} a_{m_0}(k_0) b_{n_1}(k_1, m_0) a_{n_1}(k_1, k_0) exp(i(m_0 + n_1 + n_1)\theta_{r-1}) \times \\ exp(i(k_0 + k_1 + k_1) p_{r-1}) dk_0 dk_1 dk_1 \end{aligned} \tag{3.26}$$

Iterating this relation r times we find that

$$\begin{aligned} f(p_r, \theta_r) = & \sum_{m_0, n_1, n_1, \ldots, n_r, n_r} \int_{-\infty}^{+\infty} a_{m_0}(k_0) b_{n_1}(k_1, m_0) \\ & a_{n_1}(k_1, k_0) \ldots b_{n_r}(k_r, m_0 + \sum_{s=1}^{r-1} (n_s + n_s)) a_{n_r}(k_r, k_0 + \sum_{s=1}^{r-1} (k_s + k_s)) \\ & exp(i(m_0 + \sum_{s=1}^{r-1} (n_s + n_s))\theta_0) \\ & exp(i(k_0 + \sum_{s=1}^{r-1} (k_s + k_s)) p_0) dk_0 dk_1 dk_1 \ldots dk_r dk_r \end{aligned} \tag{3.27}$$

The general correlation function C_r is then of the form

$$\begin{aligned} C_r = \quad & lim_{\tau \to \infty} \frac{1}{\tau} \int_0^{\tau} \sum_{n_0, m_0, n_1, n_1, \ldots, n_r, n_r} \int_{-\infty}^{+\infty} a_{m_0}(k) a_{m_0}(k_0) b_{n_1}(k_1, m_0) \\ & a_{n_1}(k_1, k_0) \ldots b_{n_r}(k_r, m_0 + \sum_{s=1}^{r-1} (n_s + n_s)) a_{n_r}(k_r, k_0 + \sum_{s=1}^{r-1} (k_s + k_s)) \\ & exp(i(k + k_0 + \sum_{s=1}^{r-1} (k_s + k_s)) p_0) dk dk_0 dk_1 dk_1 \ldots dk_r dk_r dp_0 \end{aligned} \tag{3.28}$$

The sum is taken over all the integers satisfying the relation

$$n_0 + m_0 + \sum_{s=1}^{r}(n_s + n_s) = 0 \tag{3.29}$$

The only case where C_r is nonvanishing is when the integral over all the k's is independent of p_0 that is when

$$\sum_{n_0,m_0,n_1,\ldots,n_r,s_r} a_{n_0}(k)a_{m_0}(k_0)b_{n_1}(k_1, m_0)$$
$$a_{n_1}(k_1, k_0)\ldots b_{n_r}(k_r, m_0 + \sum_{s=1}^{r-1}(n_s + n_s))$$
$$a_{n_r}(k_r, k_0 + \sum_{s=1}^{r-1}(k_s + k_s))$$
$$\propto \delta(k + k_0 + \sum_{s=1}^{r}(k_s + k_s)) \tag{3.30}$$

where the sum is again taken over all the integers satisfying the condition (3.29). An obvious solution to this functional equation is where the Fourier decompositions $a_m(k), a_m(k,k'), b_m(k,k')$ are themselves singular. In fact it is plausible that this is the only possible solution.

Importantly we may conclude that the only area preserving maps of the cylinder that show corrections to the quasilinear result for the diffusion coefficient are those maps for which the Fourier decompositions of $\exp(ik'f)$ and $\exp(ik'g)$ have a singular part in the reciprocal of p, that is k. Such maps are for example those that have f and g which are periodic in p or are linear in p, in which case they can be written as maps of the torus. This result extends the work of Hatori et al [HKI85] who, using a different method, studied a special form of area preserving maps of the cylinder namely the radial twist maps

$$p_{n+1} = p_n + kf(\theta_n) \tag{3.31}$$

$$\theta_{n+1} = \theta_n + a(p_{n+1}) \tag{3.32}$$

They found that the only map of this form that gives corrections to the quasilinear result is the standard map, that is the map where a is linear in p.

3.4 Higher Dimensional Symplectic Maps

In this section we use the method given in section 2 to study diffusion in higher dimensional symplectic maps but restricted to radial twist maps. We then have:

$$\mathbf{p}_{n+1} = \mathbf{p}_n + \mathbf{K}\mathbf{f}(\theta_n) \tag{3.33}$$

$$\theta_{n+1} = \theta_n + \mathbf{a}(\mathbf{p}_{n+1}) \tag{3.34}$$

where $(\mathbf{p}, \theta) \epsilon \mathbf{R}^d \times S^d$.

A simple example of such maps is the Froeschlé map [F72] which due to a special form of the coupling can be written as a map of the torus $S^d \times S^d$. This map is the following

$$p_{1,n+1} = p_{1,n} + a_1 sin(\theta_{1,n+1}) + bsin(\theta_{1,n+1} + \theta_{2,n+1}) \tag{3.35}$$

$$\theta_{1,n+1} = \theta_{1,n} + p_{1,n} \tag{3.36}$$

$$p_{2,n+1} = p_{2,n} + a_2 sin(\theta_{2,n+1}) + bsin(\theta_{1,n+1} + \theta_{2,n+1}) \tag{3.37}$$

$$\theta_{2,n+1} = \theta_{2,n} + p_{2,n} \tag{3.38}$$

Let us assume the following Fourier decompositions

$$f^i(\theta) = \sum_{\mathbf{m}} a^i_{\mathbf{m}} exp(i\mathbf{m}.\theta) \tag{3.39}$$

$$exp(i\sigma a^i(\mathbf{p})) = \int_{-\infty}^{+\infty} a^i(\mathbf{k}, \sigma) \exp(i\mathbf{k}.\mathbf{p}) d\mathbf{k} \tag{3.40}$$

where f^i and a^i are the ith components of the vector functions f and a respectively.

The quasilinear approximation to the diffusion tensor , namely C^{ij}_0 may then be written in the form:

$$C^{ij}_0 = K^2 < f^i(\theta_0) f^j(\theta_0) >_R \tag{3.41}$$

$$= K^2 < \sum_{\mathbf{m}\,\mathbf{n}} a^i_{\mathbf{m}} a^j_{\mathbf{n}} exp(i(\mathbf{m}+\mathbf{n}).\theta_0) >_R \tag{3.42}$$

$$= K^2 \sum_{\mathbf{m}} a^i_{\mathbf{m}} a^j_{-\mathbf{m}} \tag{3.43}$$

For radial twist maps of any dimension the quasilinear result is non zero.

Let us now look at the higher order correlation functions:

$$C^{n}_{\tau} = K^{2} < f^{*}(\theta_{\tau}) f^{n}(\theta_{0}) >_{R} \tag{3.44}$$

As before the region R on which the averaging is performed is assumed to be the whole cylinder.

Using the Fourier decompositions introduced above and defining $F(\mathbf{k}, \mathbf{m})$ by the following relation:

$$exp(i\mathbf{k}.\mathbf{f}(\theta)) = \sum_{\mathbf{m}} F(\mathbf{k}, \mathbf{m}) exp(i\mathbf{m}.\theta) \tag{3.45}$$

we find

$$f^{*}(\theta_{\tau}) = \sum_{\mathbf{m_0}} a^{*}_{\mathbf{m_0}} exp(i\mathbf{m_0}.\theta_{\tau}) \tag{3.46}$$

$$= \sum_{\mathbf{m_0}} a^{*}_{\mathbf{m_0}} exp(i\mathbf{m_0}.\theta_{-1}) \Pi^{d}_{s=1} exp(im^{s}_{0}.a^{s}(\mathbf{p}_{\tau})) \tag{3.47}$$

$$= \sum_{\mathbf{m_0}} \int_{-\infty}^{+\infty} a^{*}_{\mathbf{m_0}} exp(i\mathbf{m_0}.\theta_{-1}) \Pi^{d}_{s=1} a^{s}(\mathbf{k}^{s}, m^{s}_{0}) exp(i\mathbf{k}^{s}_{\mathbf{0}}.\mathbf{p}_{\tau}) d\mathbf{k}^{s}_{\mathbf{0}} \tag{3.48}$$

where $\mathbf{m_0} = (m^{1}_{0}, ..., m^{d}_{0})$. The above equation can be written as

$$\begin{aligned} f^{*}(\theta_{\tau}) = \textstyle\sum_{\mathbf{m_0}} \int_{-\infty}^{+\infty} a^{*}_{\mathbf{m_0}} exp(i\mathbf{m_0}.\theta_{-1}) \times \\ \Pi^{d}_{s=1} a^{s}(\mathbf{k}^{s}, m^{s}_{0}) exp(iK\mathbf{k}^{s}_{\mathbf{0}}.\mathbf{f}(\theta_{-1})) exp(i\mathbf{k}^{s}_{\mathbf{0}}.\mathbf{p}_{\tau-1}) d\mathbf{k}^{s}_{\mathbf{0}} \end{aligned} \tag{3.49}$$

$$\begin{aligned} = \textstyle\sum_{\mathbf{m_0}, \mathbf{m_1}} \int_{-\infty}^{+\infty} a^{*}_{\mathbf{m_0}} F(K(\sum_{s=1}^{d}(k^{s}_{0})), \mathbf{m}^{s}_{1}) exp(i(\mathbf{m_0} + \mathbf{m_1}).\theta_{\tau-1}) \times \\ exp(i(\textstyle\sum_{s=1}^{d} \mathbf{k}^{s}_{\mathbf{0}}).\mathbf{p}_{\tau-1}) \Pi^{d}_{s=1} a^{s}(\mathbf{k}^{s}_{\mathbf{0}}, m^{s}_{0}) d\mathbf{k}^{s}_{\mathbf{0}} \end{aligned} \tag{3.50}$$

Iterating this relation τ times we get:

$$\begin{aligned} f^{*}(\theta_{\tau}) = \sum_{\mathbf{m_0}, \mathbf{m_1}, ..., \mathbf{m}_{\tau}} \int_{-\infty}^{+\infty} a^{*}_{\mathbf{m_0}} F(K(\sum_{s=1}^{n} \mathbf{k}^{s}_{\mathbf{0}}), \mathbf{m}_{1}) ... F(K(\sum_{s=1}^{n} \sum_{l=0}^{\tau-1} \mathbf{k}^{s}_{\mathbf{l}}), \mathbf{m}_{\tau}) \\ \Pi^{d}_{s=1} a^{s}(\mathbf{k}^{s}_{\mathbf{0}}, m^{s}_{0}) ... \Pi^{d}_{s=1} a^{s}(\mathbf{k}^{s}_{\tau-1}, (\sum_{l=0}^{\tau-1} \mathbf{m}_{l})^{s}) \\ exp(i \sum_{l=0}^{\tau} \mathbf{m}_{l}.\theta_{0}) exp(i(\sum_{s=1}^{d} \sum_{l=0}^{\tau-1} \mathbf{k}^{s}_{\mathbf{l}}).\mathbf{p}_{0}) \Pi^{\tau-1}_{l=0} \Pi^{d}_{s=1} d\mathbf{k}^{s}_{\mathbf{l}} \end{aligned} \tag{3.51}$$

Then the τ th correlation function can be written in the form

$$C^{n}_{\tau} = \lim_{\epsilon \to 0} \epsilon^{-d} \int_{\Omega} \sum_{\mathbf{m_0}, \mathbf{m_1}, ..., \mathbf{m}_{\tau}, s} \int_{-\infty}^{+\infty} a^{*}_{\mathbf{m_0}} n^{s}_{0} F(K(\sum_{s=1}^{d} \mathbf{k}^{s}_{\mathbf{0}}), \mathbf{m}_{1})$$

$$\cdots \delta(K(\sum_{s=1}^{d}\sum_{l=0}^{\tau-1} \mathbf{k}_l^s), \mathbf{m}_\tau)\Pi_{s=1}^{d} a^s(\mathbf{k}_0^s, \mathbf{m}_0^s)\cdots$$

$$\Pi_{s=1}^{d} a^s(\mathbf{k}_{\tau-1}^s, \sum_{l=0}^{\tau-1} \mathbf{m}_l)^s) exp(i(\sum_{s=1}^{d}\sum_{l=0}^{\tau-1} \mathbf{k}_l) \cdot \mathbf{p}_0)$$

$$\Pi_{l=0}^{\tau-1}\Pi_{s=1}^{d} d\mathbf{k}_l^s d\mathbf{p}_0 \tag{3.52}$$

where the sum is taken over all the integer vectors satisfying the relation

$$\mathbf{n} + \mathbf{m}_0 + \mathbf{m}_1 + \ldots + \mathbf{m}_\tau = \mathbf{0} \tag{3.53}$$

The averaging over $\mathbf{p}_0$ would give a nonvanishing result only in the case where the a^i's are of a form such that:

$$\sum_{\mathbf{m}_0,\mathbf{m}_1,\ldots,\mathbf{m}_\tau,\mathbf{n}} a^i_{\mathbf{m}_0} a^i_{\mathbf{n}} \Pi_{s=1}^{d} a^s(\mathbf{k}_0^s, \mathbf{m}_0^s)\ldots\Pi_{s=1}^{d} a^s(\mathbf{k}_{\tau-1}^s, (\sum_{l=0}^{\tau-1} \mathbf{m}_l)^s)$$

$$\propto \delta(\sum_{s=1}^{d}\sum_{l=0}^{\tau-1} \mathbf{k}_l^s) \tag{3.54}$$

where the summation is again taken over all the integer vectors satisfying the relation (3.53).

That means that for a finite contribution to the correlation functions all the functions a^i have to be of a singular form that is of the form

$$a^i(\mathbf{k}_l, \mathbf{m}^l) \propto \delta(\mathbf{k}_l - \mathbf{m}^l) \tag{3.55}$$

where k_l is a scalar function of the components of the vector $\mathbf{k}_l$. If the a's are such that this condition does not hold then the quasilinear result for the diffusion coefficient will be valid for all values of K where the motion is chaotic over large regions of the whole phase space.

Let us now see what this condition means for the allowed form of the functions $\mathbf{a}(\mathbf{p})$. It essentially means that **all** the a^i's have to be **linear** or **periodic** functions of the momenta. Some examples will make this remark more clear.

Example1 First let us assume that the a's are linear functions of the momenta:

$$a^i(\mathbf{p}) = \sum_{s=1}^{d} c_s^i p_s \tag{3.56}$$

Then

$$exp(\imath\sigma a^i(\mathbf{p})) = \Pi_{s=1}^{d} \exp(\imath c_s^i p_i)$$

$$= (2\pi)^{-d}\Pi_{s=1}^{d} \int_{-\infty}^{+\infty} \delta(k_i - \sigma c_s^i) exp(i\mathbf{k}.\mathbf{p}) d\mathbf{k} \tag{3.57}$$

where k_i and p_i are the ith components of $\mathbf{k}$ and $\mathbf{p}$ respectively. Thus

$$a^l(\mathbf{k},\sigma) = \Pi_{i=1}^{d}\delta(\mathbf{k}_i - \sigma c_1^l) \tag{3.58}$$

and is of a singular nature, and if the force functions are chosen appropriately so that

$$\mathbf{k_1} + \mathbf{k_2} + ... + \mathbf{k_p} = \mathbf{0} \tag{3.59}$$

then for such a map there are finite corrections to the the quasilinear value for the diffusion tensor. Since all the force functions are linear there is a proper coordinate change so that the map can be written as a map on the torus and the averaging over the cylinder is then equivalent to averaging over the torus $S^d \times S^d$ which is properly defined and convergent. This is the case for the Froeschle map where corrections to the quasilinear result for the diffusion tensor, of an oscillatory form were found both numerically and analytically [KM90].

Example 2. Let us now suppose that there is a nonlinearity in one of the force functions $a^l(\mathbf{p})$. Take for example

$$a^l(\mathbf{p}) = p_1 + p_2^2 \tag{3.60}$$

Its Fourier decomposition would then be

$$a^l(\mathbf{k}^l,\sigma) = \int_{-\infty}^{+\infty} \exp(i\sigma(p_1+p_2^2))\exp(-ik_1^l p_1 - ik_2^l p_2)dp_1 dp_2 = \delta(k_1^l - \sigma)A(k_2^l,\sigma) \tag{3.61}$$

where k_j^l is the ith component of $\mathbf{k}^l$ and A is a non singular function of k_2^l. Fourier amplitudes of such form will not have a contribution $\mathbf{k_1} + ... + \mathbf{k_p} = \mathbf{0}$ and so the corrections to the quasilinear results for the diffusion coefficient will be zero.

As mentioned above the linear case is not the only one that gives corrections to the quasilinear result. A singular Fourier decomposition for $a^l(\mathbf{p})$ is obtained in the case where $a(\mathbf{p})$ is a periodic function of $\mathbf{p}$, or a sum of periodic and linear functions. This is clearly shown in the following examples.

Example 3. Suppose $a^l(\mathbf{p}) = a\sin(p_1 + p_2)$. Then

$$\begin{aligned} a^l(\mathbf{k}^l,\sigma) &= \int_{-\infty}^{+\infty} exp(ia\sigma sin(p_1+p_2))exp(-ik_1^l p_1 - ik_2^l p_2)dp_1 dp_2 \\ &= \sum_n J_n(a\sigma)\delta(k_1^l + n)\delta(k_2^l + n) \end{aligned} \tag{3.62}$$

The Fourier decomposition is then of a singular form so that corrections to the quasilinear result for the diffusion tensor of such a map are possible.

Example 4. Suppose $a^1(\mathbf{p}) = asinp_1 + p_2$.Then

$$\begin{aligned} a^1(\mathbf{k},\sigma) &= \int_{-\infty}^{\infty} exp(i\sigma(asinp_1 + p_2)exp(-ik_1p_1 - ik_2p_2)dp_1dp_2 \\ &= \sum_n J_n(a\sigma)\delta(k_1 - n)\delta(k_2 - n - \sigma) \end{aligned} \tag{3.63}$$

The Fourier decomposition is still of a singular form and corrections to the quasilinear results are again possible.

Example 5. Suppose $a^1(\mathbf{p}) = asinp_1 + p_2^2$. Then

$$\begin{aligned} a^1(\mathbf{k}^1,\sigma) &= \int_{-\infty}^{\infty} exp(i\sigma(asinp_1 + p_2^2)exp(-ik_1^1p_1 - ik_2^1p_2)dp_1dp_2 \\ &= \sum_n \int_{-\infty}^{\infty} J_n(a\sigma)exp(inp_1)exp(i\sigma p_2^2)exp(-ik_1^1p_1 - ik_2^1p_2)dp_1dp_2 \\ &= \sum_n J_n(a\sigma)\delta(k_1^1 - n)A(k_2^1,\sigma) \end{aligned} \tag{3.64}$$

where

$$A(k_2^1,\sigma) = \int_{-\infty}^{\infty} exp(ip_2^2\sigma)exp(ik_2^1p_2)dp_2 \tag{3.65}$$

is a non singular function of k_2^1.

Since the function $\mathbf{a(p)}$ does not have a singular Fourier decomposition in all the $\mathbf{k}^1$ coordinates there will be no corrections to the quasilinear result for the diffusion tensor. Thus it can be seen that a small nonlinearity in one of the force functions makes the diffusion tensor for the map equal to the quasilinear result.

3.5 Numerical Experiments.

To check the results obtained in the previous sections we have obtained numerically the diagonal terms of the diffusion tensor of a generalised Froeschle map which is a four dimensional symplectic map (d=2). The map is of the following form

$$p_{1,n+1} = p_{1,n} + \epsilon_1 sin\theta_{1,n} + \epsilon_2 sin(\theta_{1,n} + \theta_{2,n}) \tag{3.66}$$

$$\theta_{1,n+1} = \theta_{1,n} + a^{(1)}(p_{1,n+1}, p_{2,n+1}) \tag{3.67}$$

$$p_{2,n+1} = p_{2,n} + c_4 sin(\theta_{1,n} + \theta_{2,n}) \tag{3.68}$$

$$\theta_{2,n+1} = \theta_{2,n} + a^{(2)}(p_{1,n+1}, p_{2,n+1}) \tag{3.69}$$

If the a's are linear functions and specifically $a^{(1)}(p_{1,n+1}, p_{2,n+1}) = p_{1,n+1}$ and $a^{(2)}(p_{1,n+1}, p_{2,n+1}) = p_{2,n+1}$ the above map is just the Froeschle map studied numerically and analytically by Kook and Meiss [KM90]. The diffusion tensor is obtained numerically by direct iteration of $10^2 \times 10^2$ orbits of the map for time T=50 and using the definition given in section 3.2. The calculated quantity is the diagonal term of the diffusion tensor associated with the second degree of freedom, D_{22} This has been done for a number of functions $a^{(1)}, a^{(2)}$ among which is the linear case where the results of Kook and Meiss [KM90] are reproduced. Other choices were $a^{(1)}(p_1, p_2) = p_1 + \epsilon p_1^2$, $a^{(2)}(p_1, p_2) = p_2$ for various choices of the parameter ϵ, $a^{(1)}(p_1, p_2) = p_1 sin p_2$, $a^{(2)}(p_1, p_2) = p_2$, and $a^{(1)}(p_1, p_2) = p_1$, $a^{(2)}(p_1, p_2) = p_2 sin p_1$ and $a^{(1)}(p_1, p_2) = 0.1 p_1^2$, $a^{(2)}(p_1, p_2) = p_2$

The results are shown in figures 3.1,3.2,3.3 and 3.4 in the form of plots of the ratio of the numerically calculated diffusion coefficient to the theoretically calculated quasilinear value as a function of the parameter c_4. The results in figure 3.1 show that as the nonlinear parameter ϵ increases the diffusion coefficient rapidly approaches the quasilinear result. Figures 3.2,3.3 and 3.4 illustrate how for other nonlinear force functions corrections to the quasilinear value are negligible.

3.6 Conclusions.

The correlation function method for the calculation of the diffusion coefficient of chaotic maps has been extended so that it may be used for maps on the cylinder. Using this method we have shown that for a D-dimensional symplectic map there exist corrections to the quasilinear result only if **all** the force functions $\mathbf{a(p)}$or more generally $\mathbf{g(p,\theta)}$ have purely singular Fourier decompositions in the coordinates reciprocal to the $\mathbf{p}$ variables. By purely singular we mean that the coefficients $\mathbf{\hat{a}(k)}$ as defined by (3.14) are singular in every single coordinate

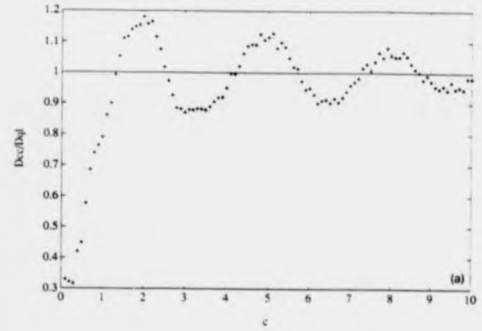
Dcc/Dsj
c
(a)

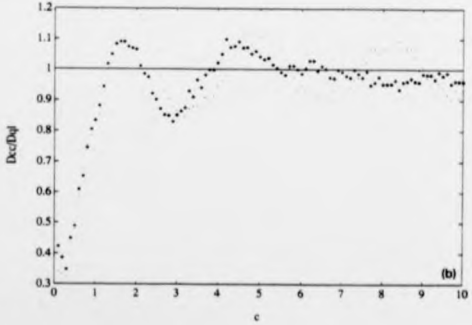
Dcc/Dsj
c
(b)

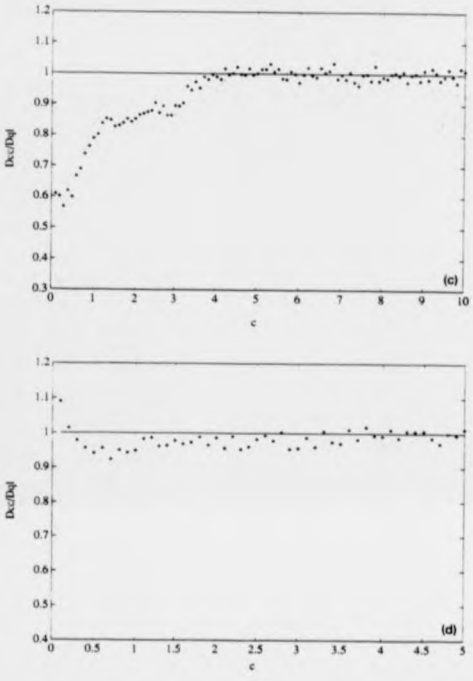

Figure 3.1. Plot of the ratio of the numerically calculated diffusion coefficient to the theoretically calculated quasilinear value for the generalised Froeschlé map with $a^{(1)}(p_1, p_2) = p_1 + \epsilon p_1^2$ and $a^{(2)} = p_2$ for various values of the parameter ϵ (a) $\epsilon = 0.0001$, (b) $\epsilon = 0.01$, (c) $\epsilon = 0.1$, (d) $\epsilon = 1$ (*) and for the generalised Froeschlé map with linear term $\epsilon = 0$.

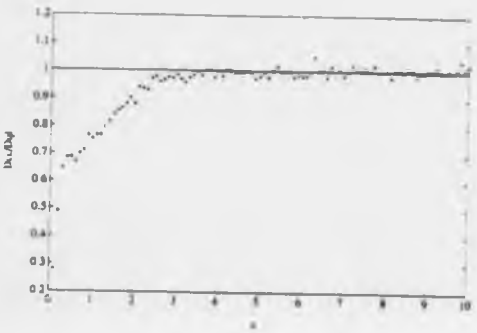

Figure 3.2. Plot of the ratio of the numerically calculated value for the diffusion coefficient to the theoretically calculated quasilinear value for the generalised Froeschlé map with $a^{(1)}(p_1, p_2) = p_1 \sin p_2$ and $a^{(2)}(p_1, p_2) = p_2$ (°) and for the generalised Froeschlé map with linear force functions (.).

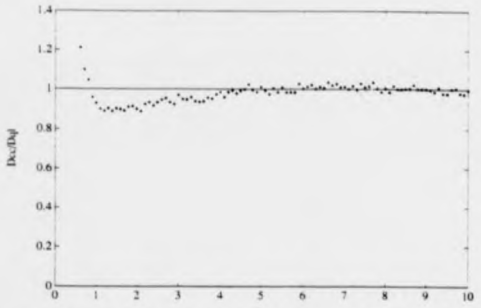

Figure 3.3. Plot of the ratio of the numerically calculated value for the diffusion coefficient to the theoretically calculated quasilinear value for the generalised Froeschle map with $a^{(1)}(p_1, p_2) = p_1$ and $a^{(1)}(p_1, p_2) = p_2 \sin p_1$ (•) and for the generalised Froeschle map with linear force functions (·).

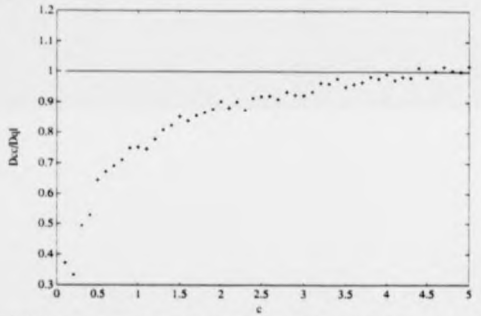

Figure 3.4. Plot of the ratio of the numerically calculated value for the diffusion coefficient to the theoretically calculated quasilinear value for the generalised Froeschle map with $a^{(1)}(p_1, p_2) = 0.1p_1^2$ and $a^{(1)}(p_1, p_2) = p_2$ (•) and for the generalised Froeschle map with linear force functions (·).

of the vector $\mathbf{k}$. This means that the functions a will either have to be linear functions of the momenta or periodic functions of the momenta or a mixture of the two. Any nonlinearity in any of the functions a (which is not periodic) result in the higher order correlation functions becoming zero. In this case the quasilinear result for the diffusion tensor is exact.

These results are in agreement with those obtained by Hatori et al [HK85] for the two dimensional radial twist map. Our results apply to more general maps and further give forms for the force functions a(p) that give corrections to the quasilinear value.

An interesting problem that remains is what is the essential difference that makes a map satisfying the conditions of linearity or periodicity of the force functions (that is a map on the torus) have corrections to the quasilinear value whereas for a map on the cylinder (not periodic in the momenta) the quasilinear value for the diffusion tensor is exact. Since the corrections to the quasilinear value arise from correlation effects (memory) as a particle moves through phase space, a possible reason would be that in the case of maps of the torus the structures that may cause memory effects are repeated regularly on a 'lattice' throughout phase space whereas for the general map of the cylinder such structures are localised in parts of phase space. (Those structures could be remnants of periodic orbits, islands or even accelerator modes which can be shown to exist only in the case of maps periodic in the momenta coordinates as well.) That is the existence of a regular lattice of such structures is expected to have a greater effect on the motion through phase space than the case where such structures are localised in parts of phase space. So the existence of corrections to the quasilinear value in the case of double periodicity, that is when regular lattices of such structures exist is expected. A formal proof of this intuitive result is given in appendix 3.1.

Also using the results of Mackay and Meiss [MM92] on the anti-integrable limit we show in Appendix 4.3 that chaotic orbits formally exist for some class of radial twist maps for perturbation parameters smaller than in the case of the standard map. While this is not a proof it serves as an indication that in

radial twist maps we can have fully chaotic trajectories for smaller values of the perturbation parameter and thus the correlation function method for the calculation of the diffusion coefficients converges faster for radial twist maps and hence gives results closer to the quasilinear result.

Chapter 4

Calculation of Diffusion Coefficients for Chaotic Maps

4.1 Introduction

The advantages of the Fokker Planck description of a chaotic dynamical system is that it provides an easy to handle description of the complicated dynamical process and can be used to give estimates for measurable quantities such as the kinetic energy of a distribution of particles or loss rates from particular parts of phase space. Thus, an important problem is the numerical or analytical calculation of the transport coefficients that enter into the Fokker-Planck description. In the present context the Fokker-Planck equation is equivalent to the time dependent diffusion equation and the only transport coefficient is the diffusion coefficient.

In the past, several methods for the calculation of the diffusion coefficient for maps have been proposed. These are based on the calculation of the diffusion coefficient D, making use of the well known formula for such a process $D = lim_{t\to\infty} \frac{<I^2>}{2t}$ where I is an action variable whose time evolution is modeled by the diffusion process,$<>$ denotes a suitable average and t the time (see for example [MCG83], [KRW82], [C79])

In this chapter, a new numerical method is proposed for the calculation of diffusion coefficients for chaotic maps. In this method the number of particles

remaining in a closed domain as a function of time is calculated using the map and is compared with that calculated analytically using the diffusion equation. The comparison is used to obtain the best estimate of the diffusion coefficient that appears in the diffusion equation. The method presents advantages over previous methods in that it can be used for a wider class of maps, for example maps for which the chaotic region is bounded. Also where the usual methods give values of D which are oscillatory in time [YR91] . Furthermore, it can be used in the calculation of diffusion coefficients for cases where these coefficients are functions of position in phase space. In the examples studied below, the present method uses an order of magnitude less computer time than previous methods.

4.2 Description of the method

The basic idea of the method of calculation of a diffusion coefficient is as follows:

A volume of phase space with a suitable geometry is chosen. (For example for a map which is already written in action-angle form, such as the standard map, the suitable geometry is that of an infinite slab , the infinite direction corresponding to the periodic variable and the other direction corresponding to the action variable.) A uniform distribution of initial points is then taken in the chosen volume and by iteration using the map the evolution of these points is followed until they leave the domain. The number of points that remain in the volume as a function of the number of iterations, which is equivalent to time, is calculated. Typical results are shown in figure 4.1 .

For the same geometry the time dependent diffusion equation is solved analytically and the total density that remains inside the given volume obtained as a function of time. This functional dependence is parametrised by the value of the diffusion coefficient.

The value of the diffusion coefficient appropriate to the map is then found by fitting the numerical results for the probability of points remaining in the domain as a function of time to the density obtained by solving analytically the diffusion equation. The value of the diffusion constant used in the analytical

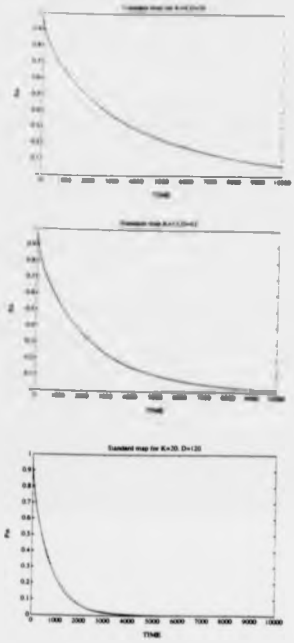

Figure 4.1. Probability that particles remain in the slab as a function of time for the standard map for different values of the parameter K. The solid line represents the values obtained by iterating the map whilst the broken line is the analytical result given by formula (4.6).

solution is treated as the fitting parameter. The 'best' value of D is obtained by making a least square fit.

The method is applied below to three well known chaotic maps, namely the standard map [C79],the web map [ZSU89] and the Fermi map [MLL85]. The results obtained are comparable to those obtained in earlier treatments of the various problems.

4.3 Standard Map

The standard map is of the form

$$p_{n+1} = p_n + K sin\theta_n \tag{4.1}$$

$$\theta_{n+1} = \theta_n + p_{n+1} \tag{4.2}$$

For large enough values of the parameter K the dynamics of the standard map is chaotic and can be modeled by a diffusion process (see for example [C79] or [RRW81]). As was mentioned before the appropriate geometry for the standard map is that of the infinite slab of width L. The diffusion equation takes the form

$$\frac{\partial P(p,t)}{\partial t} = D\frac{\partial^2 P(p,t)}{\partial p^2} \tag{4.3}$$

where P(p,t) is the probability density of points in the slab and it is assumed that the diffusion coefficient D is constant. The solution of the diffusion equation in the geometry with the boundary condition that P is zero on the boundary of the slab is [CJ59]

$$P(p,t) = \sum_n a_n exp(-\frac{Dn^2\pi^2 t}{L^2})sin(\frac{n\pi}{L}p) \tag{4.4}$$

Assuming a homogeneous initial density of points in the slab, the probability distribution becomes

$$P(p,t) = \frac{4}{\pi}\sum_n \frac{1}{2n+1} exp(-\frac{D(2n+1)^2\pi^2 t}{L^2})sin(\frac{(2n+1)\pi}{L}p) \tag{4.5}$$

The probability that particles remain in the slab as a function of time is then given by the expression:

$$P_{in}(t) = \frac{1}{L}\int_0^L P(p,t)dp = \frac{8}{\pi^2}\sum_{l=0}^{\infty}\frac{1}{(2l+1)^2} exp(-\frac{D(2l+1)^2\pi^2 t}{L^2}) \tag{4.6}$$

In figure 4.1 this probability is shown as a function of time as calculated from a numerical simulation using the map and also from using the analytical formula given above. A comparison is shown between such analytical and numerical results for a particular value of K and two different values of D in figure 4.2 . The best value of D for a particular value of K is easily obtained and it is clear that the analytic solution then fits the numerical data very closely once sufficient time is allowed for transients to decay. The found value of D agrees to within a few per cent with that obtained in [RW80]. Such a difference is within the usual computational errors associated with numerical simulations.

4.4 Web map

As discussed in detail in Chapter 2, the web map is the Poincaré map for a harmonic oscillator which is periodically kicked by a sinusoidal force [ZSU89]. It is expressed in terms of the x,p coordinates, which are the position and the momentum of the oscillator respectively. The map can be written in the form

$$u_{n+1} = (u_n + K\sin v_n)\cos\alpha + v_n\sin\alpha \tag{4.7}$$

$$v_{n+1} = -(u_n + K\sin v_n)\sin\alpha + v_n\cos\alpha \tag{4.8}$$

where $\alpha = 2\pi/q$ and K is proportional to the strength of the force. The variables u and v are proportional to x and p and defined by $u = \frac{kp}{\omega_0}$ and $v = -kx$ where k and ω_0 are the wavelength and frequency, respectively of the central mode of the wave packet. For the web map, the appropriate geometry is that of a disc since diffusion occurs in the action coordinate which is proportional to $u^2 + v^2$. The diffusion equation takes the form

$$\frac{\partial P(r,t)}{\partial t} = \frac{1}{r}\frac{\partial}{\partial r}(rD\frac{\partial P(r,t)}{\partial r}) \tag{4.9}$$

and is to be solved for a disc of radius r_0 with the boundary condition that $P(r_0,t)=0$, for all t. In the above equation r is the square root of the action. The solution of this diffusion equation is of the form

$$P(r,t) = \sum_n A_n J_0(\alpha_n r)e^{-D\alpha_n^2 t} \tag{4.10}$$

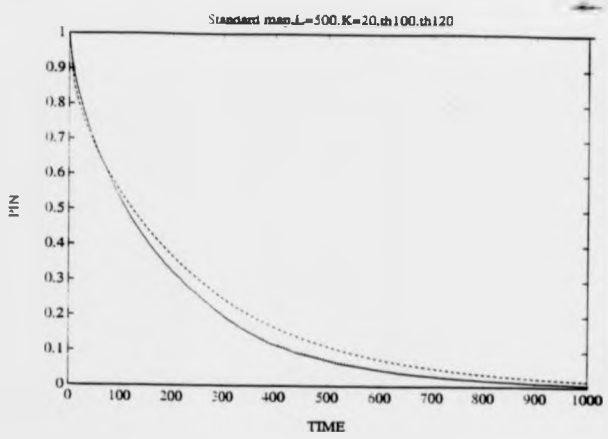

Figure 4.2. Probability that particles remain in the slab as a function of time. The numerical results (solid line) are for the standard map with K=20 and the analytical results (broken lines) for two different diffusion coefficients D=100 and D=120 are shown for comparison.

where the a_n's satisfy the equation

$$J_0(ar_0) = 0 \tag{4.11}$$

If we start with a uniform density of points in the disc the appropriate form of the probability density is

$$P(r,t) = \frac{2}{r_0} \sum_{n=1}^{\infty} e^{-Da_n^2 t} \frac{J_0(a_n r)}{a_n J_1(r_0 a_n)} \tag{4.12}$$

The density of points remaining in the disc as a function of time is given by

$$P_{in}(t) = \frac{2}{r_0^2} \int_0^{r_0} rP(r,t)dr = \frac{4}{r^2} \sum_{n=1}^{\infty} \frac{1}{a_n^2} exp(-Da_n^2 t) \tag{4.13}$$

A comparison between the numerics and the analytic value given by equation (4.13) is shown in figure 4.3 . The numerical simulations were done using the web map exhibiting four-fold symmetry (q=4). First of all it is clearly seen that the dynamics of the web map are well approximated by a diffusion process in action space. The graphs on the right of figure 4.3 give an estimate of the error E as a function diffusion coefficient D, where E is defined such that $E(D) = \frac{\sum^N |P_{in}(t=n)-P_n|^2}{N}$ where P_n is the density of particles in the disc after n iterations of the map. The value of D for which this error is minimum is the chosen one.

It is seen that the value of the diffusion coefficient obtained as above for the same value of K depends on the radius of the disc, r_0 . This is unlike the results obtained for the standard map where the diffusion coefficients were independent of the thickness of the slab chosen. This dependency on r_0 reflects the fact that the dynamics for the web map is not well approximated by a constant diffusion coefficient as in the case of the standard map. This dependency on r_0 can be interpreted as due to the diffusion coefficient being a function of the action variable. This observation agrees with the results of Zaslavskii et al [ZSU80], who, using the quasilinear approximation showed that D was action dependent and of the form

$$D(r) = D_0(1 - \frac{J_1(ar)}{2ar}) \tag{4.14}$$

where a is some constant. It is worth noting that the quasilinear diffusion coefficient for the standard map is equal to a constant [LL83].

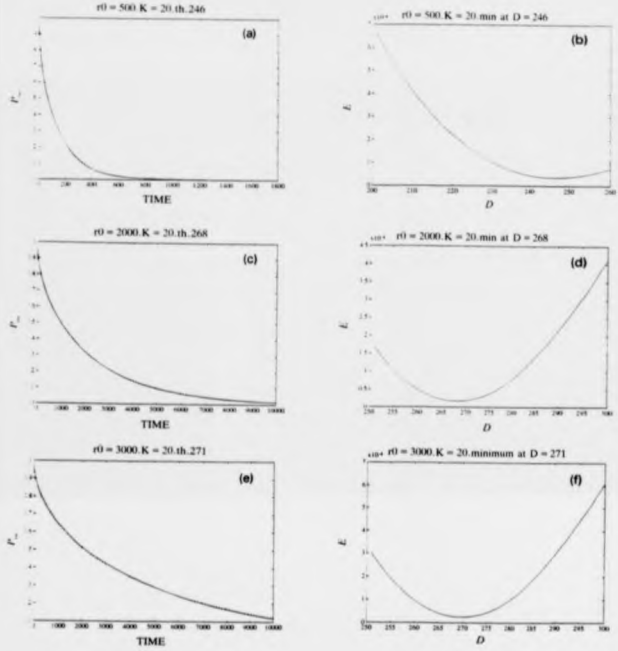

Figure 4.3. Probability that the particles remain in the disc as a function of time for the web map (four-fold symmetry) for various values of the parameter K. The solid line is the numerical simulation and the broken line is the analytical result obtained using equation (4.13) with the value of D chosen to give the best fit. The figures on the right hand side of the page show the error E defined in section 4.3, as a function of the fitting parameter D.

The method is found to work sufficently well for a range of values of the perturbation parameter K. However one must be careful to choose K large enough so that the transport through phase space does not resemble an anomalous diffusion because of the presence of islands and accelerators modes. In that case fitting to a different analytical diffusion equation may be necessary [HR86], [P92].

The method as described above has also been applied to the case of the quasi-crystal symmetries of the web map which are exhibited when q=5,7,8,... . It has been found that in these cases as well, the dynamics in phase space can well be approximated by a diffusion process with diffusion coefficient very close to the quasilinear value even for moderate values of the perturbation parameter confirming the analysis given in Chapter 3 and [YR92].

An interesting point which arises from this investigation is the following: For the special values of q=3,4,6 the web map can be written in doubly periodic form and can be considered as a map on (a properly defined) unit torus. Now consider keeping the perturbation parameter K fixed but allowing q to take real values. Then we find for q=3,4,6 a periodic arrangement of thin stochastic layers which allow diffusion in phase space. Whereas if q changes to non-integer real values, the chaotic regions become wider and have no clear periodicity, thus allowing easier diffusion through phase space. This phenomenon is revealed in the values of the diffusion coefficient. Our numerical method has been applied to the study of the diffusion coefficient for constant K but allowing q to vary in the neighbourhood of the values of q where crystal symmetry is present. The results obtained for K=4 and q in the vicinity of 4 are shown in figure 4.4 . It will be seen that there is a quick transition from the diffusion coefficient value equal to 3 as appropriate for q=4 to a constant value approximately equal to 8 as q is changed from the value q=4. The behaviour away from q=4 agrees well with the value for D (namely $K^2/2$ for the particular case of the web map) as calculated in Chapter 3 (or [YR92]) as expected for a non doubly periodic map. Similar behaviour is found for q=3,4,6, though because there in no symmetry we do not get this behaviour around q=5. For all values near q=5 quasilinear

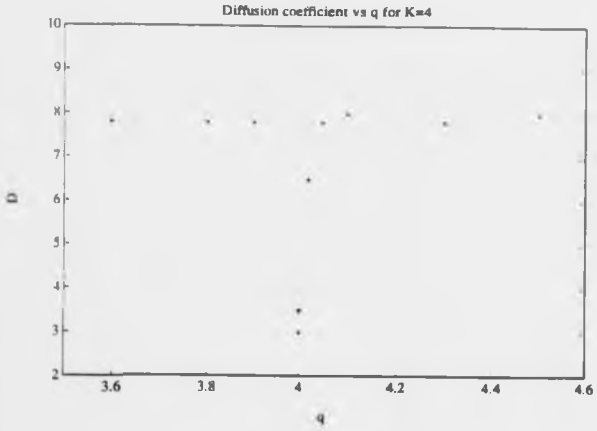

Figure 4.4. Diffusion coefficient for the web map for K=4 and for values of q around q=4 .

theory is valid.

The value of the diffusion coefficient at q=3,4,6 can be higher or lower than the quasilinear value depending on the value of K. This phenomenon is due for example to the presence of accelerator modes and is discussed in Chapter 2 and [YR91].

Finally, the boundary condition needed in the analytical solution of the diffusion equation is not the only one which could have been used. This condition depends crucially on the numerical procedure used. For example in the numerical procedure discussed in the paper, an ensemble of particles was initially started in a large disc and these particles were followed under iterations of the map until they left the disc and then they were taken out of the ensemble. This procedure corresponds to an absorbing boundary condition on the boundary of the disc. In the case of the web map with q=3,4,6, where the map is periodic, the problem could be formulated in a different but equivalent way. An ensemble of particles can now be initiated in a smaller disc but one contained in the fundamental unit torus. The diffusion equation must now be solved analytically using periodic boundary conditions on the unit torus. Now the whole initial ensemble will have to be traced for all times since we are not allowed to remove a particle from it as soon as it crosses the boundary of the disc. (Since we can no longer impose the absorbing boundary contition a particle that leaves the disc can now re-enter.) Changing our algorithm in this way both boundary conditions (that is ignoring periodicity but imposing absorbing boundary condition or taking into account the periodic boundary condition but necessarily ambadoning the absorbing boundary condition) should give the same result for the diffusion coefficient. However the disadvantage of using the second method is that the numerical part of the method will now take longer than before since we are not allowed to remove particles that leave the disc from our initial ensemble, and we now have to trace the full ensemble (which is usually a large one to minimise the statistical errors associated with the random distribution of initial conditions, of the order of 10000 particles) for the time required. Importantly, by not chosing the periodic boundary conditions,

we have a more general method valid for a wider class of maps, which arise in many applications [LL83],[HK185].

4.5 WKB solution of the diffusion equation with slowly varying diffusion coefficient.

Our numerical results and subsequent parameter fitting and the quasi-linear results of [ZSU89], suggest that the diffusion coefficient must be considered to be dependent on the action. However, it is apparent from the variation of D with r_0, found numerically, that the variation of D with action should be relatively slow. In this section we extend our method for the calculation of diffusion coefficients to allow for such slow variation of the diffusion coefficient with space.

Thus, we write our model diffusion equation in cylindrical coordinates in the following form

$$\frac{\partial P(r,t)}{\partial t} = \frac{1}{r}\frac{\partial}{\partial r}(rD(\epsilon r)\frac{\partial P(r,t)}{\partial r}) \tag{4.15}$$

where ϵ is a small parameter allowing D to have a slow variation with space. A full solution to this problem can be obtained only for special forms of the diffusion coefficient . To be able to give more general results we use an approximate solution to this equation based on the WKB method (see for example [Mb53]).

Separating variables we obtain the solution to equation (4.15) in the form

$$P(r,t) = \sum_n A_n \phi_n(r) e^{-\lambda_n^2 t} \tag{4.16}$$

(assuming a discrete eigenvalue spectrum) where the functions ϕ_n and the numbers λ_n satisfy the eigenvalue equation.

$$\frac{1}{r}\frac{d}{dr}(rD(\epsilon r)\frac{d\phi_n}{dr}) = -\lambda_n^2 \phi_n \tag{4.17}$$

For a general $D(\epsilon r)$ it is not possible to obtain an analytic solution to this equation and hence it is necessary to introduce an approximate procedure. In the case of a constant diffusion coefficient the eigenvalue equation reduces to Bessel's equation of order zero and then by imposing the condition that the

probability distribution remains finite at the origin, the solution is given in terms of the Bessel functions of zero order and of the first kind, namely $J_0(r)$. In the case of a slowly varying diffusion coefficient we assume a solution to the eigenvalue problem of the form

$$\phi(r) = A(\epsilon r) J_0(\frac{1}{\epsilon} f(\epsilon r)) \tag{4.18}$$

where for convenience we have dropped the subscripts n labeling the eigenvalues and the eigenfunctions.

Substituting this form into the eigenvalue equation we get

$$\begin{aligned} -\lambda^2 A(\epsilon r) J_0(s) = \quad & \frac{\epsilon}{\epsilon} D(\epsilon r) A'(\epsilon r) J_0(s) + \epsilon^2 D'(\epsilon r) J_0(s) A'(\epsilon r) \\ & + \epsilon^2 A''(\epsilon r) D(\epsilon r) J_0(s) + \epsilon D(\epsilon r) A'(\epsilon r) J'(s) f'(\epsilon r) \\ & + \frac{1}{\epsilon} D(\epsilon r) A(\epsilon r) J_0'(s) f'(\epsilon r) + \epsilon D'(\epsilon r) A(\epsilon r) J_0'(s) f'(\epsilon r) \\ & + \epsilon D(\epsilon r) A'(\epsilon r) J_0'(s) f'(\epsilon r) - D(\epsilon r) A(\epsilon r) J_0(s) (f'(\epsilon r))^2 \\ & + \frac{\epsilon}{f(\epsilon r)} D(\epsilon r) A(\epsilon r) (f'(\epsilon r))^2 J_1(s) \\ & + \epsilon D(\epsilon r) A(\epsilon r) J_0'(s) f''(\epsilon r) \end{aligned} \tag{4.19}$$

where dashes denote differentiation with respect to the argument of the function and $s = \frac{f(\epsilon r)}{\epsilon}$. We assume that $\epsilon r = y$ is O(1) (of order 1 in our ordering scheme) and then if in the above equation we separate terms of different order to get

$$O(1) : f'(\epsilon r) = \frac{\lambda}{D^{\frac{1}{2}}(\epsilon r)} \tag{4.20}$$

$$O(\epsilon) : (\frac{1}{2\epsilon r} + \frac{1}{2}\frac{D'(\epsilon r)}{D(\epsilon r)} - \frac{f'(\epsilon r)}{2f(\epsilon r)} + \frac{f''(\epsilon r)}{2f'(\epsilon r)}) A(\epsilon r) = -A'(\epsilon r) \tag{4.21}$$

The O(1) equation (4.20) is readily integrated to give

$$f(\epsilon r) = \int_0^{\epsilon r} \frac{\lambda}{D^{\frac{1}{2}}(\epsilon r_1)} d(\epsilon r_1) \tag{4.22}$$

We use this result to integrate the O(ϵ) equation (4.21) to get the form of the function $A(\epsilon r)$. Substituting $f(\epsilon r)$ into equation (4.21) gives

$$-(\frac{1}{2y} + \frac{1}{4}\frac{D'(y)}{D(y)} - \frac{f'(y)}{2f(y)}) = \frac{A'(y)}{A(y)} \tag{4.23}$$

(where $y=\epsilon r$) which is readily integrated to give

$$A(\epsilon r) = \frac{1}{(\epsilon r)^{\frac{1}{2}}} \frac{1}{D^{\frac{1}{4}}(\epsilon r)} f^{\frac{1}{2}}(\epsilon r), \tag{4.24}$$

where $f(\epsilon r)$ is given by equation (4.22).

In the case where D is a constant the WKB solution obtained here reduces to the exact Bessel functions solution.

The approximate eigenfunctions obtained by the WKB method are orthogonal and this is demonstrated as follows. Imposing the boundary condition $\phi(r_0) = 0$ on the eigenfunctions (which is the boundary condition used in the numerical evaluation of the diffusion coefficient) we get a discrete spectrum of eigenvalues λ_n, defined by the relation

$$\frac{\lambda_n}{\epsilon} f(\epsilon r_0) = a_n \tag{4.25}$$

where a_n denotes the roots of $J_0(x) = 0$. So the eigenfunctions for our problem are

$$\phi_n(r) = \frac{1}{(\epsilon r)^{1/2}} \frac{\lambda_n^{\frac{1}{2}}}{D^{\frac{1}{4}}(\epsilon r)} f^{\frac{1}{2}}(\epsilon r) J_0(\frac{\lambda_n}{\epsilon} f(\epsilon r)) \tag{4.26}$$

Let us now check orthogonality with respect to the inner product

$$< f, g >= \int_0^{r_0} r f g dr \tag{4.27}$$

The inner product of two eigenfunctions is given by

$$I_{nm} = < \phi_n, \phi_m > = \frac{1}{\epsilon^2} \int_0^{\epsilon r_0} (\lambda_n \lambda_m)^{\frac{1}{2}} \frac{f(\epsilon r)}{D^{\frac{1}{2}}(\epsilon r)} J_0(\frac{\lambda_m}{\epsilon} f(\epsilon r)) J_0(\frac{\lambda_n}{\epsilon} f(\epsilon r)) d(\epsilon r) \tag{4.28}$$

But

$$\frac{d(\epsilon r)}{D^{\frac{1}{2}}(\epsilon r)} = df(\epsilon r) \tag{4.29}$$

and the inner product can then be written in the form

$$I_{nm} = \frac{1}{\epsilon^2} \int_0^{f(\epsilon r_0)} (\lambda_n \lambda_m)^{\frac{1}{2}} f(y) J_0(\frac{\lambda_m}{\epsilon} f(y)) J_0(\frac{\lambda_n}{\epsilon} f(y)) df(y)) \tag{4.30}$$

Using the properties of Bessel functions [AS70] and the fact that $J_0(\frac{\lambda_n}{\epsilon} f(\epsilon r_0)) = 0$ we find that

$$I_{nm} = \frac{a_n f(\epsilon r_0)}{2\epsilon} J_1^2(\frac{\lambda_n}{\epsilon} f(\epsilon r_0)) \delta_{nm} \tag{4.31}$$

showing that the eigenfunctions generated by the approximate method outlined above are orthogonal.

The full solution of the diffusion equation is then a linear combination of all the eigenfunctions and can be written in the form

$$P(r,t) = \sum_n A_n \phi_n(r) = \sum_n \frac{1}{(\epsilon r)^{\frac{1}{2}}} \frac{\lambda_n^{\frac{1}{2}}}{D^{\frac{1}{4}}(\epsilon r)} J_1^{\frac{1}{2}}(\epsilon r) J_0(\frac{\lambda_n}{\epsilon} f(\epsilon r)) e^{-\lambda_n^2 t} \qquad (4.32)$$

where the A_n's are determined by the initial condition $P(r,0)=g(r)$ in the following way

$$A_n = \frac{1}{I_{nn}} \int_0^{r_0} r \phi_n(r) g(r) dr \qquad (4.33)$$

Let us assume that we start with a homogeneous particle distribution on the disc

$$P(r,0) = P_0 \qquad (4.34)$$

The number of particles in the disc as a function of time is then given by

$$\begin{aligned} P_{in} &= \frac{2}{r_0^2} \int_0^{r_0} r P(r,t) dr \\ &= \sum_n \frac{2}{r_0^2} \int_0^{r_0} A_n r \phi_n(r) e^{-\lambda_n^2 t} dr \\ &= \sum_n \frac{2}{r_0^2} \frac{1}{I_{nn}} (\int_0^{r_0} \phi_n(r) dr)^2 e^{-\lambda_n^2 t} \end{aligned} \qquad (4.35)$$

Using the properties of Bessel functions we obtain

$$(\int_0^{r_0} r \phi_n(r) dr)^2 = \frac{1}{\lambda_{nn}} r_0 f(\epsilon r) D^{\frac{1}{2}}(\epsilon r_0) J_1^2(\frac{\lambda_n}{\epsilon} f(\epsilon r_0)) (f'(\epsilon r))^2 \qquad (4.36)$$

Then the probability that particles remain in the disc as a function of time, for the case of a uniform initial distribution function, is

$$P_{in} = \sum_n \frac{4\epsilon}{r_0 f(\epsilon r_0)} \frac{P_0}{\lambda_n^2} D^{\frac{1}{2}}(\epsilon r_0) e^{-\lambda_n^2 t} \qquad (4.37)$$

where we have used the fact that

$$f'(\epsilon r) = D^{-\frac{1}{2}}(\epsilon r) \qquad (4.38)$$

In the case where D is a constant

$$f(\epsilon r) = \epsilon r D^{-\frac{1}{2}} \qquad (4.39)$$

and all the formulas obtained by the WKB method for the probability distribution P(r,t) and the probability that particles remain in the disc P_{in} reduce to the formulas obtained in the case of constant D.

The probability that particles are in the disc at t=0 is equal to P_0 (or 1 if appropriate units are chosen). The approximate WKB solution gives

$$\sum_n \frac{4\epsilon}{r_0 f(\epsilon r_0)} \frac{1}{\lambda_n^2} D^{\frac{1}{2}}(\epsilon r_0) = 1 \tag{4.40}$$

or equivalently

$$\frac{f(\epsilon r_0) D^{\frac{1}{2}}(\epsilon r_0)}{r_0 \epsilon} = 1 \tag{4.41}$$

where we have used the identity

$$\sum_n \frac{1}{a_n^2} = \frac{1}{4} \tag{4.42}$$

which follows from (4.13) by putting t=0, where a_n are the roots of $J_0(x) = 0$. It can be seen that equation (4.41) is not true for every function f(ε r) given by formula (4.22), except for the one obtained in the case of a constant diffusion coefficient. Equation (4.41) should then be seen as an approximate relation, with the nearness of the value of the left hand side to unity giving an indication of the accuracy of our solution of equation (4.15).

We now use the approximate solution obtained above to get information on how the diffusion coefficient varies with action.

Motivated by the general functional form of the quasilinear diffusion coefficient given above we assume that the diffusion coefficient can be written in the form

$$D = D_1 + D_2 \epsilon^{\nu} \tag{4.43}$$

with D_2 and ν negative. This diffusion coefficient approximates well the general features of the theoretically predicted diffusion coefficient as given by (4.14)(see fig.4.5). The advantage of a diffusion coefficient of this form is that it is easy to calculate analytically the function f giving

$$f(y) = -\frac{\lambda}{D_1^{\frac{1}{2}}}(ln(D^{\frac{1}{2}}(y) - D_1^{\frac{1}{2}}) - ln(D^{\frac{1}{2}} + D_1^{\frac{1}{2}}) - ln((D_1 + D_2)^{\frac{1}{2}} - D_1^{\frac{1}{2}}) + ln((D_1 + D_2)^{\frac{1}{2}} + D_1^{\frac{1}{2}})) \tag{4.44}$$

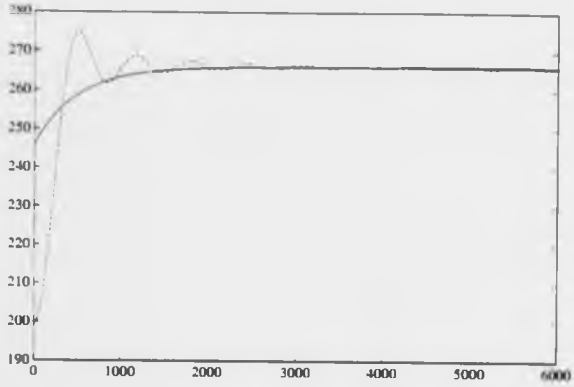

Figure 4.8. Approximation of the analytical quasilinear diffusion coefficient of equation (4.14) by the exponential law of equation (4.45).

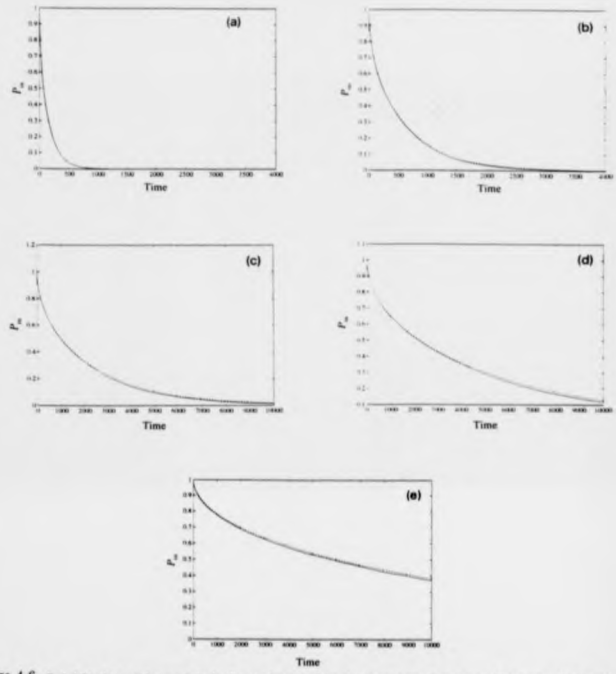

Figure 4.6. Probability that particles remain in the disc as a function of time for the web map. Comparison of the numerics (solid line) and the WKB solution (broken line). (a) $r_0 = 500$, $K = 20$; (b) $r_0 = 1000$, $K = 20$; (c) $r_0 = 2000$, $K = 20$; (d) $r_0 = 3000$, $K = 20$; (e) $r_0 = 5000$, $K = 20$, $D = 268$.

The eigenvalues and the eigenfunctions for the particular form of the diffusion coefficient are then obtained by the equations given above with the substitution of this specific form for the function f.

Then from a comparison of the analytic form and simulation results for the probability that particles remain in the disc as a function of time we get estimates for the values of D_1,D_2 and ϵ needed to model properly the web map. This has been done in the case of the web map exhibiting four-fold symmetry (see fig.4.6) . The value for D_1, which is the asymptotic value of the diffusion coefficient for large enough radii, can be found from comparison of numerics and our analytic formula (4.37) obtained for the case of constant diffusion coefficient. We find that $D_1 = 266$. Then by taking smaller values of the radius r_0 going down to $r_0 = 500$ we find that the evolution of the web map is well approximated by a diffusion process with a diffusion coefficient of the form

$$D(r) = 266 - 20e^{-0.002r} \tag{4.45}$$

Throughout these calculations the parameter K appearing in equations (4.7) and (4.8) was kept constant and equal to 20. A constant diffusion coefficient is not good enough to model the system. Importantly other functional forms for the dependence of D on r can be fitted using the present method.

4.6 The Fermi map

The method has been applied to a map for which the whole of phase space is not chaotic and where confining KAM curves exist. A well known example of such a map is the Fermi map which is of the form

$$p_{n+1} = p_n + \sin\theta_n \tag{4.46}$$

$$\theta_{n+1} = \theta_n + \frac{2\pi M}{p_{n+1}} \tag{4.47}$$

where p is the action variable and M is a parameter.

In the Fermi map, the phase plane is chaotic for actions $p < p_0$ and above this critical action p_0, the phase space is foliated by KAM tori (fig 4.7) . As

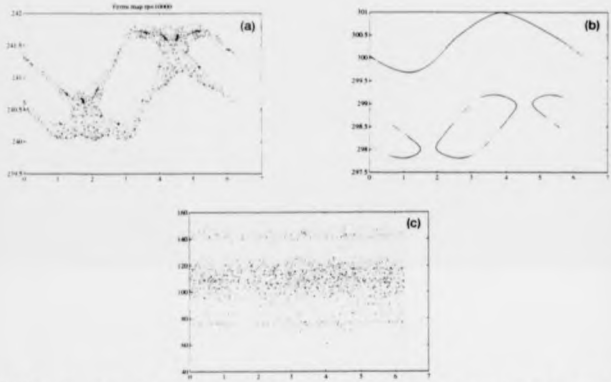

Figure 4.7. Phase plane plots for the Fermi map for $M = 10\,000$. The existence of KAM surfaces and ordered motion for large enough values of the action is shown.

is evident, particles starting in parts of phase space with $p < p_0$ are confined to stay in this region by the existence of the KAM tori. In this case the mean square displacement of those particles can not grow linearly as a function of time because of the trapping by the first KAM curve encountered. In this case the usual asymptotic method for the calculation of the diffusion coefficient namely $D = \frac{\langle \Delta p^2 \rangle}{2t}$ will give a zero value for large values of t which is not really appropriate. This is because the dynamics is controlled by the KAM surface and not by the chaotic motion.

However the method proposed in this paper gives finite values for the diffusion coefficient. The appropriate geometry for the Fermi map is the geometry of the slab as in the case of the standard map. The expression for P_{in} to be used for the Fermi map is the same as for the standard map and is given by (4.6).

The variation of $P_{in}(t)$ with t for the Fermi map calculated directly using the map and using the diffusion equation (4.3) are shown in figure 4.8. The fit is very good, but it is found that the value of D depends on r_0. This dependency is shown in figure 4.8 . The diffusion coefficient obtained is more or less constant if the thickness of the slab is smaller than some critical value r_c (which itself depends on the parameter M) and then starts to decrease abruptly as the thickness of the slab is increased to include the first KAM curve and the island structure around it. It should be noted here that since the variation of the diffusion coefficient for the Fermi map is steep, because of the KAM surface, the WKB method proposed in the previous section is not appropriate but the approximation of a constant D for $p < p_0$ is good.

The values of the diffusion coefficient for the Fermi map obtained here are to be compared to the ones obtained by Murray, Lieberman and Lichtenberg [MLL85] using a more complicated method and shown in their figure 4.10 . The complicated oscillations shown in this figure and due to the presence of small scale structure in the phase space, are not present in figure 4.9 because our method is designed to give an average value for the diffusion coefficient in such cases. Note also that the values for the diffusion coefficient obtained by

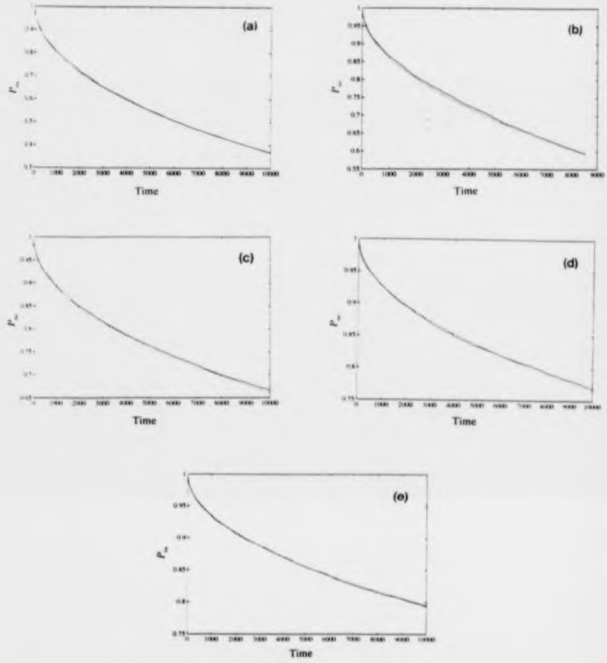

Figure 4.8. Probability that particles remain in the slab as a function of time for the Fermi map with $M = 10\,000$. Comparison between the numerical simulation (solid line) and the analytical result given by eq. (6) (broken line) is shown. The thickness of the slab changes in the different figures and so does the resulting diffusion coefficient. (a) $r_0 = 150$, $D = 0.18$; (b) $r_0 = 180$, $D = 0.125$; (c) $r_0 = 200$, $D = 0.09$; (d) $r_0 = 256$, $D = 0.07$; (e) $r_0 = 280$, $D = 0.065$.

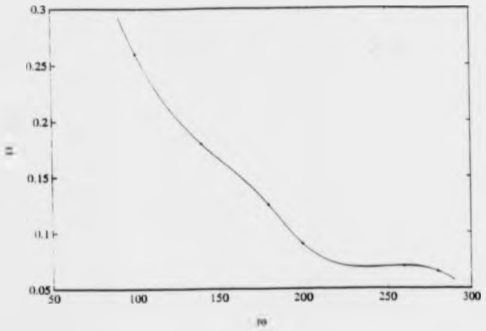

Figure 4.9. The calculated diffusion coefficient for the Fermi map as a function of the thickness of the slab r_0.

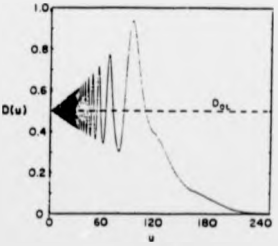

Figure 4.10. The results for the diffusion coefficient as a function of the momentum (action) after Murray, Lieberman and Lichtenberg [MLL85].

Murray, Lieberman and Lichtenberg [MLL85] are two times larger than the ones we obtain but this is due to the fact that they write their diffusion equation in the form (4.3) but with $D=\frac{D_1}{2}$ and in their figure they plot D_1.

The long tail on the variation of D with r_0 as shown in figure 4.9 is due to the fact that the straight line boundaries we take in our analytic calculations do not coincide with a KAM surface.

4.7 Conclusions

The advantages of the method described above and used for the determination of diffusion coefficient are:

1) It works for systems where the chaotic part of phase space is bounded. Such systems often occur in a number of physical problems (e.g. Fermi map) [MLL85]. For such systems the calculation of the diffusion coefficient using the expression $D = lim_{t\to\infty}\frac{\Delta I^2}{2t}$ is difficult since $D \to 0$ because the chaotic region is bounded by KAM curves.

2) The calculation of the diffusion coefficient using the present method is easier because one avoids the problem of dealing with the oscillations of the diffusion coefficient as a function of time which are due to the fine structure of the phase space (islands etc) [YR91]. The present method averages over these effects and reveals the gross variation of the diffusion coefficient in phase space. The method also gives information on the behavior of the phase flow for intermediate times which can be used to calculate loss rates and other such quantities.

3) Any variation of the diffusion coefficient with position in phase space is revealed as a variation of the calculated diffusion coefficient as a function of the radius or the slab thickness used in the calculation.

Such a dependence though revealed by time oscillations in D, cannot be easily obtained using other methods since it would involve calculations initiated in different regions of phase space.

In the two examples given, this effect was shown to exist for the web map, but not for the standard map. This is consistent with results obtained analyti-

cally.

4) It is fast and efficient. Results obtained for the standard map show that the method is about an order of magnitude faster than other methods used previously.

5) Finally the main error in the present method arises from the fact that the numerical simulation uses a random number generator to create the initial uniform probability distribution of particles in the bounded domain used. As a result the initial probability distribution is different for different realisation of the numerical simulation and this introduces a statistical error in the measurements of the diffusion coefficient. This error can be controlled by taking a sufficiently large number of initial conditions. For example in the case of the web map in the expression for D as given by (4.45) the constant term was found to be 266 ± 8. It is found that the error is comparable to the errors in the diffusion coefficients as calculated by other methods and revealed by the fact that the diffusion coefficient oscillates with time.

Chapter 5

A Model for the Coexistence of Diffusion and Accelerator Modes in a Chaotic Area-Preserving Map

5.1 Introduction.

Consider an area preserving chaotic map in x,y which can be brought into a doubly periodic form, that is, can be written as a map of the unit torus $T = [0, 2\pi] \times [0, 2\pi]$. For such maps there exist parts of phase space called accelerator modes [LL83] where ordered motion occurs rather than stochastic motion. This ordered motion corresponds to constant acceleration of particles to remote parts of phase space and this leads to anomalous enhancement of the diffusion coefficient as calculated for such maps [C79],[KRW82]. Examples of maps where such behaviour occurs are the well known standard map [C79] or the web map [ZSU89],[YR91].

Our aim is to investigate the effect of the existence of such accelerator modes on the transport through phase space for an area preserving map (two dimensional symplectic map). The motivation for investigating such a situation

is the need to explain the fluctuations observed in the numerically calculated value of the ratio of the square of the displacement, p, divided by twice the number of iterates (time) of the map namely $\frac{<p^2>}{2n}$. Usually the asymptotic value for large n of this ratio is a constant and is identified with the diffusion constant. However for many maps and in particular the maps considered in this paper the ratio shows oscillatory behaviour and/or variation proportional to n^α even for large n. We shall refer to this ratio as the diffusion coefficient $D = \frac{<p^2>}{2n}$ but we now allow it to be a function of n. A typical example of the variation of D with n, for the web map [ZSU89],[YR91] is shown in Fig.5.1 . Of course the times of interest are longer than the time needed for the effect of initial conditions to be damped away.

5.2 Formulation of the Problem.

The variation of the diffusion coefficient D with n for systems under consideration show very complicated behaviour. This behaviour we associate with the presence of accelerator modes and with regions of non-chaotic behaviour in the phase space. The exact structure of phase space is extremely complicated. In order for an analytical treatment to be feasible, some simplifications are necessary.

The phase space is modelled as follows. It is assumed to be infinite and two dimensional. In the space there exists a periodic array of points which corresponds to accelerator modes. For simplicity we assume that the accelerator modes form an infinite orthogonal lattice of points in the space. Whenever a particle reaches such a point it can make a finite jump to another point of the lattice (that is to another accelerator mode) rather than diffuse to neighboring points in the space.

Besides the accelerator modes we also take into account the effects of the existence of islands surrounding stable periodic points. Whenever a particle approaches a stable fixed point of the map we assume that it stays there for a certain number of iterations before continuing to diffuse. Thus the stable periodic points act as traps in the diffusion process through phase space. For

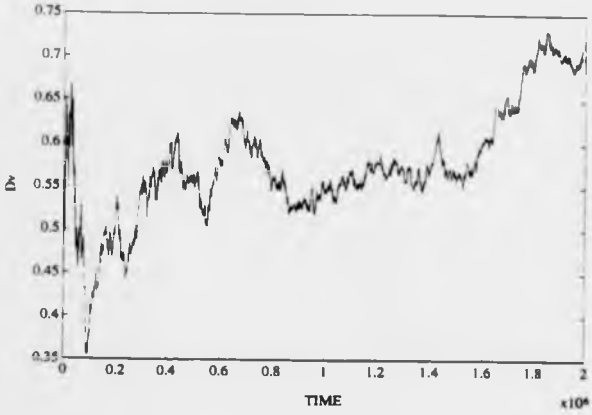

Figure 5.1. A typical numerical calculation of the diffusion coefficient as a function of time for a map containing accelerator modes.

the sake of simplicity, we also assume that the stable periodic points form an infinite orthogonal lattice in phase space. The infinity of the lattices of both the accelerator modes and the traps arises because of the double periodicity of the original map.

On every other part of phase space, the motion is assumed to be well approximated by a uniform diffusion process having a constant diffusion coefficient D.

In our model we allow particles to diffuse through phase space until they reach the vicinity of an accelerator mode or a stable island (trap). There they can be trapped with certain trapping probabilities and start performing finite jumps to other points of the lattice or remain trapped, according to whether the lattice point is an accelerator mode or a stable island. Trapping at lattice points occur for a finite number of iterations of the map m, with a probability distribution $\psi(m)$. Then detrapping occurs and the particles are allowed to diffuse again until they are brought by diffusion to the vicinity of another accelerator mode or island.

The trapping in the accelerator modes is equivalent to a diffusion process intermingled with the particle having long jumps at certain times. This is similar to the situation described by a Levy random walk, a concept which may alternatively be used to model such a chaotic system [ZSC89],[ASZ91]. The relation between this and our model is discussed later.

Half the accelerator modes correspond to orbits for which $p \to \infty$ as $n \to \infty$ and the other half correspond to orbits for which $p \to -\infty$ as $n \to \infty$. To distinguish between these two types of accelerator modes we will call the second type retardor modes. The coexistence of these two types of modes is found for example in the web map.

The accelerator modes exist on the points (nx_A, ly_A), the retardor modes exist on the points (nx_A, ly_A) and the stable islands (traps) exist on the points (nx_T, ly_T) of phase space where n,l are integers. For simplicity we allow jumps between the accelerator modes to be only in one direction, say the x direction. Generalization of the model to allow for jumps in all directions is straightfor-

ward.

5.2.1 A Discrete Model.

A suitable starting point to get a mathematical description of the random walk situation outlined above, is a discrete time - discrete space random walk model. The usual random walk model is assumed on a lattice of points so that the probability of motion to the left or to the right is equal to $\frac{1}{2}$. On this lattice there is embedded a second lattice which is the lattice of accelerator modes (retardor modes or traps). When a particle first reaches such a point it is reinjected in the normal lattice with probability (1-α) or stays trapped there performing correlated jumps with probability α. The number of correlated jumps, m, performed by the particle at such a mode is distributed with a probability distribution $\psi(m)$.

Let us assume that the accelerator modes (or traps) are situated at a distance of l lattice points apart, where l must be large enough. Then on the normal lattice the usual random walk equation

$$p(n,t) = \frac{1}{2}p(n-1,t-1) + \frac{1}{2}p(n+1,t-1) \tag{5.1}$$

is valid where p(n,t) is the probability that a particle is at lattice site n at time t, where n,t$\in \mathbf{Z}$. This equation simply states that a point of the normal lattice can be reached only from its nearest neighbours and that it takes a time unit for a particle at n+1 or n-1 to hop to n.

This equation is not valid on the accelerator modes and their nearest neighbours. An accelerator mode cannot only be reached from its nearest neighbours but also from particles which were on other accelerator modes.

Any particle that just got into the accelerator mode $(N-s)l$ by diffusion and is going to spend more than s iterations in this mode is going to end up in s time units at Nl. This is a process that takes s time units to be completed, so the rate of particles into the accelerator mode Nl at time t, due to contributions from other accelerator modes is

$$\alpha\frac{\psi(s)}{s}\frac{1}{2}(p(Nl-sl-1,t-s-1)+p(Nl-sl+1,t-s-1)) \tag{5.2}$$

where $\alpha\psi(s)$ is the probability that a particle stays in an accelerator mode for more than s iterations. For brevity of presentation let us define the operator T_1 which acts on the probability function in the following way:

$$T_1 p(n,t) = \frac{1}{2}(p(n+1,t-1) + p(n-1,t-1)) \tag{5.3}$$

where by 1 we denote the unit length of the normal lattice. The quantity $T_1 p((N-m)l, t-m)$ is the number of particles which just diffused in to the mode $(N-m)l$ from the normal lattice at time t-m.

At time t, at most t accelerator modes can contribute to Nl because particles in accelerator modes (N-s)l with $s > t$ have not had sufficient time to reach Nl. However at time t, particles which just entered (N-s)l at time t-s for $s < t$ and are going to be trapped there for m iterates, where $m > t$, can contribute to Nl at t.

The total rate of particles into the point Nl at t, from the other accelerator modes is then

$$\sum_{s=1}^{t} \frac{\psi(s)}{s} \hat{T}_1 p(Nl - sl, t-s) \tag{5.4}$$

The rate out of an accelerator mode is equal to $p(Nl, t-1)$, since everything that was in the accelerator mode will have to leave in one iteration (either to go to some other accelerator mode or back to the diffusion lattice).

From the previous arguments we see that the probability that a particle is found in the mode Nl at time t, is given by the equation

$$p(Nl,t) = \hat{T}_1 p(Nl,t) + \alpha \sum_{s=1}^{t} \Psi(s) \hat{T}_1 p(Nl - sl, t-s). \tag{5.5}$$

where $\Psi(s) = \psi(s)/s$.

Now let us look at the particles that reach the nearest neighbours of the accelerator modes.

First of all it is important to realise that not all the particles which were at Nl at time t-1 can contribute to $Nl+1$ and $Nl-1$ at time t. Only those which have finished their sojurn in the accelerator modes lattice are allowed to get back into the normal lattice. The rate of particles into the normal lattice from

the site Nl at time t is given by

$$p(Nl,t-1) - \alpha \sum_{s=1}^{t} \Psi(s) \hat{T}_1 p(Nl-(s-1)l, t-s). \qquad (5.6)$$

Notice that the term giving the 'loss' of particles from the nearest neighbours of the accelerator modes is the same as the one giving the 'gain' of particles to the accelerator mode itself only translated to the right by l. To see this, take, for example, the term $\frac{\gamma(m)}{m-1}\hat{T}_1 p(Nl-(m-1)l, t-m)$, which is contained in the sum which appears in the previous equation. This term corresponds to the particles which got into $(N-(m-1))l$ at time t-m and will be at Nl at time t, but will still be in an accelerator mode since they have to get to $Nl+l$ at t+1. Such particles are considered as a loss for the nearest neighbours of the lattice site Nl, and thus are attributed a minus sign in the above equation. Of course they are not a real loss because they are regained at the next accelerator mode. The term $\sum_{s=m+1}^{t} \Psi(s) \hat{T}_1 p(Nl-(s-1)l, t-s)$ just takes the contribution of all such terms for various trapping times in the same spirit as was done for the site Nl.

Half of the particles given by equation (5.6) will go to site Nl+1 and half to site Nl-1. The contribution to its nearest neighbours from the accelerator mode Nl will then be

$$\frac{1}{2} p(Nl,t-1) - \alpha \frac{1}{2} \sum_{s=1}^{t} \Psi(s) \hat{T}_1 p(Nl-(s-1)l, t-s) \qquad (5.7)$$

for each one of these sites. Apart from that, the sites Nl+1 (Nl-1) can be visited by normal random walk from sites Nl+2 (Nl-2) respectively.

According to the above reasoning, the probability of being in sites $Nl+1$ (Nl-1) at time t is given by the equation

$$p(Nl+1,t) = \frac{1}{2} p(Nl+2, t-1) + \frac{1}{2} p(Nl, t-1) - \alpha \frac{1}{2} \sum_{s=1}^{t} \Psi(s) \hat{T}_1 p(Nl-(s-1)l, t-s). \qquad (5.8)$$

The same equation applies for $p(Nl-1,t)$ only that $Nl+2$ is then replaced by $Nl-2$.

The random walk situation we are interested in, can now be described by the usual random walk equations plus an effective source term localised on the

lattice of accelerator modes and their nearest neighbours, that is

$$p(n,t) = \frac{1}{2}p(n+1,t-1) + \frac{1}{2}p(n-1,t-1) + S_A \tag{5.9}$$

where

$$\begin{aligned} S_A = & \alpha \sum_N \delta(n - Nl) \sum_{s=1}^{l} \Psi(s) \hat{T}_1 p(n - sl, t - s) \\ & - \frac{q}{2} \sum_N \delta(n - Nl - 1) \sum_{s=1}^{l} \Psi(s) \hat{T}_1 p(n - (s-1)l - 1, t - s) \\ & - \frac{q}{2} \sum_N \delta(n - Nl + 1) \sum_{s=1}^{l} \Psi(s) \hat{T}_1 p(n - (s-1)l + 1, t - s). \end{aligned} \tag{5.10}$$

This random walk model conserves the number of particles as is demanded by the physics of the problem. This can be easily shown as follows. Adding the equations (5.9-5.10) over all the lattice sites n we get

$$\sum_n p(n,t) - \sum_n p(n,t-1) = \sum_n S_A. \tag{5.11}$$

However,

$$\sum_n S_A = \alpha \sum_N \sum_{s=1}^{l} \Psi(s) \hat{T}_1 p(Nl - sl, t-1) - \alpha \sum_N \sum_{s=1}^{l} \Psi(s) \hat{T}_1 p(Nl - (s-1)l, t-1) = 0 \tag{5.12}$$

because the accelerator modes lattice is considered to be infinite. Thus $\sum_n p(n,t) = \sum_n p(n,t-1)$ for every t and the total number of particles is conserved.

The source term associated to the retardor modes, S_R, is similar to the one for the accelerator modes, only that it would be concentrated on a different infinite lattice, and the terms containing $p(n - sl)$ in S_A will have to be replaced by $p(n + sl)$ in S_R. This is due to the fact that particle in the retardor modes essentially stream in the opposite direction than particles in the accelerator modes. It is also straightforward to see that particle are conserved if we include in the normal random walk equations the source term S_R.

The source term corresponding to the effect of traps on the random walk, S_T, is going to be of a slightly different form. If a particle is caught in a trap, then it has to spend a finite time in the trap before it is released back into the normal random walk. For example, a particle that is driven into a trap by the random walk, will stay in this site for m time units, with probability $\alpha r(m)$ and then leave the trap to get back to the random walk. The parameter α does not

have to be the same for the traps and the accelerator modes, eventhough here it is considered to be the same. Note that the relevant probability distribution here is the first exit probability distribution r(s) which is related to the survival probability $\psi(s)$ (that is the probability that a particle starting in a trap at t=0 is still in the trap at t=s) by the simple relation $r(s)=-\frac{d\psi(s)}{ds}$. The probability distribution that a particle spends more than time t in the trap (or accelerator mode) is simply the integral of $\psi(s)$.

The rate into the trap at time t, is simply what gets into the trap via diffusion and is given by $T_1 p(n_T, t)$. What is important to find is the rate out of a trap site. If a fraction α of all the particles that landed in the trap are detained there for an infinite amount of time, then the rate out at time t would just be a fraction (1-α) of what was in the trap at time t-1, that is $(1-\alpha)p(n_T, t-1)$. However, we allow the possibility for particles that were trapped at time t-m, to be released from the trap, back to normal diffusion, at some later time t. Such particles will enhance the rate of particles out of the trap at time t. A particle first caught in the trap at time t-s, is going to be released from the trap with probability $\alpha r(s)$, and get back into the normal diffusion. The contribution to the rate out of the trap at time t from such particles, this is going to be $\alpha r(s) T_1 p(n_T, t-s)$. Then the total rate out of the trap is going to be

$$(1-\alpha)p(n_T, t-1) + \alpha \sum_{s=1}^{\infty} r(s) T_1 p(n_T, t-s). \qquad (5.13)$$

For particles that are forever trapped into the traps, the first exit probability is just a delta function at infinity, and the sum in the previous relation is identically zero.

The rate into the nearest neighbours to the trap site $n_T + 1 (n_T - 1)$ will be the normal rate corresponding to diffusion from $n_T + 2 (n_T - 2)$ plus half the rate out of the trap site. The rate out of the neighbouring sites is p(n_T + 1,t-1) (p(n_T − 1,t-1)) since everything on these sites will have to leave in one iteration.

Following the same reasoning as in the case of the accelerator modes, we

see that the source term S_T will be of the form

$$S_T = \alpha \sum_N \delta(n - Nl - n_T)(p(n,t-1) - \sum_{s=1}^{t} r(s)\hat{T}_1 p(n,t-s))$$
$$-\frac{\alpha}{2} \sum_N \delta(n - Nl - n_T - 1)(p(n-1,t-1) - \sum_{s=1}^{t} r(s)\hat{T}_1 p(n-1,t-s))$$
$$-\frac{\alpha}{2} \sum_N \delta(n - Nl - n_T + 1)(p(n+1,t-1) - \sum_{s=1}^{t} r(s)\hat{T}_1 p(n+1,t-s). \tag{5.14}$$

Because of the double periodicity of the map, the traps are assumed to be situated on the periodic lattice $Nl + n_T$ where $N \epsilon \mathbf{Z}$. Note that in the above source term, all the probability functions are calculated on the same point, because the particle is static for a certain time when it is trapped. It is also straightforward to check that the source term S_T conserves probability. This is consistent with the fact that a particle is counted when it is temporarily immobilised in a trap and it is not considered as lost from the system.

5.2.2 Continuous model

The discrete model proposed in the previous subsection can be written in a continuous form, which is more useful for analytical and numerical approximation.

Assume that the distance of two ordinary lattice points, 1, is taken to be infinitesimal, compared with the length scales involved in the model, but that the distance between two accelerator modes is kept finite. The time step taken for the hop between two normal sites is taken to be small, so that time can be thought of as a continuous variable. In order to avoid the introduction into the model of regions of space with infinite velocities, we assume that the jump from accelerator mode to accelerator mode takes a finite, but small, time.

Then expanding the random walk equations in small parameters which are the length scale of the normal lattice and the time unit for the hop from a normal lattice site to another lattice site we get to first order in α

$$\frac{\partial p}{\partial t} - D\nabla^2 p = \alpha S_A \tag{5.15}$$

where

$$S_A = \sum_N \delta(x - Nx_A)\delta(y - Ny_A) \times$$
$$\sum_{s=1}^{\infty} \Psi(s) H(s-t)(p(x - sx_A, y, t-s) - p(x - (s-1)x_A, y, t-s)) \tag{5.16}$$

where by H(s-t) we denote the Heaviside function and s is taken to be an integer. In the above derivation we tacitly assumed that the normal random walk, or diffusion, takes place on a two dimensional lattice but the accelerator modes make particles stream only in the x direction. In this equation x_A and y_A denote the distance between two accelerator modes.

The form of the equation is that of a diffusion equation in space with a localised source term on the accelerator mode lattice. Note that the discrete model had a source term localised on the accelerator mode lattice and the nearest neighbours but here because these lattice sites are thought of as one, the source term is replaced by one localised on the accelerator modes only. Formally the continuous source term is obtained by Taylor expanding the discrete source term in a small parameter which is the lattice length scale.

It is easy to see that the continuous model also conserves probability. Integrating over all space we get

$$\frac{\partial \int p dx dy}{\partial t} = \int S_A dx dy \tag{5.17}$$

But

$$\int S_A dx dy = \sum_{N,L} \sum_{s=1}^{\infty} \Psi(s) H(s-t)(p(Nx_A - sx_A, Ly_A, t-s) - p(Nx_A - (s-1)x_A, Ly_A, t-s)) \tag{5.18}$$

which is equal to 0, since the summation over N is a doubly infinite summation and we can shift N by s in the first sum of the right hand side of equation (5.18) and by (s+1) in the second, essentially getting the same result. Hence $\int p dx dy = const.$, which implies that the number of particles in the continuous model is conserved.

The continuous form of the source term for the retardor modes, S_R, is obtained in a straightforward way from the discrete one, and is found to be such that probability is conserved.

The continuous analogue of the source term for the traps, S_T, is of a slightly different form

$$S_T = -\frac{1}{4} \sum_{N,L} \nabla^2 [\delta(x - Nx_T - x_0)\delta(y - Ly_T - y_0)(p(x,y,t) - \sum_{s=1}^{t} r(s) p(x,y,t-s))] \tag{5.19}$$

Summarizing, we see that, both in the discrete and in the continuous case, our basic model is to consider that over the whole of phase space a diffusion equation with a constant diffusion coefficient is applicable to capture the dynamics, except on the accelerator modes and in the stable islands. To model the transfer of particles from one accelerator mode to another and the effect of the trapping of particles in the stable islands we add effective sources to the diffusion equation, localised on the lattice of structures. Treating these sources as a series of delta functions is of course an approximation but the complexity due to finite size regions can reasonably be absorbed into the definition of the $\Psi(m)$'s.

Our equations are in the form of a delay equation because of the terms p(x,y,t-m) that appear in the source terms. The existence of such terms is expected on quite general grounds due to the fact that a particle takes a finite time to make a jump from one accelerator mode to another and spends a finite time in the vicinity of a stable island.

Though equations (5.15),(5.16) and (5.19) or their discrete analogues can be solved exactly the solution is extremely complicated. A full solution in terms of a formal series in α is given in Appendix 5.3. Below we give an iterative scheme based on the smallness of α, which is a reasonable procedure for the case where most of the phase plane is chaotic. This is particularly useful when combined with the fact that we are only interested in the low moments of the distribution function, which are all that is necessary for the calculation of the effective diffusion coefficient. The perturbation scheme given below, is equally valid for the continuous and the discrete case. For brevity it is given here for the continuous case but it is the same for the discrete one, only that the discrete Green function will have to be used. More details can be found in Appendix 5.2.

We write our equation in the more compact operator form

$$D\mathrm{p}(\mathrm{x},\mathrm{y},\mathrm{t}) = \epsilon \hat{L}\mathrm{p}(\mathrm{x},\mathrm{y},\mathrm{t}) + \delta(\mathrm{x}-\mathrm{x}_0)\delta(\mathrm{y}-\mathrm{y}_0) \qquad (5.20)$$

where we have introduced a real source of particles at the point x_0, y_0 . Here $\hat{L}\mathrm{p}(\mathrm{x},\mathrm{y},\mathrm{t})$ represents the effective source term and ϵ a small parameter asso-

ciated with n. For $\epsilon = 0$ the solution of (5.20) which is the solution for the diffusion equation with the point source is just the Green's function and is given by

$$p^{(0)}(x,y,t) = \frac{D}{4\pi(t-t_0)} exp(-D\frac{(x-x_0)^2+(y-y_0)^2}{4(t-t_0)})H(t-t_0) \qquad (5.21)$$

[Ma53] where $H(t-t_0)$ is the Heavyside function. Then by writing $p = p^{(0)} + \epsilon p^1 + O(\epsilon^2)$ and going to order ϵ we have

$$Dp^{(1)}(x,y,t) = R(x,y,t) \qquad (5.22)$$

where $R(x,y,t) = Lp^{(0)}(x,y,t)$ is a known function of x,y,t. The solution to this equation is given by

$$p^{(1)} = \int G(x,y,t \mid x',y',t')R(x',y',t')dx'dy'dt' \qquad (5.23)$$

where $G(x,y,t \mid x',y',t')$ is the Green's function for the operator D and is given by (5.22) with x',y',t' replacing x_0,y_0,t_0. The integrations with respect to x' and y' are over the whole space and the integration with respect to t' is from 0 to t. Then to first order, the correction to the distribution function is given by

$$p^{(1)}(x,y,t) = \int G(x',y',t' \mid x,y,t)(S_{A,R}(p^{(0)}(x',y',t'))+S_T(p^{(0)}(x',y',t')))dx'dy'dt' \qquad (5.24)$$

where by $S_{A,R}$ we denote the sum of the source terms corresponding to the accelerator modes and the retardor modes.

5.3 Calculation of the Diffusion Coefficient.

The quantities we are primarily interested in are the moments of the probability distribution p(x,y,t). We define two effective diffusion coefficients D_x and D_y by

$$D_x(t) = \frac{M_{2,x}(t)}{tM_0} \quad and \quad D_y(t) = \frac{M_{2,y}(t)}{tM_0} \qquad (5.25)$$

where

$$M_{2,x}(t) = \int x^2 p(x,y,t)dxdy = < x^2 > \qquad (5.26)$$

$$M_{2,y}(t) = \int y^2 p(x,y,t)dxdy = < y^2 > \qquad (5.27)$$

$$M_0(x) = \int p(x, y, t) dx dy \tag{5.28}$$

and the integrations are over all space. These diffusion coefficients characterize the motion over the whole of phase space which may now be taken to be uniform. Importantly $D_x(t)$ and $D_y(t)$ are the diffusion coefficients which are to be compared with values of $\frac{\langle \Delta x^2 \rangle}{n}$ and $\frac{\langle \Delta y^2 \rangle}{n}$ obtained by iterating the maps in numerical experiments. In particular we are interested in the behaviour of $D_x(t)$ and $D_y(t)$ as functions of time for our simple stochastic model.

After some cumbersome algebra we can express the moments in the form

$$M_{2,x}(t) = Dt + A_1 + A_2 + A_T \tag{5.29}$$

$$M_{2,y}(t) = Dt \tag{5.30}$$

where the functions A_1, A_2, A_T which are functions of t, are given explicitly in Appendix 5.1. The zeroth moment M_0 is always equal to 1, because of the fact that our model preserves the number of particles. In Appendix 5.2 this perturbation method is briefly sketched for the discrete model, and is shown to give essentially the same results.

5.4 Results.

The diffusion coefficients in x and y are calculated using the analytical formulas obtained and given in Appendix 5.1 or Appendix 5.2. In the numerical results presented below the trapping time distribution is taken to be a delta function law of the form

$$\tau(m) = \sum_i A_i \delta(m - M_i) \tag{5.31}$$

For the sake of simplicity we assume that the trapping probability in an accelerator mode is the same as the trapping probability in a retardor mode or a trap. The value of the parameter α is taken to be small enough, so that the perturbative approach for the solution of the model presented here is valid. In the numerical results presented here it is taken to be of the order 10^{-1}. We observe first that the diffusion coefficient $D_x(t)$ shows fluctuations in time in

the form of big humps which correspond to the effect of trapping in the accelerator mode for a finite time (see fig.5.2) . The number of the bumps is equal to the number of peaks in the distribution function $\psi(m)$. After such jumps the diffusion coefficient $D_x(t)$ relaxes slowly to a constant value D_l larger than D_0 so that the effect of the particle being trapped in an accelerator mode for a finite number of iterations leads to the enhancement of the effective diffusion coefficient measured at infinite times. This is explained using an asymptotic analysis of the model, in Appendix 5.4.

If the effect of the accelerator modes is switched off ($\alpha = 0$) then what we find is a dip in the diffusion coefficient. This is entirely due to the presence of traps (that is the stable islands in the particle dynamics). This is illustrated in figure 5.3 .

The oscillations (fluctuations) observed in $D_x(t)$ are similar to the ones found in the calculated diffusion coefficients obtained from numerical simulations of maps (see figure 5.1 where such diffusion coefficients are plotted as functions of time for the standard and the web map). The multiple trapping in an accelerator mode which is assumed in our model in order to get more than one 'bump' in our theoretical diffusion coefficient can be observed in maps. Figure 5.4 for example shows an orbit of the web map which is trapped in an accelerator mode for a number of iterates then it is detrapped and diffuses for a long time and then it is trapped again in an accelerator mode for a long number of iterates. Therefore the multiple delta function type trapping distribution considered here models, at least qualitatively, the true particle dynamics.

The behaviour of $D_y(t)$ does not show any significant fluctuations and this is expected since we only allowed the accelerator modes to be connected in the x direction. In $D_y(t)$ we just see the effect of traps.

Before closing this section, a comparison of our results with the results of a different model for a similar situation is appropriate. Ishizaki et al [IHKM91] using a method based on a statistical mechanics formalism of dynamical systems tried to get an estimate of the long time behaviour of the diffusion coefficient as a function of time in the case of repeated sticking to an accelerator mode.

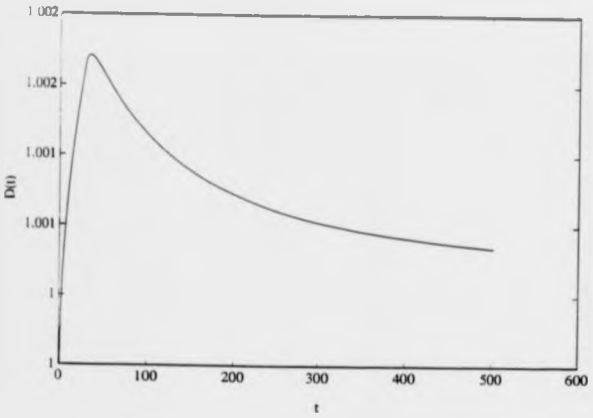

Figure 5.2. Diffusion coefficient calculated from the results of our model in the case of accelerator modes and a delta function trapping probability distribution.

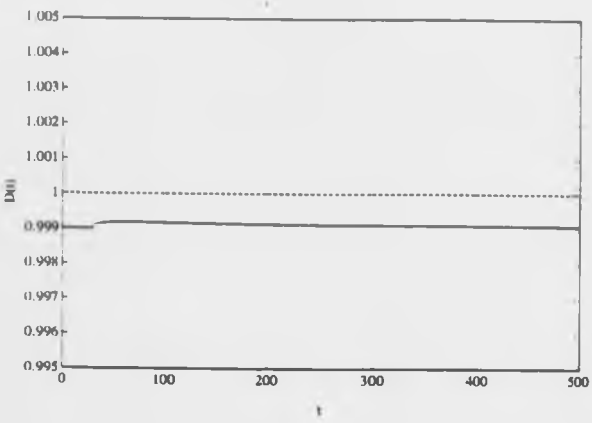

Figure 5.3. Diffusion coefficient calculated from the results of our model in the case of traps only, with a delta function trapping probability. The dashed line is the diffusion coefficient in the case of no traps. The bump is due to the release of particles from the trap after a time lag.

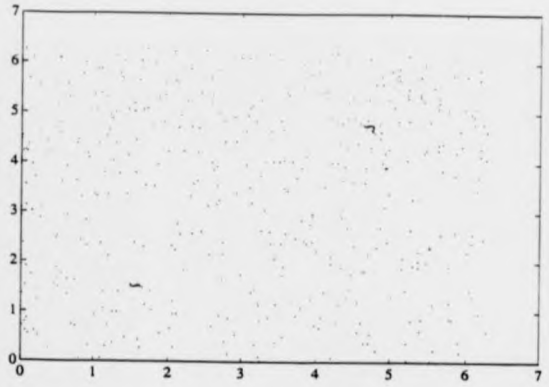

Figure 5.4. A typical single orbit of the web map. The two small continuous loops show the existence of multiple trapping in the accelerator modes that can be modeled by a multiple delta function trapping distribution.

Assuming that the probability for an orbit to stick in an accelerator mode longer than n is of the power law form $\psi(n) \sim n^{-(\beta-1)}$ for $n \gg 1$, they found that the diffusion coefficient calculated for orbits that may stick to the accelerator modes is $D \sim n^{2-\beta}$. Taking into account these orbits, as well as orbits that diffuse without getting trapped at all, the diffusion coefficient should be of the form $D(n) = D_1 + D_2 n^{2-\beta}$ where $2 > \beta > 1$.

We will show that our model can cover this case as well, giving the same asymptotic results. Assume that in our model instead of a trapping distribution function of a delta function form as in (5.31), we take a power law form, that is, assume that $\psi(n) \sim n^{-\beta}$ for $n \gg 1$. By definition $\psi(n) = \int_n^\infty \psi(n)dn$ and here $\psi(n) \sim n^{-(\beta-1)}$ namely the form used by Ishizaki et al [IHKM91]. A short note on the ψ's and ψ's used is of relevance here. As mentioned above in the formulation of the model, $r(m)$ is the probability distribution that a particle that enters an accelerator mode at time t=0 stays there for m time units and is released on the m+1 time unit. The probability that a particle which was in an accelerator mode at time t=0 is still in the accelerator mode at time t=m is equal to $\psi(m)$ where $r(m) = \frac{\psi(m)}{m}$ [MO86]. Then the probability that a particle stays in an accelerator mode for time greater than m is just $\int_m \psi(m')dm'$.

The major difference between our delta function like distribution function and this power law is that in our model the detrapping is ensured whereas using the power law distribution function the possibility of trapping for an infinite number of iterations is not excluded.

The asymptotic behaviour of our model is studied in Appendix 5.3. Using the results of Appendices 5.3 and 5.4 we find that $D_x(t) = D_1 + D_2 t^{-\beta+2}$ as $t \to \infty$ which is identical to the result obtained by Ishizaki et al [IHKM91]. The second moment and the diffusion coefficient as calculated by our model, taking into account the accelerator modes, in the case of a power law trapping distribution are shown in figure 5.5 . Our results are in remarkable agreement with the results of Ishizaki et al [IHKM91] obtained by direct iteration of the standard map.

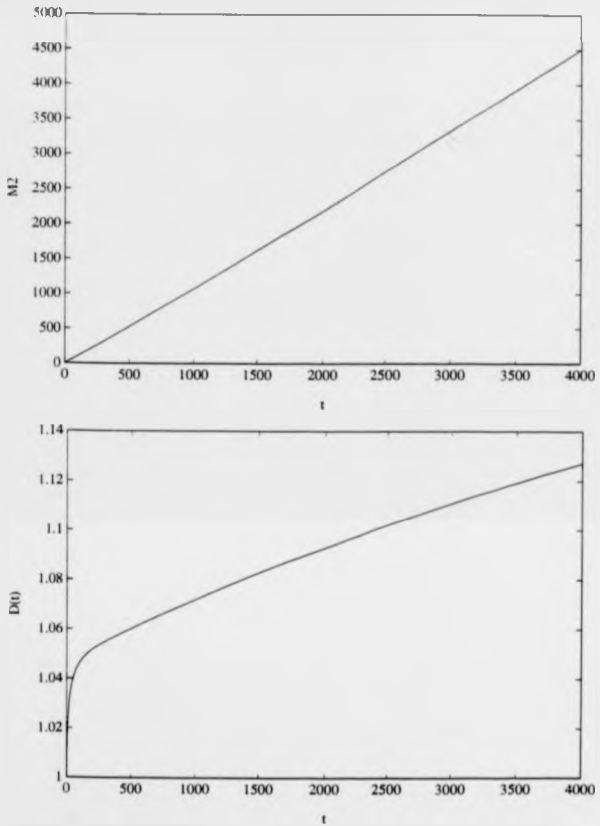

Figure 5.5. (a) Second moment and (b) Diffusion coefficient for the case of accelerator modes, considering a distribution function for the trapping times with a power law decay.

In the case where only the trap terms are present, the asymptotic time dependence is of the form $D_x(t) = D_1 + D_2 t^{-1}$ which corresponds to a diffusion coefficient decaying to the constant one. Note that the constant terms D_1 in the above expressions, are not equal to D the background diffusion constant.

The present model can also predict another interesting result concerning the effect of the form of the trapping distribution in the accelerator modes on the asymptotic time behaviour of the random walk. This is a result giving a connection between the microscopic properties of the random walk, which is actually an approximation of motion in the connected chaotic regions of the phase space, (trapping distribution in the lattice sites of the accelerator modes) with its macroscopic and easily measurable properties, that is the asymptotic time behaviour of the diffusion coefficient. Namely an exponentially decaying trapping distribution function of the form $\psi(m) = A exp(-\lambda m)$ results in a diffusion coefficient independent of time. That is the accelerator modes show no observable effects on the asymptotic time dependence of the effective diffusion coefficient. The details of the calculation, which is in the same spirit as that for the case of the power law distribution function, are presented in Appendix 5.4. This is of course in contrast to the case of a power law trapping distribution in the accelerator modes where the diffusion coefficient has a power law asymptotic behaviour in time and then the effect of the accelerator modes is shown in the asymptotic behaviour of the random walk.

In a recent paper Zaslavskii and Tippet [ZT91] studied the statistical behaviour of a dynamical system that can present long flights in certain parts of phase space, and focused their attention on the effect of the Poincare recurrence statistics on the asymptotic behaviour of the diffusion through phase space caused by the chaotic properties of the motion. According to their extensive numerical results, for certain parameter values, for which the Poincaré recurrence statistics follow an exponential law, the diffusion coefficient for the dynamical system in question, approaches a constant value for large time. In contrast, in the case where parameter values were chosen such that the Poincare recurrence statistics follow a power law, the diffusion coefficient diverges asymptotically in

time also following a power law.

We can identify the integral of the Poincare recurrence probability distribution function in the parts of phase space associated with the existence of long flights with the trapping time distribution $\Psi(m)$ in the accelerator modes used in the present model. Hence, the results that Zaslavskii and Tippet [ZT91] obtained by extensive numerical calculations can be explained analytically by the use of the theoretical model proposed in this paper. Namely when the Poincare recurrence statistics follow a power law, $\Psi(m)$ and D also follow power laws. When the Poincaré recurrence statistics follow an exponential law then $\Psi(m)$ also follows an exponential law but D is now constant.

5.5 Conclusions.

We have constructed a simple stochastic model describing the coexistence of accelerator modes and diffusion for area preserving chaotic maps. The analytically predicted forms for the effective diffusion coefficient of this simple model show the qualitative behaviour obtained by direct numerical integration. The different asymptotic time behaviour found in various numerical simulations can be calculated in terms of the trapping probability function $\Psi(m)$.

Our model is shown to be consistent in the asymptotic time behaviour with the work of Ishizaki et al [IHKM91], that studied the asymptotic behaviour of the diffusion coefficient in the presence of accelerator modes. However, our treatment of the problem using rate equations enables us to obtain intermediate time results whereas the treatment in [IHKM91] is purely asymptotic.

Furthermore, the asymptotic results of our model are shown to coincide with the numerical observations of Zaslavskii and Tippet [ZT91], in the case of a chaotic flow with occurence of jets, in which it was shown that there is a link between the microscopic properties of a chaotic motion (Poincaré recurrence) and the macroscopic properties (time dependence of the diffusion coefficient).

Finally, eventhough our model has been formulated for a very simple rectangular lattice having a periodic infinite array of structures (accelerator modes or traps), which is the situation that corresponds to an area preserving map

of the torus, the generalisation to more general lattices is in principle possible and straightforward. Also generalisation to three dimensions is straightforward, but the asymptotic results are expected to be different since for random walks of dimensions higher than two, the probability that a diffusion particle reaches any particular point, for example a trapped site, is no longer equal to 1.

Chapter 6

Conclusion.

6.1 Conclusions.

In this thesis the possibility of studying the statistical properties of strongly chaotic Hamiltonian systems using well known results from the theory of diffusion processes has been investigated.

In Chapter 2, the asymptotic statistical properties of a certain dynamical system, the web map, were studied. In particular, the diffusion coefficient for the momentum coordinates of the web map was calculated as a function of the perturbation parameter, using an analytical approach based on the assumption of ergodicity for the chaotic motion and the quick fall of velocity autocorrelation functions. The general form of the results obtained was that the diffusion coefficient depended in an oscillatory manner as a function of the perturbation parameter and relaxed to a monotonic value for large values of this parameter. The analytical results obtained agreed very well with those obtained by direct iteration of the map except at some particular values of the perturbation parameter. These discrepancies were shown to be due to the existence of structures in the phase space of the map. These structures were either accelerator modes which resulted in an increase of the diffusion coefficient, or stable islands which resulted in a decrease. It is worth mentioning, that the analytical results show an increase or decrease for these values of the perturbation parameter, although this might be smaller than the one numerically observed. This effect

is shown in the analytical results since short time correlations are incorporated in the analytical method.

The web map is a map having a special symmetry. In particular it is a map symmetric in both action and angle variables and so it can be written as a map of the torus. Other maps with the same symmetry are the standard map or the Froeschlé map. However, general maps employed in physical models may not have this special symmetry, which is called double periodicity. Good examples of such maps are the Fermi map and Chirikov's separatrix map. These maps are only periodic in the angle coordinate and can be thought of as maps on the cylinder.

In Chapter 3, the diffusion coefficient in the action (momentum) of such maps was studied, in order to see whether the same fluctuations observed in the diffusion coefficient of maps of the torus, as a function of the perturbation parameter due to correlations, would be observed in such maps. The maps that were studied were symplectic maps of dimension $n \geq 2$ for which the chaotic region was supposed to be infinite.

An analytical method was formulated for the calculation of the diffusion coefficient of maps of the cylinder in the same spirit as the method used by Karney, Rechester and White for maps of the torus. Importantly it was proved, for maps which are not doubly periodic that the quasilinear value of the diffusion coefficient, that is the one obtained if all the correlations are neglected, is the correct one. This is in contrast to what happens in the case of maps with a double periodicity where our method predicts fluctuations of the diffusion coefficient as a function of the perturbation parameter around the quasilinear result. All these results are supported by numerical investigations, where maps of the cylinder, which are obtained by a perturbation of doubly periodic maps, have been used.

The resemblance of the evolution of a chaotic system with a diffusion process has been checked using more elaborate criteria than the existence of a diffusion coefficient defined by the relation $\lim_{t\to\infty} \frac{\langle \Delta p^2 \rangle}{2t}$. In Chapter 4 the evolution of an initial distribution of particles in a bounded domain of phase space under

a chaotic map was studied and compared to the evolution of the same initial distribution under a diffusion process. It was shown that physical quantities such as the average number of particles in the bounded domain as a function of time, obtained from the evolution of the chaotic system can be very well approximated by those obtained from the diffusion equation.

This resemblance was used as a means of calculating the appropriate diffusion coefficient for chaotic systems. A numerical method for the extraction of the diffusion coefficient for a chaotic system, using the procedure described in the previous paragraph, was formulated and checked for three different maps, the standard map, the web map and the Fermi map. The results were very satisfactory, and it was shown that

1) The method is faster and more accurate than the usual way of calculating the diffusion coefficient as $\lim_{t\to\infty} \frac{\langle x^2 \rangle}{2t}$.

2) It can work for systems for which the chaotic part of phase space is bounded such as the Fermi map.

3) It can predict changes of the diffusion coefficient with position in phase space. In particular, this has been tested on the web map where the diffusion coefficient is known to be space dependent. A WKB procedure based on the slowness of the variation of the diffusion coefficient with position in phase space was used to extract the functional form of the position dependent diffusion coefficient of the web map.

4) Finally, using this method further numerical results, in favour of the theory suggested in Chapter 3 were obtained. In particular the web map was studied for various symmetries, where a crossover from double periodicity to single periodicity occurs. It was shown that there is a sharp transition to the quasilinear value for the diffusion coefficient as we pass from the doubly periodic case to the singly periodic case.

In Chapter 2, where the web map was studied, the importance of structures in the diffusion through phase space in a chaotic system was noted. Some general results on the effect of such structures in the transport through phase space would be desirable. As a starting point on this problem, a random walk

model in the presence of structures was formulated, that would serve as a model of a strongly chaotic system. In parts of phase space where chaos is dominant, motion is well approximated by a random walk (which is the discrete space and time version of the diffusion process). The particles are driven by the random walk to parts of phase space where structures exist, such as periodic orbit islands and accelerator modes. In such parts of phase space long time correlations exist and the simple random walk model is no longer sufficient. The motion there will have to be approximated differently. For example the particle will have to stop for a time interval if it lands on a stable island or it will make correlated jumps in one direction if it lands on an accelerator mode. The full motion of the particle then modelled assuming a normal random walk with some properly chosen source functions on the points where the structures exist.

This random walk model has been used to calculate the quantities that are usually computed for chaotic maps, such as the second moment of the displacement of the particle. The results obtained were seen to be in accordance with the results obtained for chaotic systems. The important feature of such a model is that it has incorporated the correlation effects that are observed in real chaotic systems, thus giving a better statistical description than an ordinary random walk (or simple diffusion equation). For instance, using this model the behaviour of the diffusion coefficient in the presence of accelerator modes has been predicted, as well as the connection between the form of the Poincare recurrence statistics and the long time asymptotic statistical behaviour of the system in terms of moments.

6.2 Further Work.

A number of problems meriting further investigation arose during the preparation of this thesis.

As a starting point it would be very interesting to conduct more detailed studies of the transport properties of maps on the cylinder for more general cases, relaxing the conditions we assumed in Chapter 3. The comparison of

the transport properties of symplectic maps on the cylinder and on the torus, both in the regions of weak chaos and strong chaos promises interesting results not only from the theoretical point of view but also from the point of view of applications.

More detailed studies of the transport through phase space when chaos coexists with regular structures such islands or accelerator modes can be made. More elaborate kinetic equations in the spirit of those given in Chapter 5 may be written, providing a more complete description of a chaotic system with a divided phase space. To this end, Markov models can be used locally, near the structures, for the determination of the proper boundary conditions and the source terms that have to be inserted in the kinetic equations.

Finally it would be of interest to apply our results or extend them, considering specific physical systems, where transport due to Hamiltonian chaos occurs, such as the advection of passive scalars or passive vectors in laminar flows. The study of such systems could be of use to a great number of applications ranging from the study of mixing of tracers in laminar flows (chaotic advection) to dynamo theory.

Chapter 7

Appendices

7.1 APPENDIX 2.1

The unperturbed hamiltonian for the q=4 web map is given by

$$H_4 = -\Pi_4(cosv + cosu) \tag{7.1}$$

where $\Pi_4 = \frac{K}{27}$. Keeping only two terms in the time dependent perturbation corresponding to the two closer to resonance with the oscillator harmonics of the wave packet the time dependent perturbation is written in the form

$$V = -\Pi_4 cosucos(\frac{\omega t}{4}) \tag{7.2}$$

For small values of the perturbation parameter K it is valid to take the solution of the set of equations generated by the Hamiltonian $H = H_4 + V$ as written in the form

$$u = u_0 + \delta u \tag{7.3}$$

$$v = v_0 + \delta v \tag{7.4}$$

where u_0 and v_0 is a solution of the unperturbed equations of motion generated by the Hamiltonian H_4 and δu and δv are considered as small deviations from the unperturbed solutions. Substituting equations (7.3) and (7.4) into the full equations of motion and linearising in δu and δv we obtain the following set of equations for the evolution of the deviations

$$\delta u = \Pi_4 cosv_0 \delta v \tag{7.5}$$

$$\dot{\delta v} = -(\Omega_4 cos u_0 + 2\Omega_4 cos u_0 cos(\frac{\omega t}{4}))\delta u - 2\Omega_4 sin u_0 cos(\frac{\omega t}{4}) \qquad (7.6)$$

In the above set of equations u_0 and v_0 are functions of time which can be computed. So the above system is a linear equation for the deviations from the unperturbed solutions with time varying coefficients.

It is important to see how δu and δv behave when u_0 and v_0 is the separatrix solution for the Hamiltonian H_4. For the separatrix solution where H_4=0 we have

$$tan(\frac{u_0}{2}) = exp(\mp\Omega_4 t) \qquad (7.7)$$

$$tan(\frac{v_0}{2}) = exp(\pm\Omega_4 t) \qquad (7.8)$$

Substituting those expressions in the equation for the evolution of δu and δv we obtain the following set of equations

$$\dot{\delta u} = \mp\Omega_4 tanh(\Omega_4 t)\delta v \qquad (7.9)$$

$$\dot{\delta v} = \mp\Omega_4 tanh(\Omega_4 t)(1 + 2cos(\frac{\omega t}{4}))\delta u - 2\Omega_4 \frac{1}{cosh(\Omega_4 t)} cos(\frac{\omega t}{4}) \qquad (7.10)$$

In the limit $t \to \infty$ the above set of equations becomes

$$\dot{\delta u} - \Omega_4^2(1 + 2cos(\frac{\omega t}{4}))\delta u = 0 \qquad (7.11)$$

and

$$\dot{\delta u} = \mp\Omega_4 \delta v \qquad (7.12)$$

The first of the above two equation is a Mathieu equation [McL64] which can be brought in the canonical form

$$\frac{d^2\delta u}{d\tau^2} + (a - 2qcos2\tau)\delta u = 0 \qquad (7.13)$$

by the transformation $\tau = \frac{\omega t}{8}$. Then for the values of a and q obtained the Mathieu equation (for small K) has alway unstable solutions (unbounded) and this is a manifestation of the instability leading to chaos near the unperturbed separatrix solution.

7.2 APPENDIX 3.1.

In this appendix we show that a regular lattice of coherent structures has a greater effect on the diffusion through phase space than a disordered one. To do this we use a simple random walk model which simulates the chaotic motion and introduce the effect of islands of coherent motion on the diffusion through phase space by considering a lattice of perfect traps (absorbing points). The effect of the presence of a trap on the random walk (diffusion through phase space) is quantified by calculating the probability that a particle is not trapped as a function of time. We consider the case of a regular lattice of traps and also a slightly disordered lattice of traps. The first case corresponding to diffusion through phase space for doubly periodic maps, the second corresponding to diffusion for maps on the cylinder close to the doubly periodic case. For simplicity we present here the case of the one dimensional random walk but our results hold in any dimension.

The model was originally introduced by Halagurov and Vaks [BV74] in a different physical context. They solved the diffusion equation in one dimension on a lattice of traps situated at the points x_i and found that the probability a particle is **not** trapped to be of the form:

$$P(t) = \sum_i \sum_{n=0}^{\infty} \frac{4}{l_i} exp(-\frac{D(2n+1)^2 t}{4l_i^2}) \frac{l_i}{(2n+1)^2 \pi^2} \tag{7.14}$$

where D is the diffusion coefficient,$l_i = x_{i+1} - x_i$ is the distance between two subsequent traps, and L is the length of the chain.

We use this result to study the difference between the case of a regular lattice of traps and a disordered lattice of traps.

A.Regular lattice.

Assume that the traps are situated on the periodic lattice $x_i = x_0 + iL_0$. Then $l_i = L_0$ for every i and

$$P_R(t) = N \sum_{n=0}^{\infty} \frac{4}{L} exp(-\frac{D(2n+1)^2 t}{L_0^2}) \frac{L_0}{(2n+1)^2 \pi^2} \tag{7.15}$$

where N is the total number of traps in the lattice.

B.Disordered lattice.

For the case of a disordered lattice of traps, with the probability distribution for the distance between two traps equal to $f(l)$

$$P_D(t) = N\sum_{n=0}^{\infty}\frac{4}{L}\int_0^{\infty} f(l)exp(-\frac{D(2n+1)^2t}{l^2})\frac{l}{(2n+1)^2\pi^2}dl \qquad (7.16)$$

An appropriate distribution function for the distance between two traps for the physical situation we are studying is a top hat distribution where $f(l) = \frac{1}{2a}$ for $L_0 - a < l < L_0 + a$ and zero elsewhere. Thus a is a measure of the disorder of the lattice of traps. This probability distribution goes to the delta function distribution $f(l) = \delta(l - L_0)$, which corresponds to a periodic lattice of traps in the limit $a \to 0$. Using the top hat distribution, the probability that a particle is not trapped becomes

$$P_D(t) = \frac{N}{2a}\sum_{n=0}^{\infty}\frac{4}{L}\int_{L_0-a}^{L_0+a} exp(-\frac{D(2n+1)^2t}{l^2})\frac{l}{(2n+1)^2\pi^2}dl \qquad (7.17)$$

It is easy to prove that

$$\int_{x_0-\epsilon}^{x_0+\epsilon} f(x)dx > 2\epsilon f(x_0) \qquad (7.18)$$

for functions such that $f(x) > 0$ and $f''(x_0) > 0$. If we take $f_n(x)$ to be

$$f_n(x) = exp(-\frac{D(2n+1)^2\pi^2t}{2x^2})\frac{x}{(2n+1)^2\pi^2} \qquad (7.19)$$

we find that every term in the sum defining $P_D(t)$ is greater than the corresponding term in the sum defining $P_N(t)$ if the condition

$$D(2n+1)^2\pi^2t > L_0^2 \qquad (7.20)$$

holds. For large enough time, which is the case we are interested in, this is always true. Moreover this holds for small times as long as the mean free path of the particle is greater than the average distance between the traps. This is a very reasonable condition since in this case the particle can distinguish between the case of a disordered lattice of traps and a regular lattice of traps. Assuming this condition is satisfied we have that $P_D(t) > P_N(t)$ for every t. Thus correlation effects are more pronounced for a regular array of traps and hence corrections to the quasilinear value for the diffusion coefficient are expected to be larger than for a disordered array.

7.3 APPENDIX 3.2.

Another important point that arises is whether the diffusion coefficient as defined in equation (3.6) can take nonzero values for the more general case of maps on the cylinder. To answer this problem it is necessary first to be able to prove that the maps can have chaotic orbits which are unbounded in the momenta. To do this we use the results obtained by Aubry and Abramovicci [AA90] in the anti-integrable limit. According to a theorem proved by these authors, a particular symplectic map in one dimension defined by a Frenkel-Kontorowa model which has an energy functional of the form

$$W(u) = \sum_i \epsilon L(u_i, u_{i+1}) + V(u_i) \tag{7.21}$$

where L(x,y) is the interaction term between the different atoms in the chain and V(x) is a potential with which the atoms interact and satisfies several conditions that make it close enough to the potential V(x)=1-cos(x), chaotic trajectories with unbounded momenta exist for large enough values of the perturbation parameter if

$$\frac{\partial^2 L(x,y)}{\partial x \partial y} \tag{7.22}$$

is bounded for every value of x and y. We will use this theorem to show that this is the case for example in the one dimensional radial twist map of the form

$$p_{n+1} = p_n + \epsilon \sin\theta_n \tag{7.23}$$

$$\theta_{n+1} = \theta_n + a(p_{n+1}) \tag{7.24}$$

This map is given by an energy functional of the form given in equation (7.21) with $V(\theta) = 1 - cos\theta$ and $L(\theta, \theta') = \int^{\theta-\theta'} a^{-1}(\theta - \theta')d(\theta - \theta')$, where a^{-1} is the inverse function of a(p) and $K = \frac{1}{\epsilon}$. For such a map, after a little algebra we obtain,

$$\frac{\partial^2 L(x,y)}{\partial x \partial y} = \frac{\partial a^{-1}(y-x)}{\partial y} \tag{7.25}$$

which is equal to

$$\frac{\partial^2 L(x,y)}{\partial x \partial y} = \frac{1}{da(p)/dp}. \tag{7.26}$$

and p is defined by the relation

$$y = x + a(p) \tag{7.27}$$

If we choose a(p) to be a monotonic function of p, such as for example $a(p) = p + \lambda p^3$, for proper values of the parameter λ, or $a(p) = p + \lambda p^4$ an we concentrate on orbits with positive p, then we get that

$$\frac{\partial^2 k(x,y)}{\partial x \partial y} \tag{7.28}$$

is a bounded function for all x and y. So for certain radial twist maps there exist chaotic orbits with unbounded momenta and the diffusion coefficient defined as in equation (3.6) is non vanishing. Similar results are expected to hold for the higher dimensional cases and hence the diffusion tensor for higher dimensional symplectic maps on the cylinder is defined as in equation (3.6) and is nonzero.

7.4 APPENDIX 3.3

In this appendix we use the results obtained by Mackay and Meiss [MM92] on the minimum perturbation parameter for which one can formally prove the existence of chaotic orbits coming from the anti-integrable limit for the case of the standard map and a standard like map with some nonlinear perturbation in the force function a(p). Using a Frenkel-Kontorowa model like the one defined in Appendix 3.2 the orbits of the symplectic map that corresponds to this energy functional are given by sequences u_i that make this energy functional stationary. Let us choose a stationary sequence in the anti-integrable limit u_i and define

$$b(u) = sup_{i,N} \mid D_2L(u_{i-1}, u_i) + D_1L(u_i, u_{i+1}) \mid \qquad (7.29)$$

Let us denote by Σ_B all the sequences u_i for which $b(u) \leq B$. According to a theorem proved by Mackay and Meiss [MM92] given $B > 0$ there exists $\epsilon_0(B) > 0$ such that all stationary states of Σ_B persist for $\epsilon < \epsilon_0$ and remain nondegenerate.

The usual perturbation parameter K we use in the definition of the symplectic maps in the text is inversely proportional to the ϵ mentioned in the theorem. An upper bound on ϵ_0 is given by the authors as $\epsilon_0 < \frac{\alpha^2\beta}{B+2\beta}$ where the parameters in the above formula are defined by $\mid u_i - u_i^{AI} \mid \leq \delta, \mid D^2V(u_i)^{-1} \mid < \alpha^{-1}$, $\mid\mid DG \mid\mid \leq \beta$ and $\mid\mid G(0) \mid\mid \leq B$ where G is the operator defined by $G(u_i) = -D_2L(u_{i-1}, u_i) - D_1L(u_i, u_{i+1})$. In the previous relation D_1 and D_2 denote differentiation with respect to the first and the second argument of the function respectively.

We take two maps with the same potential function V so that the stationary sequences for both maps in the anti-integrable limit are the same and we change L in such a way that in the first case we have the standard map and in the second case we have a perturbation to the standard map with a nonlinear force function. In this case the values of α and δ for the two maps are the same but B and β are different.

The maximum estimate for ϵ_0 will be given if in the inequality that gives

the upper bound for ϵ_n we substitute the minimum estimates for B and β. This would then give the minimum estimate for K, K_{min} such that if $K > K_{min}$ the stationary sequence from the anti-integrable limit persists and remains non degenerate. That is for $K > K_{min}$ we have well defined chaotic orbits δ-close to the ones we had in the anti-integrable limit.

We study maps of the form

$$p_{n+1} = p_n + Kf(\theta_n) \tag{7.30}$$

$$\theta_{n+1} = \theta_n + a(p_{n+1}) \tag{7.31}$$

which are given by an action of the form

$$h(\theta, \theta') = \sum [cL(\theta, \theta') + V(\theta)] \tag{7.32}$$

with

$$L(\theta, \theta') = L(\theta - \theta') = \int^{\theta - \theta'} a^{-1}(\theta - \theta')d(\theta - \theta') \tag{7.33}$$

and $K_{min} \sim \frac{1}{\alpha'_0}$. For such maps B depends on the value of $a^{-1}(\theta - \theta')$ on the sequence chosen and β depends on the value of $\frac{\partial a^{-1}(\theta - \theta')}{\partial \theta}$ + $\frac{\partial a^{-1}(\theta'' - \theta)}{\partial \theta}$ on the sequence chosen. The inverse function of a is nothing else than p as a function of θ_{n+1} and θ_n that is $a^{-1}(\theta_{n+1} - \theta_n) = p_{n+1}(\theta_{n+1} - \theta_n)$.

We will now compare the values of β and B for a map of this form with a(p) linear in p and a more general map on the cylinder.

A. a(p)=p (Standard map)

In this case $a^{-1}(\theta_{n+1} - \theta_n) = \theta_{n+1} - \theta_n$ and $\frac{\partial a^{-1}}{\partial \theta} = 1$.

B. $a(p) = p + \lambda f(p)$

Then $a(p_{n+1}) = \theta_{n+1} - \theta_n$, while $\frac{\partial a^{-1}(\theta_{n+1} - \theta_n)}{\partial \theta_n} = \frac{\partial p_{n+1}}{\partial \theta_n}$. Differentiating the previous equation for $\theta_{n+1} - \theta_n$ we get that

$$\frac{\partial a^{-1}}{\partial \theta_n} = \frac{1}{1 + \lambda \frac{\partial f}{\partial p}} \tag{7.34}$$

where $\frac{\partial f}{\partial p}$ is now a function of $\theta_{n+1} - \theta_n$. If we chose maps for which $\lambda \frac{\partial f}{\partial p} > 0$ then $\frac{\partial a^{-1}}{\partial \theta} < 1$ and we may chose $\beta < 1$ so that $\beta^{NM} > \beta^{NTM}$. A concrete example of that is the case where $a(p) = p + \lambda p^3$.

B depends on the value of $a^{-1}(\theta_{n+1} - \theta_n) - a^{-1}(\theta_n - \theta_{n-1}) = p_{n+1} - p_n$ for a given sequence. Suppose $a(p) = p + \lambda f(p)$. This is a deviation of the standard map force function if $\lambda \neq 0$. For the standard map the minimum estimate for the value of B can be given as the maximum of $| \theta_{n+1} + \theta_{n-1} - 2\theta_n |$ for a given anti-integrable sequence. For a general RTM map the value of B can be given as the maximum of $| p_{n+1} - p_n |$ where the p's are related to the anti-integrable θ sequence by the relation

$$\theta_{n+1} - \theta_n = a(p_{n+1}) \tag{7.35}$$

It is easy to see that $| p_{n+1} - p_n | \leq | \theta_{n+1} + \theta_{n-1} - 2\theta_n |$ in the above equation considered as a mapping of p to θ is expanding. This is equivalent to taking the function a(p) to be an increasing function of p. So for a RTM with a force function which is an increasing function of p, such as for example $a(p) = p + \lambda p^3$ for λ positive the following inequality is true $B^{SM} > B^{RTM}$.

Using the above results we find that $\epsilon_0^{SM} < \epsilon_0^{RTM}$, that is $K_{crit}^{SM} > K_{crit}^{RTM}$. This means that the existence of chaotic orbits coming from the anti-integrable limit can be rigorously proved for a general radial twist map (RTM) for smaller values of the perturbation parameter K than for the standard map. This is an indication that a RTM becomes chaotic more easily than the standard map (the first being a map of the cylinder the latter being a map of the torus) which may be one more reason why the correlation function method converges faster to the quasilinear result for maps on the cylinder than for maps of the torus.

Of course one might argue that the Lebesgue measure of the chaotic orbits the existence of which can be rigorously proved is zero as conjectured by Aubry and Abramovici [AA90]. Even if this conjecture is true, these chaotic orbits originating from the anti-integrable limit form a skeleton (a web) supporting the full set of chaotic orbits so their existence is basic to the chaotic behaviour in the phase space.

7.5 APPENDIX 5.1

In this appendix we give explicitly the algebraic forms of the functions involved in the calculations of the diffusion coefficients.

$$A_1 = \int_0^t dt' \sum_{l=-\infty}^{+\infty} \sum_{m=1}^{[t']} \Psi(m) \frac{2m-1}{t'-m} exp(-\frac{(n-x_0)^2 + (l-y_0)^2}{t'-m}) H(t'-m) \quad (7.36)$$

where x_0 and y_0 are the starting points of the particle. If we assume that $(x_0, y_0) \neq (0,0)$ then the above expression can be simplified to

$$\begin{aligned} A_1 \simeq & \int_0^t \sum_{m=1}^{[t']} \Psi(m) \frac{2m-1}{t'-m} exp(-\frac{n^2+y_0^2}{t'-m}) \\ & + \int_0^t \sum_{m=1}^{[t']} \frac{2m-1}{t'-m} (\frac{4K}{\pi} - 1) \end{aligned} \quad (7.37)$$

where K is the complete elliptic integral and the following relation hold

$$q = exp(-\frac{1}{t'-m}) = exp(-\frac{\pi K'}{K}). \quad (7.38)$$

The term A_2 for the retardor modes is similar.

7.6 APPENDIX 5.2.

In this appendix the first order perturbative solution is obtained for the discrete random walk model presented in section 5.2.1. and is shown to agree well with the results obtained from the first order perturbative solution of the continuous model.

The probability distribution for the discrete model to first order in α is given by

$$p^{(1)} = \sum_{t'=0}^{t} \sum_{n'} G(n-n', t-t')(S_A(p^{(0)}(n', t')) + S_T(p^{(0)}(n', t'))) \qquad (7.39)$$

where

$$G(n-n', t-t') = \int_{-\pi}^{\pi} exp(ik(n-n'))(cos(k))^{(t-t')}dk \qquad (7.40)$$

is the Green function for the simple random walk on a lattice and

$$p^{(0)}(n', t') = G(n'-n_0, t'). \qquad (7.41)$$

The correction to the probability distribution of the normal random walk, due to the accelerator modes, to first order in α is then

$$p^{(1)}(n,t) = \sum_{N,t'}^{\infty} \int_{-\pi}^{\pi} dq (cosq)^{t-t'} exp(i(n-Nl)q) \sum_{s=1}^{t'} \Psi(s) T_1 p(Nl-sl, t'-s)$$
$$- \sum_{N,t'}^{\infty} \int_{-\pi}^{\pi} dq (cosq)^{t-t'} cosq\, exp(i(n-Nl)q) \sum_{s=1}^{t'} \Psi(s) T_1 p(Nl-(s-1)l, t'-s) \qquad (7.42)$$

From this equation it is obvious that the Fourier transform of this correction term is

$$F(p^{(1)}) = f(q) = \sum_{N,t'}^{\infty} (cosq)^{t-t'} exp(-iNlq) \sum_{s=1}^{t'} \Psi(s) T_1 p(Nl-sl, t'-s)$$
$$- \sum_{N,t'}^{\infty} (cosq)^{t-t'} cosq\, exp(-iNlq) \sum_{s=1}^{t'} \Psi(s) T_1 p(Nl-(s-1)l, t'-s) \qquad (7.43)$$

and since we are interested in first order in α we will substitute the source terms appearing in this expression by

$$T_1 p(x,t) = \int_{-\pi}^{\pi} dk (cosk)^t exp(ikx). \qquad (7.44)$$

The correction to the zeroth moment which is the total number of particles due to the existence of the accelerator modes is given by

$$\Delta M_0 = f(0) = 0 \qquad (7.45)$$

as expected by particle conservation. The correction to the second moment, due to the existence of the source term related to the accelerator modes is given by

$$\Delta M_2 = -f''(0) \tag{7.46}$$

where the double dashes denote differentiation with respect to q. Performing the differentiations we get that

$$\Delta M_2 = \sum_{0}^{t}(t-t')(A_1(t')-A_2(t'))+\sum_{0}^{t} N^2 l^2 (A_1(t')-A_2(t'))-\sum_{0}^{t} tA_2(t') \tag{7.47}$$

where

$$A_1(t')-A_2(t') = \sum_{s=1}^{t'} \Psi(s) \int_{-\pi}^{\pi} dk (cosk)^{(t'-s)} exp(ik(Nl-sl))(1-exp(ikl)). \tag{7.48}$$

Using the identity

$$\sum_{N=-\infty}^{\infty} exp(ikNl) = \sum_{N=-\infty}^{\infty} \delta(k-\frac{2\pi N}{l}) \tag{7.49}$$

we can do the summations over N in the equation giving ΔM_2 and thus get

$$\Delta M_2 = -\sum_{t'}^{t}\sum_{s=1}^{t'} \Psi(s) \int_{-\pi}^{\pi} dk \sum_{N} \frac{\delta}{dk}(cosk)^{t'-s} exp(-iksl)(1-exp(ikl))\delta(k-\frac{2\pi N}{l}) \\ -\sum_{t'}^{t}\sum_{s=1}^{t'} t'\Psi(s) \sum_{N=-l/2}^{l/2} cos(\frac{2\pi N}{l})(t'-s). \tag{7.50}$$

We finally get for the real part of ΔM_2

$$\Delta M_2 = C_1 \sum_{t'}^{t}\sum_{s=1}^{t'} s\Psi(s)A(t'-s) - C_2 \sum_{t'}^{t}\sum_{s=1}^{t'} \Psi(s)A(t'-s) \tag{7.51}$$

where

$$A(t'-s) = \sum_{N=-l/2}^{l/2} cos(\frac{2\pi N}{l})(t'-s) \tag{7.52}$$

and

$$C_1 = 2l^2 \\ C_2 = l^2 + 1. \tag{7.53}$$

The function $A(t'-s)$ is bounded

$$|A(t'-s)| \leq l \tag{7.54}$$

for all values of $t' - s$. A calculation of $A(t'-s)$ shows that it can take both positive and negative values, but they are distributed in such a way that ΔM_2 is always a positive quantity. Furthermore for $t \to \infty$

$$\Delta M_2 \simeq C_1 \sum_{t'}^{t} \sum_{s=1}^{t'} s\Psi(s) - C_1 \sum_{t'}^{t} \sum_{s=1}^{t'} \Psi(s). \tag{7.55}$$

The behaviour of the second moment can now be calculated, by use of the discrete relation (7.51) without having to go to the continuous limit. It is also seen, that the discrete model gives the same results with the continuous one as far as asymptotic in time results are concerned. This can be easily seen comparing the discrete relation (7.55) with the relation for ΔM_2 obtained for the continuous case, which is given in Appendix 5.1, or even better its Fourier-Laplace transform given in Appendix 5.3.

The correction to the normal random walk, due to the presence of the source term corresponding to traps is calculated in a similar way. The final result is

$$\Delta M_2 = -\alpha \sum_{t'}^{t} B(t'-1) + \alpha \sum_{t'}^{t} \sum_{s=1}^{t'} r(s) B(t'-s) \tag{7.56}$$

where

$$B(t'-s) = \sum_{N=-l/2}^{l/2} cos(\frac{2\pi N}{l})^{t'-s} cos(\frac{2\pi N n_T}{l}) \tag{7.57}$$

The function $B(t'-s)$ has similar properties as the function $A(t'-s)$ defined above. It is such that the correction to the second moment due to the trap terms is always negative, thus giving rise to a decrease in the effective diffusion coefficient as expected. Furthermore for $t \to \infty$

$$\Delta M_2 \simeq -\alpha t + \alpha \sum_{t'}^{t} \sum_{s=1}^{t'} r(s). \tag{7.58}$$

It can be easily seen that this is just the discrete counterpart of the continuous relation for the case of traps, given in Appendix 5.3.

7.7 APPENDIX 5.3.

In this appendix we give the complete solution of the continuous diffusion model given in section 5.2.2 in Fourier-Laplace space. Even though this solution is not easily transformed back into real space and used to give results for intermediate times, it can be illuminating as far as asymptotic results for the second moment of the probability distribution are concerned.

We start by taking into account only the accelerator modes term. If we take the Fourier transform of the diffusion equation proposed in section 5.2.2 we get

$$\frac{\partial}{\partial t}\hat{p}(k,t) + Dk^2\hat{p}(k,t) = \sum_N e^{ikNx_A} \sum_{s=1}^{[t]} \Psi(s)(p(Nx_A - sx_A, Ny_A, t-s) - p(Nx_A - (s-1)x_A, Ny_A, t-s)) + \delta(t) \tag{7.59}$$

Manipulating the sum in the right hand side of the above equation we get

$$\frac{\partial}{\partial t}\hat{p}(k,t) + Dk^2\hat{p}(k,t) = (1 - exp(-ik_x Nx_A)) \sum_{s=1}^{[t]} \Psi(s) exp(ik_x sx_A) \times \sum_{\mathbf{N}} exp(i\mathbf{k}.\mathbf{N}x_A)p(\mathbf{N}x_A, \mathbf{N}y_A, t-s) + \delta(t) \tag{7.60}$$

where $\hat{p}(\mathbf{k},t)$ is the Fourier transform of $p(\mathbf{x},t)$. Since the above model is formally two dimensional, $\mathbf{k}$ is considered as a two dimensional vector, and because the communication of the accelerator modes is done in the x direction only, it is the x-coordinate of $\mathbf{k}$ that enters the multiplicative factor in front of the Fourier transform of the source term.

Writing

$$p(Nx_A, t-s) = \int_{-\pi}^{\pi} dq\, exp(-iNx_A q)\hat{p}(q, t-s) \tag{7.61}$$

and using the fact that

$$\sum_N exp(i(k-q)x_A N) = \delta((k-q)x_A - 2\pi N) \tag{7.62}$$

we can rewrite equation (7.60) in the form

$$\frac{\partial}{\partial t}\hat{p}(k,t) + Dk^2\hat{p}(k,t) = (1 - exp(-ik_x x_A)) \sum_{s=1}^{[t]} \Psi(s) exp(ik_x sx_A) \sum_{\mathbf{N}} \hat{p}(\mathbf{k} + \frac{2\pi}{x_A}\mathbf{N}, t-s) + \delta(t). \tag{7.63}$$

We now take the Laplace transform of this equation. This gives

$$u\hat{p}(k,u) + Dk^2\hat{p}(k,u) = \\ a(1 - exp(-ik_x x_A))\Psi(u - ik_x x_A)\sum_N p(k + \frac{2\pi}{x_A}N, u) + 1 \tag{7.64}$$

where the convolution sum has been replaced by an integral. In the above equation, $\Psi(u)$ is the Laplace transform of the function Ψ, and $p(k,u)$ is the Fourier-Laplace transform of p(x,y,t). The approximation of the convolution sum by an integral does not introduce new behaviour in the system, since the full dispersion relation of the discrete model using the discrete Fourier transform and the z-transform, where one makes no approximations of this sort, is analogous to the one obtained here for the continuous model and gives similar asymptotic results. The derivation of the dispersion relation for the discrete model is similar to the one presented here, only that it does not involve any of the approximations necessary to be done in the continuous case.

We solve the operator equation for $p(k,u)$ using the iteration scheme

$$p^{(m)}(k,u) = G^0(k,u) + af(k)G^0(k,u)\Psi(u - ik_x x_A)\sum_N p^{(m-1)}(k + \frac{2\pi}{x_A}N, u) \tag{7.65}$$

where

$$G^0(k,u) = \frac{1}{u + Dk^2} \tag{7.66}$$

and

$$f(k) = 1 - exp(-ik_x x_A) \tag{7.67}$$

As the zeroth order approximation we use $p^0(k,u) = G^0(k,u)$ which is the Fourier-Laplace transform of the diffusion equation in the case of no sources ($a = 0$).

It is clear that this iterative scheme is just the Fourier-Laplace space version of our perturbative solution of the diffusion equation employed in section 5.3. The advantage of using this method in Fourier Laplace space for the solution of the dispersion relation, is that, we can get iterations of this scheme up to any order we like, thus getting a formal series in a for the complete solution of the problem. The full solution to the problem is then

$$p(k,u) = G^0(k,u) + \sum_{n=1}^{\infty} a^n \hat{p}_n(k,u) \tag{7.68}$$

where

$$p_n(k,u) = f(k)G^0(k,u)\Psi(u - ikx_A)\sum_{m_1,\ldots,m_n}\prod_{i=1}^{n-1} f(k + A\sum_{i=1}^{i} m_i)$$
$$G^0(k + A\sum_{i=1}^{i} m_i, u)\Psi(u - ikx - iA\sum_{i=1}^{i} m_i)G^0(k + A\sum_{i=1}^{n} m_i, u) \tag{7.69}$$

and $A = \frac{\beta\delta}{\tau_A}$.

It is easy to see that the full solution to the problem gives

$$\hat{p}(0,u) = \frac{1}{u} \tag{7.70}$$

which is equivalent to the conservation of particles.

We now use equation (7.68) to get the Laplace transform for the second moment of the probability distribution. As is well known second moments are given by

$$\mathbf{M_2}(u) = -\frac{d^2\hat{p}(\mathbf{k},u)}{d\mathbf{k}^2}\Big|_{\mathbf{k}=0} \tag{7.71}$$

Differentiating $\hat{p}(\mathbf{k},u)$ twice we get

$$\frac{d^2\hat{p}(\mathbf{k},u)}{d\mathbf{k}^2} = -\frac{2D}{(u+Dk^2)^2} + \frac{2D^2k^2}{(u+Dk^2)^3} + \sum_{n=1}^{\infty}\alpha^n\frac{d^2\hat{p}_n(\mathbf{k},u)}{d\mathbf{k}^2} \tag{7.72}$$

where

$$\begin{aligned}\frac{d^2p_0(\mathbf{k},u)}{d\mathbf{k}^2} &= f''(k)G^0(k,u)\Psi(u - ikx_A,u)F_1(k,u)\\ &+ f'(k)G^{01}(k,u)\Psi(u - ikx_A,u)F_1(k,u)\\ &+ f'(k)G^0_1(k,u)\Psi'(u - ikx_A,u)F_1(k,u)\\ &+ f(k)G^0_1(k,u)\Psi(u - ikx_A,u)G_{11}(k,u)\\ &+ f'(k)G^{01}(k,u)\Psi(u - ikx_A,u)G_{12}(k,u)\\ &+ f'(k)G^{01}(k,u)\Psi(u - ikx_A,u)G_{13}(k,u)\\ &+ f'(k)G^{01}(k,u)\Psi(u - ikx_A,u)G_{14}(k,u)\end{aligned} \tag{7.73}$$

and

$$\begin{aligned}F_1(k,u) = \sum_{m_1,\ldots,m_n}\prod_{i=1}^{n-1} f(k + A\sum_{i=1}^{i} m_i)G^0(k + A\sum_{i=1}^{i} m_i,u)\\ \Psi(u - ix_Ak_x - iA\sum_{i=1}^{i} m_i)G^0(k + A\sum_{i=1}^{n} m_i,u)\end{aligned} \tag{7.74}$$

$$\begin{aligned}G_{11}(k,u) = \sum_{n=0}^{n-1}\sum_{m_1,\ldots m_n} f'(k + A\sum_{i=1}^{n_0} m_i)G^{01}(k + A\sum_{i=1}^{n_0} m_i)\\ \Psi(u - ix_Ak_x - iA\sum_{i=1}^{n_0} m_i)\\ \prod_{i=1,i\neq 0}^{n-1} f(k + A\sum_{i=1}^{i} m_i)G^0(k + A\sum_{i=1}^{i} m_i,u)\\ \Psi(u - ix_Ak_x - iA\sum_{i=1}^{i} m_i)G^0(k + A\sum_{i=1}^{n} m_i,u)\end{aligned} \tag{7.75}$$

$G_2(k,u)$ is the same as the above but with $G^{0'}$ instead of f', $G_3(k,u)$ is again the same as the above but with Ψ' instead of f' and finally $G_4(k,u)$ is the same as F_1 but the last G^0 function is differentiated with respect to k, that is, it is substituted by a $G^{0'}$. It is obvious that the terms containing f' and Ψ' are non zero only if derivatives with respect to k_x are taken.

The asymptotic behaviour of the second moment, is given in the limit $u \to 0$ and $k = 0$. The terms diverging as $u \to 0$ are those which are of interest. Terms of the form $G^{n_1}(k + A\sum_{i=1}^{j} m_i, u)$ are going to diverge as $u \to 0$, only if $\sum_{i=1}^{j} m_i = 0$. However, because of the presence of terms of the form $f(\sum_{i=1}^{j} m_i)$ in the series giving the Laplace transform of the second moment as k=0, and of the property f(0)=0, we are not free to have as many G^0's diverging at $u \to 0$ as we like. Observing the structure of the series and taking into account that $f'(0) \neq 0$ and $G^{0'}(0) = 0$ we see that the only possible diverging terms as $u \to 0$ are such that

$$M_{2x}(u) = \frac{1}{u^2} + C_1\frac{\tilde{\Psi}'(u)}{u^2} + C_2\frac{\tilde{\Psi}^2(u)}{u^3} \tag{7.76}$$

whereas $M_{2y}(u)$ is just equal to $\frac{1}{u^2}$. The first term in the above sum is just the normal diffusive behaviour $M_2 = t$. The second term, in real space corresponds to a behaviour of the form

$$\Delta M_2(t) \equiv \int_0^t \int_0^\tau s\Psi(s)dsd\tau \tag{7.77}$$

and the third term in a behaviour of the form

$$\Delta M_2(t) \equiv \int_0^t (t-u)^2\Psi * \Psi(u)du \tag{7.78}$$

where * denotes the convolution product.

Thus the full solution to the diffusion model for the second moment in x, is given by equations (7.76-7.78).

In the case where the trap term is introduced into the system, the same procedure should be followed. By taking the Fourier-Laplace transforms of the continuous equations we get

$$u\tilde{p}(k,u) + Dk^2\tilde{p}(k,u) = \frac{\alpha}{2}k^2(1 - H(u))\sum_N e^{ma}\tilde{p}(k+N,u) + 1 \tag{7.79}$$

where $R(u)$ is the Laplace transform of $r(s)$ and we have assumed that the traps are situated on a periodic lattice which without loss of generality can be taken of the form $x_0 + 2\pi N$.

This is an equation for $\bar{p}(k,u)$ which can be solved using the following iterative scheme

$$\bar{p}^{(m+1)}(k,u) = G^0(k,u) + \frac{\Omega}{2}k^2(1 - R(u))G^0(k,u)\sum_N exp^{iNx_0}\bar{p}^{(m)}(k+N,u) \tag{7.80}$$

where

$$G^0(k,u) = \frac{1}{u + Dk^2} \tag{7.81}$$

is the Fourier-Laplace transform of the Green function for the diffusion process when $a = 0$. In the above may be considered as a vector or a scalar according to the dimension of the diffusion process. Since the trapping process does not create a prefered direction, as in the case of the accelerator modes where the streaming was defining a prefered direction, it is not of great importance to think of k as a vector.

Starting with $\bar{p}^{(0)}(k,u) = G^0(k,u)$ we get the full solution

$$\bar{p}(k,u) = G^0(k,u) + \frac{1}{2}\sum_{n=1}^{\infty} a^n k^2(1 - R(u))^n G^0(k,u)F_n(k,u) \tag{7.82}$$

where

$$F_n(k,u) = \sum_{n_1 \ldots n_s} exp(i(n_1 + \ldots + n_s)x_0)(k+n_s)^2 G^0(k+n_s,u)\ldots$$
$$(k + n_s + n_{s-1} + \ldots + n_2)^2 G^0(k + n_s + n_{s-1} + \ldots + n_2, u)G^0(k + n_s + \ldots + n_1, u) \tag{7.83}$$

The second moment we are interested in, is equal to $-\bar{p}''(0,u)$ which is

$$\bar{p}''(0,u) = G^{0''}(0,u) + \sum_{n=1}^{\infty} a^n(1 - R(u))^n G^0(0,u)F_n(0,u). \tag{7.84}$$

We are interested in terms diverging as $u \to 0$, because these are the terms which give asymptotic contributions in time. It can be seen that the only case where $F_n(0,u)$ can diverge is when $n_1 + \ldots + n_s = 0$ while all the other sums $n_m + \ldots + n_s \neq 0$ where $m \geq 2$. This gives a divergence of $1/u$ which is due to the $G^0(0,u)$ term.

So, $\tilde{p}^{\infty}(0, u)$ diverges as

$$-\frac{1}{u^2} + \sum_{s=1}^{\infty} \alpha^s \frac{(1 - R(u))^s}{u^2} \tag{7.85}$$

The correction of the second moment due to the trap terms is then

$$\Delta M_2 = -\sum_{s=1}^{\infty} \alpha^s \frac{(1 - R(u))^s}{u^2} \tag{7.86}$$

This gives a contribution

$$\Delta M_2 = -\frac{\alpha}{1-\alpha}\frac{1}{u^2} + \sum_{s=1}^{\infty} A_s \frac{R(u)^s}{u^2} \tag{7.87}$$

where A_s are constant terms that can be obtained from the expansion of $(1 - R(u))^s$.

Transforming back to time, this relation becomes

$$\Delta M_2(t) = -\frac{\alpha}{1-\alpha} t + \sum_{s=1}^{\infty} A_s \int^t \int^{t'} (r(\tau))^{*s} d\tau dt' \tag{7.88}$$

where f^{*s} denotes the convolution of f, s-times with itself.

7.8 APPENDIX 5.4.

In this appendix, the asymptotic results for $M_2 x$ are obtained for various forms of the waiting time probability distribution $\psi(s)$.

1. Power law

Assume the the trapping probability distribution in the accelerator modes behaves asymptotically in time like a power law

$$\psi(t) \sim t^{-1-\beta}, \quad t \to \infty, \quad 1 < \beta < 2. \tag{7.89}$$

Then, from the definition of $\Psi(t)$ we see that

$$\Psi(t) \sim t^{-\beta}, \quad t \to \infty. \tag{7.90}$$

In the previous appendix it was shown that in the presence of accelerator modes, the second moment has the following corrections as $t \to \infty$

$$\Delta M_2^{(1)}(t) \sim \int_{\tau_r}^{t} \int_{\tau_r}^{t'} s\Psi(s) ds dt' \tag{7.91}$$

and

$$\Delta M_2^{(2)}(t) \sim \int_{t_r}^{t} (t-u)^2 \Psi * \Psi(u) du. \tag{7.92}$$

where τ_r and t_r are times for which our asymptotic forms for $\Psi(t)$ are valid. For $\Psi(t) \sim t^{-\beta}$ as $t \to \infty$ it is easy to see that

$$M_2^{(1)}(t) \sim t^{3-\beta}. \tag{7.93}$$

The convolution $\Psi * \Psi$ will behave asymptotically as $t^{1-\beta}$ for $t \to \infty$ so that

$$\Delta M_2^{(2)}(t) \sim t^{4-2\beta} \tag{7.94}$$

For $1 < \beta < 2$ the dominant contribution as $t \to \infty$ is that of $M_2^{(1)}$.

In the case where trap terms are introduced the asymptotic behaviour for the corrections to the second moment is

$$\Delta M_2^{(1)}(t) \propto -\frac{u}{1-u} t \tag{7.95}$$

and

$$M_2(t) \simeq \int_{t_c}^{t} \int_{t_c}^{t'} (r(\tau))^{**} d\tau dt' \tag{7.96i}$$

which for $r(t) \sim t^{-1-\gamma}$ as $t \to \infty$ behaves like

$$M_2(t) \sim t^{2-\gamma} \tag{7.97}$$

which for every $s \geq 1$ decays to 0 as $t \to \infty$.

2.Exponential form

If the distribution function $\psi(t)$ decays exponentially then in general $\psi(t)$ will decay as $exp(-\lambda t)$ as $t \to \infty$.

In that case

$$\Delta M_2^{(1)} \sim \int^t \int^s s exp(-\lambda s) ds dt \sim exp(-\lambda t) \tag{7.98}$$

So the term $\Delta M_2^{(1)}$ will not contribute for $t \to \infty$ in the case of an exponential trapping distribution. The same happens with the term $\Delta M_2^{(2)}$. If $\psi(t) \sim t^{-n} exp(-\lambda t)$ then $\Psi(t) < f(t) = exp(-\lambda t)$ for $t > 1$ and $\Psi * \Psi(t) < f * f(t) = t exp(-\lambda t)$. Then

$$\Delta M_4^{(2)} < \int^t (t-u)^2 u exp(-\lambda u) du \tag{7.99}$$

and this last integral decays exponentially to zero as $t \to \infty$. So $\Delta M_4^{(2)}$ again will not contribute to the second moment for $t \to \infty$ in the case of an exponential trapping distribution.

The same is true for the correction term due to the presence of traps.

Bibliography

[AS70] Abramowitz M. and I. A. Stegun (eds) (1970) Handbook of Mathematical Functions, Dover

[A88] De Almeida A. M. O. , 'Hamiltonian Systems: Chaos and Quantization', Cambridge University Press, 1988.

[Ar89] Arnold V. I. , 'Mathematical Methods of Classical Mechanics', 2nd ed. , Springer Verlag, 1989.

[AA90] Aubry S. and G. Abramovici (1990), Physica D **43**, 199

[ACSZ90] V. V. Afanasiev, A. A. Chernikov, R. Z. Sagdeev and G. M. Zaslavskii, Physics Letters A **144** (1990) p. 229

[ASZ91] Afanasiev V. V. , R. Z. Sagdeev and G. M. Zaslavskii (1991), Chaos **1**, 143

[BV74] Balagurov B. Y. and V. G. Vaks (1974), Soviet Physics JETP **38**, 968

[BK84] Bensimon D. and L. Kadanoff (1984) Physica **13D**, 82.

[BR86] Bland A. S. and G. Rowlands (1986) in Nonlinear Phenomena and Chaos, ed. S. Sarkar, Adam Hilger

[CJ59] Carslaw H. S. and J. C. Jaeger (1959) Conduction of Heat in Solids, Clarendon Press

[C79] Chirikov B. V. (1979), Physics Reports **52**, 263

[CR81] Cohen R. H. and G. Rowlands (1981) Phys. Fluids **24**, 2295

[CM81] Cary J. R. and J. D. Meiss (1981) Phys. Rev. A **24**, 2664

[CNP87] Chernikov A. A. , M. Y. Natenzon, B. A. Petrovichev, R. Z. Sagdeev and G. M. Zaslavskii (1987) Phys. Let. A **122**, 39

[CSU87] Chernikov A. A. , R. Z. Sagdeev, D. A. Usikov and G. M. Zaslavskii (1987) Phys. Let. A **125**, 101

[CSZ88] Chernikov A. A. , R. Z. Sagdeev and G. M. Zaslavskii (1988) Physica **D33**, 65

[DMP89] Dana I. , N. W. Murray and I. C. Percival (1989) Phys. Rev. Lett. **62**, 233.

[D90] Dana I. (1990) Phys. Rev. Lett **64**, 2339.

[E86] Easton R. W. (1986) Trans. A. M. S **294**, 2.

[F72] Froeschle C. (1972), Astronomy and Astrophysics **16**, 172

[G80] Goldstein H. , 'Classical Mechanics', 2nd ed. , Addison-Wesley, Reading, Massachusetts, 1980.

[GH83] Guckenheimer J. and P. Holmes, 'Nonlinear Oscillations, Dynamical Systems and Bifurcations of Vector Fields', Springer Verlag, 1983

[HK185] Hatori T. , T. Kamimura and Y. H. Ichikawa (1985) Physica **14D**, 193

[HHKM91] Ishizaki R. , T. Horita, T. Kobayashi and H. Mori (1991), Prog. Theor. Phys. **85**, 1013

[KRW82] C. F. F. Karney, A. B. Rechester and R. B. White, Physica **4D** (1982) p. 425

[KM90] Kook H. and J. D. Meiss (1990) , Physical Review A **41**, 4143

[LL83] A. J. Lichtenberg and M. A. Lieberman: Regular and stochastic motion Springer Verlag 1983

[L89] Liboff R. L. , 'Kinetic Theory: Classical, Quantum and Relativistic Descriptions', Prentice Hall, 1989

[Ma53] Morse P. M. and H. Feshbach, 'Methods of Theoretical Physics', Vol. I McGraw-Hill 1953.

[Mb53] Morse P. M and H. Feshbach 'Methods of theoretical Physics', Mc Graw Hill. Vol II 1953.

[McL64] rLachlan N. W. 'Theory and application of Mathieu functions', Dover, 1964

[MCG83] Meiss J. D. , J. R. Cary, C. Grebogi, J. D. Crawford, A. N. Kaufman and H. D. I. Abarbanel (1983), Physica **6D** . 375

[MMP84] Mackay R. S. , J. D. Meiss and I. C. Percival (1984) Physica **13D**, 55.

[MLL85] Murray N. W, M. A. Lieberman and A. J. Lichtenberg (1985) Phys. Rev. A **32**, 2413

[M85] Mackay R. S. 'Introduction to the Dynamics of Area-Preserving Maps', Proceedings for the US Particle Accelerator School SLAC', ed. M. Month 1985.

[MO86] Meiss J. D. and E. Ott (1986), Physica **20D**, 387

[MMP87] Mackay R. S. , J. D. Meiss and I. C. Percival (1987), Physica **D27**, 1.

[MM92] Mackay R. S. and J. D. Meiss (1992), Nonlinearity **5** . 149

[O89] J.M.Ottino, The Kinematics of Mixing, Chaos and Transport C.U.P., 1989

[P62] Prigogine I. 'Nonequilibrium Statistical Mechanics' Interscience, 1962.

[P84] Petrosky T. Y. (1984) Phys. Rev. A **29**, 2078

[P85] Petrosky T. Y. (1985) Phys. Rev. A **32**, 3716

[P92] Pikovsky A. S. (1992) J. Phys. A:Math. Gen. **25**, L477

[RW80] Rechester A. B. and R. B. White (1980), Phys. Rev. Lett. , **44** , 1586

[RRW81] Rechester A. B. , Rosenbluth M. N. and R. B. White (1981), Phys. Rev. A. **23** , 2664

[SBGC84] Schechtman D. , I. Blech, D. Gratias and J. W. Cahn (1984) Phys. Rev. Let. **53**, 951

[YR91] Yannacopoulos A. N. and G. Rowlands (1991), Phys. Lett. A **155** , 133

[YR92] Yannacopoulos A. N. and G. Rowlands (1992), Physica **57D**, 355

[W92] Wiggins S. , 'Chaotic Transport in Dynamical Systems', Springer-Verlag, 1992.

[ZC72] Zaslavskii G. M. and Chirikov B. V. (1972) Soviet Physics Uspekhi **14**, 549

[ZZS86] G. M. Zaslavskii, M. Y. Zakharov, R. Z. Sagdeev, D. A. Usikov and A. A. Chernikov, Soviet Physics JETP**64** (1986) p. 294

[ZSC89] Zaslavskii G. M. , R. Z. Sagdeev, D. K. Chaikovskii and A. A. Chernikov (1989), Soviet Physics JETP **68**, 995

[ZSU89] G. M. Zaslavskii, R. Z. Sagdeev, D. A. Usikov and A. A. Chernikov, Soviet Physics Uspekhi **31** (1989) p. 887 and references therein

[Z191] Zaslavsky G. M. and M. K. Tippett (1991), Phys. Rev. Letters **67**, 3251